Lehrstuhl für Informationstechnische Regelung
Technische Universität München

Cooperative multi-robot manipulation under uncertain kinematic grasp parameters

Sebastian Erhart

Vollständiger Abdruck der von der Fakultät für Elektrotechnik und Informationstechnik der Technischen Universität München zur Erlangung des akademischen Grades eines

Doktor-Ingenieurs (Dr.-Ing.)

genehmigten Dissertation.

Vorsitzender: Prof. Gordon Cheng, Ph.D.

Prüfer der Dissertation:

1. Prof. Dr.-Ing. Sandra Hirche

2. Prof. Domenico Prattichizzo, Ph.D.,

    (schriftliche Beurteilung)

3. Prof. Dr.-Ing. Klaus Diepold (mündliche Prüfung)

Die Dissertation wurde am 20.01.2016 bei der Technischen Universität München eingereicht und durch die Fakultät für Elektrotechnik und Informationstechnik am 07.11.2016 angenommen.

Abstract

Autonomous robotic systems are nowadays the key technology in a variety of industrial, logistic and domestic applications. The increasing demand for performance leads successively to task specifications which exceed the capacity of a single robot. A team of cooperating robots outperforms naturally the functionality of a single robot due to the intrinsic redundancy and the potentially heterogeneous team member skills. Typical examples include industrial robots manipulating cooperatively large metal profiles or loading heavy cargo between different carriers as well as transportation tasks conducted by means of cooperating aerial robots. When employing several robots, the core challenge is the coordination of the robotic team while incorporating the distributed sensing and actuation capabilities of the individual robots. This holds true, in particular, for cooperative manipulation tasks in which a direct physical interaction between the robots takes place.

The present thesis addresses the major issues arising in cooperative manipulation tasks when autonomous robots with distributed sensing and actuation capabilities cooperate and no global coordinate system is available for accomplishing the task. To this end, the central manipulation task objective is distributed to the manipulator ensemble by computing suitable setpoints, which in turn are tracked by the robots' local force/motion controllers. At this stage, even small errors in the kinematic coordination may result in large interaction forces damaging the object and thus missing the task objective. In this thesis, the cooperative manipulation task is reformulated as a robust force/motion tracking problem under uncertain kinematic parameters. Careful attention is paid to the fact that in general each robot has only access to its local sensing and actuation capacities while interacting globally through the object with the rest of the manipulator ensemble. The distributed character of the robotic system needs to be properly addressed in the modeling, the analysis and the control design in order to achieve the manipulation task objective when no precise global coordination is available. An open problem in the area of cooperative manipulators is the modeling of the occurring end effector forces, which are a crucial prerequisite for the stability analysis in cooperative force/motion tracking tasks. Moreover, the kinematic coordination of the manipulator ensemble without global coordinate frame is a major challenge faced beyond dedicated laboratory environments which has not yet been treated by the robotics community.

The main contributions of this thesis can be divided into three parts. First, a novel and physically consistent modeling of the interaction dynamics is presented. This model incorporates an explicit mathematical expression for the emerging manipulator wrenches and is based on the Dirac structure imposed by the kinematic constraints through the object. Second, a thorough analysis of this model provides a new characterization and decomposition of internal and external manipulator wrenches. This analysis leads to a completely new approach to the design of a more general decoupling control scheme for internal/external forces, a new paradigm for the choice of the load distribution between manipulators and the synthesis of the resulting object dynamics. Third, an adaptive control scheme is described which achieves robust force/motion tracking under uncertain kinematic grasp parameters without relying on a global coordinate frame for planar, quasi-static cooperative manipulation tasks.

Zusammenfassung

Autonome Robotersystems sind heutzutage die Schlüsseltechnologie in zahlreichen industriellen, logistischen und häuslichen Anwendungen. Die steigenden Anforderungen an deren Leistungsfähigkeit führen sukzessive zu Aufgabenstellungen, die von einzelnen Robotern nicht mehr bewältigt werden können. Ein Team von kooperierenden Robotern übertrifft naturgemäß die Funktionalität eines einzelnen Roboters aufgrund der intrinsischen Redundanz und der potentiell verschiedenartigen Fähigkeiten der Team-Mitglieder. Typische Anwendungsbeispiele umfassen industrielle Roboter, die große Metallprofile manipulieren oder schwere Lasten verfrachten, aber auch Transportaufgaben, die von fliegenden Robotern durchgeführt werden. Sobald mehrere Roboter kooperieren, stellt die größte Herausforderung deren Koordination im Hinblick auf die Integration der auf die einzelnen Roboter verteilten Sensorik und Aktuierung dar. Dies gilt im Besonderen für kooperative Manipulationsaufgaben, bei denen eine direkte physikalische Interaktion zwischen den Robotern stattfindet.

Die vorliegende Dissertation behandelt die bedeutendsten Aspekte kooperativer Manipulationsaufgaben im Falle autonomer Roboter mit verteilter Sensorik und Aktuierung unter der Annahme, dass kein globales Koordinatensystem für die Aufgabenausführung zur Verfügung steht. Zu diesem Zweck wird das zentrale Ziel der Manipulationsaufgabe in Form von geeigneten Sollwerten für die Kraft-/Bewegungs-Regler auf die einzelnen Roboter verteilt. An dieser Stelle führen selbst kleine kinematische Koordinationsfehler zu großen Interaktionskräften, die das Objekt beschädigen können und damit das Aufgabenziel verfehlen. Die vorliegende Arbeit formuliert die kooperative Manipulationsaufgabe als ein Problem der robusten Kraft-/Bewegungs-Folgeregelung unter unsicheren kinematischen Parametern. Besondere Aufmerksamkeit ist der Tatsache gewidmet, dass im Allgemeinen jeder Roboter nur Zugriff auf seine lokale Sensorik und Aktuatorik besitzt, während er durch das Objekt global mit dem gesamten restlichen Manipulatorensemble interagiert. Der verteilte Charakter des Robotersystems muss dementsprechend in der Modellierung, der Analyse und dem Regelungsentwurf abgebildet werden um das Manipulationsziel auch zu erreichen, wenn keine akkurate globale Koordination möglich ist. Ein offenes Problem auf dem Gebiet der kooperativen Manipulation stellt die Modellierung der auftretenden Endeffektor-Kräfte dar, die eine wesentliche Voraussetzung für die Stabilitätsanalyse von kooperativen Kraft-/Bewegungs-Reglern ist. Besonders außerhalb von dedizierten Laborumgebungen findet sich in der kinematischen Koordination der Manipulatoren unter Verzicht auf ein globales Koordinatensystem eine bedeutende Herausforderung, die bisher innerhalb der Robotik nicht behandelt wurde.

Die zentralen wissenschaftlichen Beiträge dieser Dissertation gliedern sich in drei Teile. Erstens wird ein physikalisch konsistentes Modell der Interaktionsdynamik eingeführt. Dieses Modell umfasst einen expliziten mathematischen Ausdruck für die auftretenden Endeffektor-Kräfte und basiert auf der durch die vom Objekt vorgegebenen kinematischen Zwangsbedingungen und der damit verbundenen Dirac-Struktur. Zweitens führt eine sorgfältige Analyse dieses Modells zu einer neuen Charakterisierung und Zerlegung von internen und externen Manipulatorkräften. Diese Analyse führt zu einem komplett neuartigen Ansatz für den Entwurf einer verallgemeinerten Entkoppelungsregelung für interne/externe Kräfte, einem neuen Paradigma für die Wahl der Lastverteilung zwischen

den Manipulatoren und der Synthese der resultierenden Objektdynamik. Drittens wird ein adaptives Regelgesetz vorgestellt, das für planare, quasi-statische Manipulationsaufgaben und fehlerbehaftete kinematische Parameter robuste Kraft-/Bewegungs-Folgeregelung garantiert, ohne dabei auf eine globales Koordinatensystem zurückzugreifen.

Preface

This thesis summarizes the results of an intensive period of research conducted at the Institute of Information-Oriented Control (ITR) at Technische Universität München. The presented studies would not have been possible without the great support from many people to whom I am deeply indebted.

I would like to express my sincere gratitude to my doctoral advisor and head of the institute Prof. Sandra Hirche for her continuous encouragement, countless scientific stimuli and her firm commitment to excellence in research. Not least because of her ITR provides an outstanding research ambiance for the permanent staff, students and visitors.

Likewise, I would like to thank all my colleagues for numerous scientific discussions and for their prompt help in fixing the hardware and software architecture whenever a robot broke down. Many thanks as well to the administration and technical staff for providing support whenever needed.

I am deeply grateful to Prof. Danica Kragic, director of the Centre for Autonomous Systems at KTH, Stockholm, for receiving me twice for a short-term research stay. Moreover, I would like to thank particularly Yiannis Karayiannidis from the Computer Vision and Perception Lab at KTH who took care of a great part of the organizational issues for the two research stays and to whom I am much obliged for many intensive and inspiring discussions about adaptive control theory.

Munich, January 2016 Sebastian Erhart

Contents

Notations

Symbols

General

$\mathbb{R}^n$	Real coordinate space of n dimensions
$\mathbb{R}^{m \times n}$	Set of $m \times n$ matrices
$\mathbb{R}^+$	Set of non-negative real numbers
I_3	3×3 identity matrix
0_3	3×3 zero matrix
R	3×3 rotation matrix

Operators

$*$	Quaternion product
$\times$	Cross-product
$S(\cdot)$	Skew-symmetric matrix performing the cross-product, i.e. $a \times b = S(a)b$
A^T	Matrix transpose of the matrix A
M^{-1}	Matrix inverse of the matrix M
q^{-1}	Inverse of the unit quaternion q
$A^\dagger$	Moore-Penrose inverse of the matrix A
A^+	Generalized inverse of the matrix A
$\|v\|$	Euclidean norm of the vector v

Manipulator and object kinematics

ξ	Manipulator joint space angle vector
J	Manipulator Jacobian matrix
x	Rigid body pose
p	Position vector
q	Unit quaternion representing a rigid body orientation
η	Scalar part of the unit quaternion
ϵ	Vector part of the unit quaternion
ω	Angular velocity
r	Grasp vector
δq	Grasp orientation

Manipulator and object dynamics

Λ Joint space inertia matrix

τ Joint torque vector

M Task space inertia matrix

C Task space Coriolis matrix

D Task space damping matrix

K Task space stiffness matrix

$\mathcal{I}$ Moment of inertia matrix

h Task space wrench vector

Coordinate frames

$\{i\}$ Coordinate frame attached to the end-effector of the i-th manipulator

$\{\underline{i}\}$ Coordinate frame attached to the base of the i-th manipulator

$\{o\}$ Coordinate frame attached to the object's center of mass

$\{w\}$ Inertial world frame

Subscripts, Superscripts and Accents

x_i End effector pose of the i-th manipulator

x_i^d Desired value of x_i

$\hat{r}_i$ Estimate of the grasp vector r_i

$\tilde{r}_i$ Estimation error of the grasp vector

$^o r_i$ Grasp vector r_i expressed in the coordinate frame $\{o\}$

$^o R_w$ Rotation matrix transforming a vector from frame $\{w\}$ to frame $\{o\}$

$\tilde{\tau}_i$ Joint torque disturbance

$\tilde{h}_i$ End effector wrench disturbance

$\bar{h}_i$ Reaction wrench to the wrench h_i, i.e. $\bar{h}_i = -h_i$

List of Figures

1 Introduction

Autonomous robotic systems are nowadays the key technology in a variety of application domains ranging from manufacturing, construction, agriculture and forestry to service robotics, search and rescue but also aerial transportation. The increasing demand for performance of such robotic systems is often met by employing an ensemble of robots for performing a task. A team of cooperating robots outperforms naturally the functionality of a single robot due to the intrinsic redundancy and the potentially heterogeneous team member skills in terms of sensing and actuation capabilities. Applications of classical multi-agent system theory include area coverage and surveillance (e.g. for forest fire detection) and formation control (e.g. for search and rescue tasks). When the cooperative task involves manipulation of an object, the multi-robot system is said to perform a cooperative manipulation task. Typical examples include industrial robots manipulating cooperatively large metal profiles or loading heavy cargo between different carriers as well as transportation tasks conducted by means of cooperating aerial robots. In the long term, scenarios in which a human operator interacts actively with the multi-robot team show promise to yield a maximum benefit in regard to the achievable task efficiency. An exemplary cooperative multi-robot manipulation scenario with human interaction is depicted in Fig. 1.1.

Fig. 1.1: Cooperative multi-robot manipulation scenario with human-robot interaction

In such tasks, the human operator provides not only high-level task directives to the robots but also gets simultaneously feedback from the multi-robot team about the current task progress. In this way, the human cognitive skills and the robots' distributed sensing and actuation capacities contribute to an increasing task performance. In order to enable

the human to adopt a supervising role, the multi-robot team is required to maintain a high level of autonomy during the task, allowing to reduce the human intervention to a minimum.

In this perspective it becomes obvious that the benefits of using a team of robots for manipulating a common object come at the cost of an increased complexity for coordinating the manipulator ensemble. The variety of potential applications motivates the tremendous research on multi-agent coordination strategies during the past decades. Recently, multi-agent approaches are employed for the coordination of cooperating manipulators, too. However, as detailed in the sequel of this thesis, the dynamics in cooperative manipulation tasks are intrinsically different from the dynamics encountered in conventional multi-agent systems. In general, the emerging behavior of the cooperative manipulator system is complex due to a direct coupling of the nonlinear manipulator dynamics and the dynamics of the manipulated object. Aiming for a successful task achievement, the interplay between the cooperative coordination strategy and the manipulator force/motion control schemes needs to be thoroughly understood and analyzed. This work starts with discussing coordination strategies for general multi-robot systems and specifying the particular features of the system dynamics encountered in cooperative manipulation tasks.

1.1 Coordination strategies for multi-robot systems

Coordination strategies for multi-robot systems are part of the broader field of multi-agent system theory. This research field unites algorithmic, game-theoretic and logical approaches in order to develop new methods for multi-robot systems, distributed optimization or reinforcement learning [1]. According to [2], multi-agent systems are characterized by three distinct features: 1) the agents are (at least partially) *autonomous*; 2) the agents have only a *local view*, i.e. no agent has a full global view on the system and 3) the coordination between is *decentralized*, i.e. there is no designated controlling agent.

Typically, methods developed within the framework of multi-agent system theory address multi-robot problems such as the consensus [3] or rendez-vous problem [4], formation control [5] or coverage control problem [6]. Particular emphasis is put on maintaining network connectivity [7] and the formation stability in terms of graph rigidity [8]. While the greater part of multi-agent coordination methods are developed for configuration spaces, a framework based on differential geometry for motion coordination on the Euclidean group is presented in [9]. By construction, all cited coordination strategies above do comply with the requirements on multi-agent systems in view of their autonomy, the local view and the decentralization.

At this point it is crucial to recognize that in classical multi-agent systems the emerging system dynamics result from a *coupling through feedback*. This is illustrated by means of the formation control problem in the following Fig. 1.2.

Initially, the agent position (denoted by the gray triangles) does not match the desired formation shape. In the present example, the desired formation shape is an equilateral triangle. Through sensing of the agents' relative positions and appropriate feedback design the ensemble performs a transient (denoted by the black dotted lines) which reaches the desired formation eventually (denoted by the black triangles).
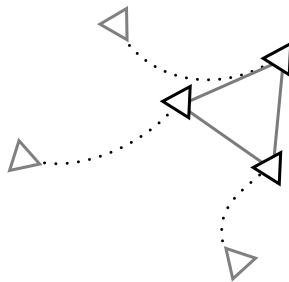
Fig. 1.2: Illustration of a multi-robot system performing a formation control task

In cooperative manipulation tasks the situation is different. Consider Fig. 1.3 for an illustration of the system dynamics encountered in cooperative manipulation tasks.
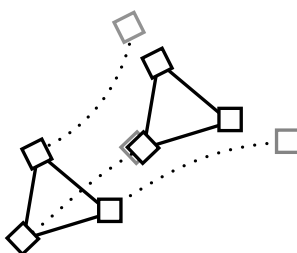
Fig. 1.3: Illustration of a multi-robot system performing a manipulation task

The manipulators (depicted by the black boxes) grasp the rigid object (denoted by the black lines) firmly. All manipulators try to track their individual force/motion setpoints (denoted by the gray boxes) by means of their local feedback loops. Note that those setpoints do not necessarily need to comply with the object shape. However, due to the object rigidity, the manipulators are at any time of the manipulation task forced to maintain their initial relative positions (unless end effector slippage occurs or the object breaks). In case the manipulator setpoints do not match the object shape, the manipulator ensemble will be subject to constraining forces which ensure that the end effectors maintain the geometric constraint. From a system theoretic point of view, this means that each manipulator implements a local feedback loop but that the individual dynamics are *coupled through a kinematic constraint* (not through feedback as for conventional multi-agent systems).

Given this observation on the resulting system dynamics, one needs to check carefully to which extent a cooperative manipulator exhibits the features of a multi-agent system as discussed at the beginning of this section. Clearly, any manipulator ensemble complies with the requirement 1) since each manipulator is able to operate and manipulate objects autonomously. Moreover, each manipulator has a priori only access to its local sensing and actuation capabilities. This is in line with the requirement of each agent having only a local view on the system. Due to the rigid coupling of the manipulation dynamics, coordination strategies for cooperative multi-robot manipulation tasks are typically *centralized* in the sense that there exists a dedicated agent which generates the desired object motion and from which the individual manipulator setpoints are derived. The following section discusses the assumptions and implications of such centralized coordination strategies which will lead naturally to the challenges in cooperative manipulation tasks.

1.2 Challenges in cooperative manipulation tasks

A core challenge faced in today's robotics research is the realization of highly autonomous robot behavior in unstructured environments. This holds particularly true for cooperative multi-robot manipulation tasks in which accurate coordination among the robots is required but in which also direct interaction with a human takes place. In the context of manipulation tasks, the human safety, the design of interfaces for the information and signal exchange between humans and robots and the predictability of the robotic behavior are major prerequisites for a successful synergy of human and robot skills.

There exist a couple of challenges related to the autonomy of a cooperating multi-robot team when performing a manipulation task in an unstructured environment. The term unstructured shall refer to environments which are not modified in order to accommodate or compensate limitations of the robot [10]. In this sense, any model provided to the robotic manipulator system might be interpreted as an a priori knowledge about the manipulation task which needs to be adapted during the task execution as a function of the encountered task situation. The ability to incorporate updates on the task knowledge is crucial in order to keep a high level of autonomy for the robotic system. The particular challenges concerning the manipulation task model and occurring uncertainties are as follows.

Cooperative manipulator dynamics   Cooperative manipulation tasks are characterized by the tight coupling of the individual, commonly nonlinear manipulator and object dynamics. Traditionally, the interplay between the manipulators is coordinated in task space, i.e. the manipulator force/motion setpoints are derived from the desired object motion and its inertial properties. At the same time, existing modeling approaches for the cooperative manipulator dynamics are commonly derived in joint space. As a consequence, there is an obvious gap between the system theoretic modeling of the cooperative manipulator system in joint space and the available coordination and control strategies in task space. This clearly impedes a smooth and compact analysis of the interaction between plant and control dynamics. In fact, there is currently no analytic closed-form expression for the emerging end effector forces which is indisputably a crucial ingredient for the analysis of any manipulation task.

Dynamic force/motion tracking   As a direct consequence of the apparent gap between existing modeling approaches in joint space and control strategies in task space as described above, relevant ingredients for an accurate system analysis of the cooperative manipulator system are missing. So far, existing results on stability or tracking in task space are based on ad-hoc assumptions or involve limiting simplifications such as quasi-static manipulation of objects. Without an explicit closed-form expression for the emerging end effector forces at hand, central issues such as achieving force/motion tracking can not properly be discussed when aiming for general, dynamic manipulation tasks. Moreover, the apparent dynamic behavior of the manipulator ensemble is crucial when interacting with the environment in view of bounding the potential interaction forces. While in centralized control schemes this apparent dynamics is usually imposed, in manipulation tasks with decentralized coordination, one is clearly interested in finding and deriving the apparent,

global behavior from the local manipulator and object dynamics. There exists currently no methodology for this purpose. Eventually, the force tracking task is commonly split into the tracking of internal and external force components. However, this decomposition is not unique and it is controversially discussed in the literature.

Distributed coordinate knowledge A particular challenge arises from the fact that the coordination of cooperating manipulators is traditionally performed in a centralized fashion with access to a common coordinate system. This centralized approach to the problem of manipulator coordination works well for manipulation tasks in structured environments as e.g. dedicated laboratory spaces, in which each manipulator can be localized accurately. As an immediate consequence, any coordination approach based on a global reference frame neglects the autonomous character of the individual manipulators as represented by their distributed sensing, actuation and computation capabilities. In case no global coordinate frame is available for the task coordination, the cooperating manipulators are forced to employ potentially inaccurate on-board measurements of the relative kinematics between them. This leads inevitably to uncertainty in the relative grasp parameters and to undesired interaction forces which - in the worst case - might even destroy the manipulated object. Currently, there are no coordination schemes available which are able to exploit the distributed knowledge on the available coordinate systems in order to eliminate the fundamental dependency on a global coordinate frame.

Example Consider the cooperative aerial transportation task with three quadcopters depicted in Fig. 1.4.
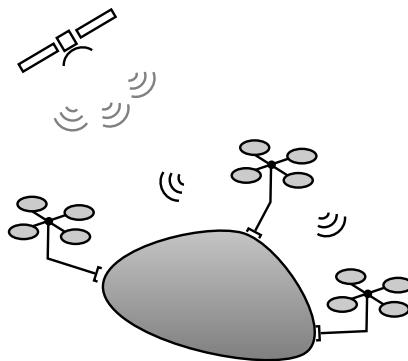
Fig. 1.4: Illustration of global and local localization systems for the coordination in a cooperative aerial manipulation task

In case of outdoor aerial manipulation, one potential global reference frame is provided by the global positioning system (GPS). This is depicted in Fig. 1.4 by the satellite, which makes it possible to locate all quadcopters in a common coordinate system (depicted by the gray localization signals). For indoor manipulation the same global localization mechanism applies when an optical, potentially marker-based tracking system is available. However, when such global localization is not available (or with limited accuracy as in the case of GPS), the cooperating manipulators need to rely on their local on-board sensing for measuring their relative position. This is depicted by the black localization signals in

Fig. 1.4. Obviously, it is desirable to employ coordination strategies which take into account the distributed character of the local on-board sensing and which are simultaneously able to deal efficiently with the arising uncertainty in the kinematic grasp parameters.

Remark   The challenges stated above are particularly relevant in conventional multi-robot manipulation tasks as e.g. cooperative manipulation of an object with several anthropomorphic or industrial manipulators. All of the named challenges are however also relevant to other domains in greater or lesser extent. While the cooperative manipulator dynamics and the force/motion tracking goal appear equally relevant for in-hand manipulation and thus for the grasping community, the distributed coordinate knowledge aspect is probably less significant in this domain since the individual fingers are mounted to a common base (the palm) providing a common coordinate system. In aerial manipulation tasks a proper dynamic modeling and efficient treatment of arising uncertainties due to inaccurate on-board sensing is again of prior importance. A similar situation is encountered in cooperative underwater manipulation tasks.

1.3 Outline and contributions

This thesis intends to provide a complete and physically consistent treatment of the dynamics in cooperative manipulation tasks with emphasis on the manipulator interaction when dealing with rigid objects and uncertainties in the kinematic grasp parameters for the manipulator coordination. Moreover, the present study tries to highlight the intersection and links between existing cooperative manipulation control schemes and particular coordination schemes developed within the framework of multi-agent theory.

To this end, the structure of this thesis is borrowed from the classical approach in control design, starting with the modeling of the cooperative manipulator dynamics in Chapter 2 followed by a thorough analysis of this model in Chapter 3. Chapter 4 formulates the general problem setting of cooperative force/motion tracking when no global localization system is available and presents an adaptive control approach which is able to deal with the arising uncertainties in the kinematic grasp parameters. Appendix A reviews and summarizes some basic concepts from adaptive control and system identification which are extensively used in Chapter 4. Conclusions of this study and potential future works are presented in Chapter 5.

The related work and open problems are reviewed in detail at the beginning of each chapter. The contributions of the individual chapters with respect to the challenges as previously presented in Section 1.2 are as follows.

Chapter 2: Modeling of the dynamics in cooperative manipulation tasks

This chapter develops one of the core results of this thesis by means of a complete dynamical model of the cooperating manipulators in task space incorporating both the constrained system kinematics and an analytic and explicit expression for the manipulators' interaction forces. The derivation of this result is based on Gauss' principle known from constrained

multi-body systems and highlights the significant role of the kinematic constraints imposed to the manipulator ensemble by firmly grasping a common object. The chapter presents a comprehensible methodology which links the dynamics of the individually feedback controlled manipulators in task space with the dynamics of the manipulated object. This new perspective on the cooperative manipulator system as a constrained multi-body system provides simultaneously a very convenient way for the simulation of multi-robot manipulator systems since it transforms the initial, implicit system description as a set of differential algebraic equations (DAE) to an explicit system model by means of a set of ordinary differential equations (ODE) which can be solved conveniently by standard engineering tools. The contributions of this chapter are based on [11].

Chapter 3: Analysis of the cooperative manipulator model

Based on the explicit cooperative manipulator model in task space as presented in Chapter 2, this chapter focuses on the system theoretic properties of the interaction dynamics. Given the non-ideal feedback linearization of individual manipulator control loops in practice, robust stability for the manipulator ensemble coupled through the object is derived. Simultaneously, the apparent dynamics of the cooperating manipulators when interacting with the environment is presented and evaluated in an experimental study. Eventually, the formulation of the cooperative manipulator system as constrained multi-body systems is exploited for introducing a new paradigm for the description of internal and external force components as needed for cooperative force/motion tracking. This new definition unites and generalizes previous results on force decomposition by invoking the principle of virtual work. As an immediate consequence of this model-based approach to the control design, a decoupled control scheme for simultaneous internal and external force/motion tracking is presented. The contributions of this chapter are based on [11], [12] and in parts on two of my students master's theses [13, 14].

Chapter 4: Adaptive control for cooperative multi-robot manipulation

This chapter deals with the cooperative manipulator coordination when no global localization frame is available and only estimates of the kinematic grasp parameters are at hand. First, the general problem setting is expressed as a robust force/motion control problem with respect to uncertain kinematic grasp parameters. An explicit condition for the identifiability of the kinematic grasp parameters are derived for the relevant special case of planar manipulation for which existing identifiability criteria do not apply. Finally, a robust control law for planar manipulation tasks is proposed which guarantees exponential force/motion tracking under initially biased grasp parameters in case the object's inertial forces remain small. The contributions of this chapter are in parts based on [15], [16] and previously unpublished material elaborated at least in parts during two consecutive research periods (January/February and May/June 2015) with Yiannis Karayiannidis at the Computer Vision and Active Perception Lab (CVAP) at KTH, Stockholm, Sweden.

2 Modeling of the dynamics in cooperative manipulation tasks

This chapter deals with the modeling of the dynamics in cooperative manipulation tasks. The employed dynamical model plays a vital role for system analysis and control design. The material presented in this chapter is consequently the foundation of this thesis. The cooperative manipulation task model derived in the sequel meets the two typically opposed requirements encountered in dynamical system theory: on the one hand, the abstract model should incorporate all characteristic features of the physical system. On the other hand, the model should remain simple and compact enough to facilitate system analysis and control design. The key result of this chapter is a physically consistent model of the cooperating manipulators, providing an explicit analytical expression for the emerging interaction forces and torques.

This chapter is structured as follows. First, the related work on dynamic modeling of cooperative manipulator system is reviewed and open problems are discussed. Subsequently, a general formulation of the manipulator dynamics in joint and task-space is presented in Section 2.1, while particular emphasis is put on impedance controlled end effectors. Section 2.2 briefly covers the rigid body dynamics of the manipulated object. Section 2.3 addresses the kinematic constraints which arise when the robotic end effectors are rigidly grasping the manipulated object. Finally, the dynamics of the cooperative manipulator system is derived in Section 2.4 wherein an explicit link between the kinematic constraints and the emerging interaction wrenches is drawn by means of the Gauss principle.

Related work and open problems

The dynamics of cooperative manipulator systems have been studied for more than three decades. A pioneering work on the dynamics of a robotic multi-arm system under motion constraints is given in [17]. The *augmented object model* describing the apparent dynamics of a cooperating manipulator system is presented in [18]. The authors of [19, 20, 21, 22] present a model of the cooperative manipulator dynamics illustrating the interaction effects in joint space. More recently, the modeling of the redundant manipulator dynamics are interpreted in the context of constrained multi-body systems [23, 24]. These previous works build on the formulation of the interaction dynamics in joint space without addressing relevant interaction effects between the manipulators in task space. In [25] the interaction between cooperative manipulators is modeled in task space by means of port-Hamiltonian systems without addressing the underlying Dirac structure. The Dirac structure however determines the interaction wrenches and is thus a central quantity for manipulation tasks. As will be detailed in the sequel, manipulation of a rigid object gives rise to kinematic constraints between the manipulators' end effectors, leading to an *implicit* port-Hamiltonian

system endowed with a Dirac structure and thus to a mixed set of differential and algebraic equations (DAEs) [26]. The Dirac structure induced from a constraint distribution may be represented in various ways [27] among which the Lagrange multiplier formulation is the most common. The Dirac structure and the underlying rigidity constraints between the end effectors have not been explored for the modeling of cooperating manipulators in the robotics literature. A general framework for simulating constrained multi-body systems based on a projection operator for control applications is presented in [28].

A very similar situation in view of modeling and control design is encountered in dexterous manipulation of objects with multi-fingered hands. Interestingly, common models for the dynamics in dexterous manipulation *do* actually incorporate the coupling between fingertips and object in terms of a kinematic (velocity) constraint [29]. The interaction wrenches between fingers and object have a straightforward interpretation as the Lagrange multiplier associated to the kinematic constraints [30]. However, inertia terms are neglected and quasi-static manipulation is assumed when computing explicit values for the resulting interaction wrenches. A notable exception is reported in [31], where a linearized and quasi-static (i.e. neglect of inertial terms) approximation of the cooperative dynamics is employed to compute explicit values for the Lagrange multipliers.

Recent works on cooperative aerial manipulation as e.g. [32] assume quasi-static manipulation or employ a dynamic manipulation task model for which the under-determined interaction forces are computed based on differential flatness conditions [33].

In summary, there exists currently no explicit closed-form solution for computing the manipulators' end effector wrenches in task space when cooperatively manipulating an object. It is obvious that such an expression is the core instrument for the analysis of cooperative manipulation tasks, since it allows to quantify the end effector wrenches applied to the object and provides insight on how the interaction between manipulators and object actually takes place.

2.1 Manipulator dynamics

This thesis foces on the dynamics and the interaction analysis of cooperative manipulators in task space. The dynamics of a single manipulator are however naturally expressed in joint and a desired end effector behavior in task space is rendered by means of an additional control loop. This section describes how to achieve a certain end effector behavior in task space for a single manipulator starting from the dynamics in joint space.

2.1.1 Joint space dynamics

A single robotic manipulator is composed of several mechanical links and joints which are additionally actuated in order to perform a desired task. The number of joints for the i-th manipulator is denoted by n_i. For each joint, the current position is commonly available through explicit measurement by means of a dedicated joint angle sensor while the actuation is implemented through an electric motor connected to a gear mechanism applying a desired force/torque about this joint. The stacked vector of joint angles and joint torques is denoted $\xi_i \in \mathbb{R}^{n_i}$ and $\tau_i \in \mathbb{R}^{n_i}$ respectively. Given the set of joint angles ξ_i, the

pose of the i-th end effector $x_i \in SE(3)$ is uniquely determined by the forward kinematics map $\Phi_i : \mathbb{R}^{n_i} \to SE(3)$ of the manipulator given by

$$x_i = \Phi_i(\xi_i). \tag{2.1}$$

Differentiation of (2.1) leads to a relation between the joint space velocities $\dot{\xi}_i \in \mathbb{R}^{n_i}$ and the resulting end effector velocity $\dot{x}_i \in se(3)$ according to

$$\dot{x}_i = J_i(\xi_i)\dot{\xi}_i \tag{2.2}$$

with the manipulator Jacobian J_i defined by

$$J_i(\xi_i) := \frac{\partial \Phi_i}{\partial \xi_i}. \tag{2.3}$$

The dynamics of robotic manipulators is most conveniently derived in joint space, meaning that the joint angles are employed as the (generalized) coordinates in the Lagrange formulation. The most general form of the manipulator dynamics is given by

$$\Lambda_i(\xi_i)\ddot{\xi}_i + \Gamma_i(\xi_i, \dot{\xi}_i) = \tau_i \tag{2.4}$$

wherein $\Lambda_i \in \mathbb{R}^{n_i \times n_i}$ is the symmetric positive-definite joint space inertia matrix and $\Gamma_i \in \mathbb{R}^{n_i}$ is a vector incorporating the Coriolis and gravity terms. In general, the matrix Λ_i and the vector Γ_i induce a coupling between the manipulator joints in terms of the apparent inertial properties and the Coriolis forces.

Joint space feedback control

In view of implementing a desired manipulator behavior independent of the current joint space configuration, feedback linearization is commonly applied which additionally decouples the individual joint variables. Choosing

$$\tau_i = \hat{\Lambda}_i(\xi_i)\mu_i + \hat{\Gamma}_i(\xi_i, \dot{\xi}_i) + \tau_i^d \tag{2.5}$$

with $\tau_i^d = 0_{n_i \times 1}$ and based on the estimates of the inertia matrix $\hat{\Lambda}_i$ and $\hat{\Gamma}_i$ respectively and substituting (2.5) in (2.4) yields the decoupled, second order joint space dynamics

$$\ddot{\xi}_i = \mu_i \tag{2.6}$$

for $\hat{\Lambda}_i = \Lambda_i$ and $\hat{\Gamma}_i = \Gamma_i$ and the new motion control input $\mu_i \in \mathbb{R}^{n_i}$.

Exemplarily, for motion control in joint space a PD-controller with feed forward term is implemented by letting

$$\mu_i = \ddot{\xi}_i^d + K_{P,i}(\xi_i^d - \xi_i) + K_{D,i}(\dot{\xi}_i^d - \dot{\xi}_i) \tag{2.7}$$

wherein $\xi_i^d(t)$ is the desired joint space trajectory and $K_{P,i}, K_{D,i} \in \mathbb{R}^{n_i \times n_i}$ are some positive-definite matrices. It is straightforward to verify that the tracking error $\tilde{\xi}_i = \xi_i^d - \xi_i$ satisfies

$$\ddot{\tilde{\xi}}_i + K_{D,i}\dot{\tilde{\xi}}_i + K_{P,i}\tilde{\xi}_i = \Lambda_i^{-1}\tilde{\tau}_i \tag{2.8}$$

when subject to a disturbance $\tilde{\tau}_i \in \mathbb{R}^{n_i}$, e.g. due to non-ideal feedback linearization. Under some mild assumptions on the smoothness of $\xi_i^d(t)$, the boundedness of Λ_i and finiteness of the Coriolis error term [34, (8.72) through (8.74)], one can still guarantee convergence of the tracking error to zero for $\hat{\Lambda}_i \neq \Lambda_i$ and $\hat{\Gamma}_i \neq \Gamma_i$ (cf. Lemma 3 in Section 3.5). Obviously, tracking in joint space is achieved exponentially for $\tilde{\tau}_i = 0_{n_i \times 1}$.

In case of contact with the environment, an arbitrary wrench applied to the i-th end effector $\tilde{h}_i \in se^*(3)$ induces a dynamically consistent joint-torque $\tilde{\tau}_i$ according to [35]

$$\tilde{\tau}_i = J_i^T(\xi_i)\tilde{h}_i. \tag{2.9}$$

Relation (2.9) is particularly useful in order to incorporate an additional feed forward term $\tau_i^d \neq 0_{n_i \times 1}$ on the right-hand side of (2.5) which accounts for a potential payload h_i^d attached to the i-th end effector. Letting $\tau_i^d = J_i^T(\xi_i)h_i^d$ guarantees exponential convergence of the joint space tracking error $\tilde{\xi}_i(t)$ even when a payload is attached to the robotic manipulator.

2.1.2 Task space dynamics

Given the manipulator dynamics in joint space, the emphasis is now put on the behavior of the end effector. The apparent inertia of the manipulator model (2.4) in task space $M_i^\Lambda \in \mathbb{R}^{6 \times 6}$ after arbitrary feedback design in terms of τ_i or μ_i, the apparent inertia of the end effector in task space is given by the symmetric positive-definite matrix [35]

$$M_i^\Lambda = [J_i(\xi_i) \, \Lambda_i^{-1}(\xi_i) \, J_i^T(\xi_i)]^{-1}. \tag{2.10}$$

This expression clearly shows that the inertial properties of the end effector depend on both the particular values of the joint space inertia Λ_i and on the current manipulator pose ξ_i. In view of the vast variety of potential manipulation tasks and the involved requirements on the manipulator dynamics, both dependencies of the apparent manipulator inertia M_i^Λ are generally undesired.

Task space feedback control

A common measure to overcome this limitation is the use of an additional, wrist-mounted force/torque sensor [36] measuring the end effector wrench h_i. Given h_i, an arbitrary stable filter can be employed to design the desired manipulator response in terms of the resulting, commanded end effector motion $\ddot{x}_i^*$. A widely used approach to this goal is impedance control, which enforces a relation between the applied end effector wrench h_i and the resulting end effector motion according to

$$M_i \, (\ddot{x}_i^* - \ddot{x}_i^d) + D_i \, (\dot{x}_i^* - \dot{x}_i^d) + h_i^K(x_i^*, x_i^d) = h_i - h_i^d + \tilde{h}_i \tag{2.11}$$

wherein $x_i^* = (p_i^{*T}, q_i^{*T})^T$ denotes the commanded pose of the i-th end effector. The pose is split into translational and rotational coordinates with $p_i^* \in \mathbb{R}^3$ and the unit quaternion $q_i^* \in \text{Spin}(3)$. Thus each x_i^* can be mapped onto an element of the special Euclidean group $SE(3)$. The twist $\dot{x}_i^* = (\dot{p}_i^{*T}, \omega_i^{*T})^T \in se(3)$ is composed of the end effector's translational and rotational velocity denoted by $\dot{p}_i^* \in \mathbb{R}^3$ and $\omega_i^* \in \mathbb{R}^3$. The wrench $h_i = (f_i^T, t_i^T)^T$

is split into the force and torque vectors $f_i, t_i \in \mathbb{R}^3$. Desired quantities are indicated by the superscript d. An additional disturbing wrench $\tilde{h}_i$ is labeled with the tilde.

Remark (Quaternion rates and angular velocity)   Employing a slight abuse of notation, the twist $\dot{x}_i$ is *not* the pure time derivative of the pose x_i, in particular $\frac{d}{dt} q_i \neq \omega_i$. In order to compute the proper angular velocity, the unit quaternion rate needs to be mapped to the angular velocity by the following relationship [37]

$$\begin{pmatrix} 0 \\ \omega_i \end{pmatrix} = \begin{bmatrix} \eta_i & -\epsilon_i^T \\ \epsilon_i & \eta_i I_3 + S(\epsilon_i) \end{bmatrix} \dot{q}_i \tag{2.12}$$

with the unit quaternion $q_i = (\eta_i, \epsilon_i^T)^T$ composed of real and imaginary part $\eta_i \in \mathbb{R}$ and $\epsilon_i \in \mathbb{R}^3$, respectively.

Without loss of generality, the impedance parameters, denoting the desired apparent mass, damping and stiffness of the end effector are assumed to exhibit (block-)diagonal structure, i.e.

$$M_i = \begin{bmatrix} m_i I_3 & 0_3 \\ 0_3 & \mathcal{I}_i \end{bmatrix}, \tag{2.13}$$

$$D_i = \begin{bmatrix} d_i I_3 & 0_3 \\ 0_3 & \delta_i I_3 \end{bmatrix}, \tag{2.14}$$

$$K_i = \begin{bmatrix} k_i I_3 & 0_3 \\ 0_3 & \kappa_i I_3 \end{bmatrix}, \tag{2.15}$$

decoupling the translational from the rotational end effector behavior. The matrices are parameterized by the scalar values $m_i, d_i, k_i \in \mathbb{R}^+$ yielding isotropic translational behavior of the individual end effector. Isotropic impedance parameters are assumed in order to simplify subsequent expressions for the cooperative manipulator system and keep a maximum level of clarity. $\mathbb{R}^+$ denotes the set of strictly positive real numbers. The rotational dynamics are determined by the positive definite inertia matrix $\mathcal{I}_i \in \mathbb{R}^{3 \times 3}$ and the scalar parameters $\delta_i, \kappa_i \in \mathbb{R}^+$.

The geometrically consistent stiffness h_i^K [38] in (2.11) (i.e. a stiffness matrix which results from a corresponding potential function in $SE(3)$, having thus a physical equivalent) is given by

$$h_i^K(x_i, x_i^d) = \begin{pmatrix} f_i^K \\ t_i^K \end{pmatrix} = \begin{pmatrix} [k_i I_3] \, \Delta p_i \\ [\kappa_i' I_3] \, \Delta \epsilon_i \end{pmatrix}, \tag{2.16}$$

wherein the difference of actual and desired pose is defined as $\Delta p_i = p_i - p_i^d$ and $\Delta q_i = q_i * (q_i^d)^{-1}$ with $\kappa_i' = 2\kappa_i \Delta \eta_i$. For notational convenience the quaternion expressing the relative orientation is further split into $\Delta q_i = \left(\Delta \eta_i, \Delta \epsilon_i^T \right)^T$.

The positive-definite impedance parameters $M_i, D_i \in \mathbb{R}^{6 \times 6}$ represent the apparent inertia, damping and stiffness of the end effector and can in general be chosen arbitrarily.

Depending on the actual implementation of the impedance control scheme in practice,

the choice of these values might be restricted in view of the closed-loop manipulator stability [39]. In what follows, the focus is exemplarily put on the implementation called position-based impedance control, in which the output $x_i(t)$ resulting from (2.11) is translated into a joint space trajectory after differentiation of (2.2) and employing a generalized inverse of the manipulator Jacobian J_i^+ according to [40]

$$\ddot{\xi}_i^* = J_i^+(\xi_i^*)(\ddot{x}_i^* - \dot{J}_i(\xi_i^*)\dot{\xi}_i^*) + [I_{n_i} - J_i^+(\xi_i^*)J_i(\xi_i^*)]\ddot{\xi}_i^{*0} \tag{2.17}$$

with an arbitrary joint acceleration vector $\ddot{\xi}_i^{*0} \in \mathbb{R}^{n_i}$ projected onto the null space of J_i. Note that tracking of ξ_i^* in joint space is subject to the error dynamics as presented in (2.8) and in case of $\tilde{\xi}_i \neq 0_{n_i \times 1}$ one has in general

$$x_i = \Phi_i(\xi_i) \quad \neq \quad x_i^* = \Phi_i(\xi_i^*). \tag{2.18}$$

In order to focus primarily on the interaction effects of the cooperative manipulator system, the following assumption is made.

Assumption 1 (Ideal single manipulator motion tracking)**.** *The joint space tracking error $\tilde{\xi}_i$ can be made arbitrarily small for each manipulator so that*

$$x_i(t) \approx x_i^*(t), \tag{2.19}$$

i.e. commanded and actual end effector pose coincide. Therefore, no distinction is drawn in the sequel between x_i^* and x_i and the asterix is omitted for notational convenience.

Assumption 1 holds obviously for ideal feedback linearization, i.e. $\hat{\Lambda}_i = \Lambda_i$ and $\hat{\Gamma}_i = \Gamma_i$ in (2.4) and (2.5), since a consistent feed forward term $\ddot{\xi}_i^*$ can be computed from $\ddot{x}_i^*$ and the control gains $K_{P,i}$ and $K_{D,i}$ can be made arbitrarily high, leading to exponential convergence of $\tilde{\xi}_i$ to zero. Note that this assumption does not imply congruence of x_i^*/x_i with the desired manipulator pose x_i^d.

Remark (Non-ideal feedback linearization)   The case of *non-ideal feedback linearization* and the resulting disturbances on the cooperative manipulation dynamics is discussed in the subsequent chapter in Section 3.5.

Generic representation of the task space dynamics

In view of the subsequent modeling of the interaction effects of the cooperative manipulator system, a generic description of the task space dynamics is of interest. For an arbitrary manipulator control scheme the resulting task space dynamics can be written in the form

$$M_i\ddot{x}_i = h_i^\Sigma + h_i, \tag{2.20}$$

wherein $h_i^\Sigma = h_i^\Sigma(x_i, \dot{x}_i, t)$ incorporates the specific structure of the applied manipulator control scheme and depends only on the manipulator state variables x_i, $\dot{x}_i$ and on time, e.g. through the desired trajectory $x_i^d(t)$.

Task space impedance control   Rewriting the task space impedance control law (2.11) in form of (2.20) yields

$$h_i^\Sigma = h_i^x - h_i^d + \tilde{h}_i \tag{2.21}$$

wherein all terms related to the kinematic motion control are combined into

$$h_i^x = M_i \ddot{x}_i^d - D_i[\dot{x}_i - \dot{x}_i^d] - h_i^K(x_i, x_i^d). \tag{2.22}$$

Finding similar representations for alternative force control schemes (e.g. PI force controller [41]) is straightforward whenever the end effector wrench h_i appears affine in the manipulator control law.

Task space tracking control   In this paragraph it is illustrated how to cast a pure motion control scheme into the generic form (2.20). Feedback linearization as in (2.5) combined with a PD tracking controller and feed forward acceleration term in task space [35] can be written as

$$h_i^\Sigma = M_i^\Lambda \left[\ddot{x}_i^d - K_{D,i}(\dot{x}_i - \dot{x}_i^d) - K_{P,i} \, \Delta x_i \right] \tag{2.23}$$

with the apparent inertia of the i-th end effector M_i^Λ as in (2.10), the difference of actual and desired pose $\Delta x_i = [\Delta p_i^T, \Delta \epsilon_i^T]^T$ as in (2.16) and the proportional and derivative control gains $K_{P,i}, K_{D,i} \in \mathbb{R}^{6\times 6}$. Although the tracking controller does not explicitly incorporate the end effector wrench h_i, the scheme can directly be interpreted by means of (2.20) by considering h_i as an externally applied disturbing end effector wrench. Note further that M_i^Λ is the apparent *physical* inertia, whereas M_i in (2.11) is a *virtual* and tunable parameter by means of the impedance control law. In case of the task space tracking controller (2.23), the virtual inertia M_i on the left-hand side of (2.20) needs to be replaced by the physical inertia M_i^Λ.

Remark (Alternative manipulator control schemes)   Although the focus is put in the sequel exemplarily on the case of ideal and non-ideal admittance (i.e. position-based impedance) control for the individual manipulator control loops, the generic representation of the interaction dynamics (2.20) is able to incorporate also force-based impedance control loops as e.g. presented in [42]. The mapping between forces and accelerations from joint space to task space is readily performed by employing the dynamically consistent (i.e. satisfying not only the kinematic projection but also providing a proper mapping between end-effector force/torque and joint torque vectors) Jacobians (and their inverses) as proposed in [35]. This allows to compute for any joint space controlled manipulator the end effector wrench h_i^Σ resulting from the individual control scheme in task space as required in (2.20).

2.2 Object dynamics

The equations of motion of a rigid object are derived by applying Lagrangian mechanics. The object's kinetic and potential energy are

$$T_o = \frac{1}{2}\dot{x}_o^T M_o \dot{x}_o \quad \text{and} \quad U_o = m_o \, g^T p_o \tag{2.24}$$

with $M_o = \text{diag}(m_o I_3, \mathcal{I}_o)$ and $m_o \in \mathbb{R}$ and $\mathcal{I}_o \in \mathbb{R}^{3\times3}$ are the object's mass and inertia respectively and $g \in \mathbb{R}^3$ is the gravity vector. For convenience of notation the explicit indication of dependencies such as $M_o(x_o)$ is omitted when unambiguous. Employing (2.24) for deriving the Lagrange equations yields the object dynamics w.r.t. its center of mass

$$M_o \ddot{x}_o + C_o \dot{x}_o + h_g = h_o + \tilde{h}_o \tag{2.25}$$

wherein h_o is the effective wrench acting on the object, $\tilde{h}_o$ is an additional, external disturbance and h_g and C_o incorporate the gravity force and the Coriolis term, i.e.

$$h_g = \begin{pmatrix} -m_o \, g \\ 0_{3\times1} \end{pmatrix} \, , \, C_o = \begin{bmatrix} 0_3 & 0_3 \\ 0_3 & \omega_o \times \mathcal{I}_o \end{bmatrix}. \tag{2.26}$$

The generic representation of the object dynamics is written as

$$M_o \ddot{x}_o = h_o^\Sigma + h_o \tag{2.27}$$

with

$$h_o^\Sigma = \tilde{h}_o - C_o \dot{x}_o - h_g. \tag{2.28}$$

2.3 Object manipulation and rigidity constraints

In this section, some fundamental properties of the manipulator kinematics are discussed when cooperatively holding a common object. For the subsequent analysis, the following assumption is made.

Assumption 2 (Object and grasp rigidity). *The manipulated object is assumed to be rigid and the end effectors are assumed to be rigidly connected to the object.*

Assumption 2 has two important consequences. On the one hand this means, that the deformation of the object is negligible throughout the manipulation task. Of course, there exists no ideally rigid object. However, from a practical point of view this assumption is well approximated as soon as the object stiffness exceeds the apparent stiffness of the end effectors. This manipulator stiffness can either be rendered by an appropriate control loop or might simply be the result of a finite structural stiffness of the manipulator construction components. On the other hand, based on Assumption 2, any end effector slippage is excluded, i.e. the individual grasp pose of the manipulators remains constant during the manipulation task. This assumption is more likely to be violated in practice. In Chapter 4

it is pointed out how to detect slippage and identify the modified grasp pose by means of an adaptive control scheme.

For the subsequent mathematical description of the manipulator and object kinematics, a coordinate system is attached to each rigid body. This is depicted in Fig. 2.1.
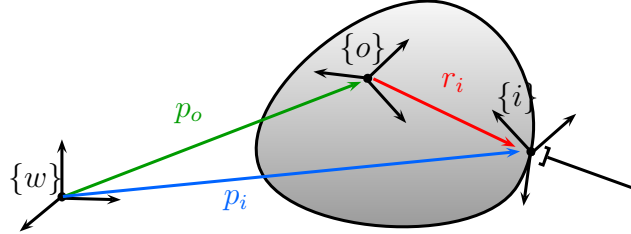
Fig. 2.1: Illustration of the coordinate systems employed for the cooperative manipulation task

The coordinate frames are denoted by curly brackets. Besides the body-fixed object frame $\{o\}$ each manipulator has its individual, local end effector frame $\{i\}$. If not stated otherwise (through a leading upper index) vectors are expressed in the (inertial) world frame $\{w\}$.

Translational constraint

The rigidity condition constrains the relative displacement of two bodies, i.e.

$$^{o}r_i = \text{const.} \tag{2.29}$$

This means that the relative position of the manipulator with respect to the body-fixed coordinate system $\{o\}$ remains constant. Using this fact one may express the position of the i-th end effector as

$$p_i = p_o +^{w} R_o(q_o)\ ^{o}r_i \tag{2.30}$$

with the 3×3 rotation matrix $^{w}R_o$ transforming a vector from frame $\{o\}$ to frame $\{w\}$. Differentiation of p_i and using $^{o}r_i = \text{const.}$ yields

$$\dot{p}_i = \dot{p}_o + \omega_o \times r_i. \tag{2.31}$$

Differentiating (2.31) again leads to

$$\ddot{p}_i = \ddot{p}_o + \dot{\omega}_o \times r_i + \omega_o \times (\omega_o \times r_i). \tag{2.32}$$

This latter condition constrains mutually the admissible accelerations of the object $\ddot{p}_o$, $\dot{\omega}_o$, the end effector $\ddot{p}_i$ and the object's angular velocity ω_o.

Rotational constraint

Furthermore the relative orientation between object and manipulators

$$^{o}\delta q_i = q_o^{-1} * q_i \tag{2.33}$$

is constrained to remain constant, i.e.

$$^{o}\delta q_i = \text{const.} \tag{2.34}$$

Differentiation of $^{o}\delta q_i$ w.r.t. time reveals that the angular velocity of the two bodies $\{o\}$ and $\{i\}$ needs to be equal [12, Lemma 1], so that

$$\omega_o = \omega_i. \tag{2.35}$$

Thus one has after differentiating again

$$\dot{\omega}_o = \dot{\omega}_i \tag{2.36}$$

imposing a constraint on the admissible angular acceleration of the object and the end effector.

Constraint matrix

In order to analyze the system dynamics under the previously discussed kinematic constraints, it is convenient to introduce the stacked state vector

$$x' = \begin{pmatrix} x_o \\ x_1 \\ \vdots \\ x_N \end{pmatrix} \tag{2.37}$$

being an element of the (N+1)-fold Cartesian product of $SE(3)$ and containing the stacked pose information of object and end effectors. The stacked acceleration vector $\ddot{x} \in \mathbb{R}^{6 \cdot (N+1)}$ reads thus

$$\ddot{x}' = \begin{pmatrix} \ddot{p}_o \\ \dot{\omega}_o \\ \ddot{p}_1 \\ \dot{\omega}_1 \\ \vdots \\ \ddot{p}_N \\ \dot{\omega}_N \end{pmatrix}. \tag{2.38}$$

The acceleration constraints (2.32) and (2.36) may be rewritten compactly as

$$A' \cdot \ddot{x}' = b' \tag{2.39}$$

with $A' \in \mathbb{R}^{6 \cdot N \times 6 \cdot (N+1)}$ and $b \in \mathbb{R}^{6 \cdot N}$ given by

$$A' = \begin{bmatrix} -I_3 & S(r_1) & I_3 & 0_3 & & 0_3 & 0_3 \\ 0_3 & -I_3 & 0_3 & I_3 & & 0_3 & 0_3 \\ \vdots & \vdots & & & \ddots & & \\ -I_3 & S(r_N) & 0_3 & 0_3 & & I_3 & 0_3 \\ 0_3 & -I_3 & 0_3 & 0_3 & & 0_3 & I_3 \end{bmatrix} \tag{2.40}$$

and

$$b' = \begin{pmatrix} S(\omega_o)S(\omega_o)r_1 \\ 0_{3\times1} \\ \vdots \\ S(\omega_o)S(\omega_o)r_N \\ 0_{3\times1} \end{pmatrix} \tag{2.41}$$

with $S(\cdot)$ denoting the skew-symmetric matrix performing the cross-product operation, i.e. $a \times b = S(a) \cdot b = -S(b)a$.

Remark (Alternative contact model) In case that the end effector contact is not rigid and e.g. relative angular motion between end effector and object is possible, the constraint formulation (2.39) remains valid while only the number of incorporated constraints is reduced in the contact model.

Remark (Inequality constraints) Note that the presented modeling incorporating equality constraints is valid for inequality constraints, too, as long as the applied end effector forces remain positive. Inequality constraints arise typically in dexterous manipulation tasks with unilateral finger contacts [43] or in aerial manipulation when cooperatively manipulating a cable-suspended load [33].

2.4 Cooperative manipulation dynamics

In this section the interaction dynamics of the cooperative manipulator system is derived when rigidly grasping a common object. In particular, an analytical closed-form expression for the emerging interaction wrenches is presented. The derivation is based on Newton's third law and the Gauss principle as applied for the analysis of constrained multi-body systems.

2.4.1 Principle of action and reaction

Whenever a manipulator is in rigid contact with the object and a wrench is applied by this manipulator, then due to Newton's third law, there is always a wrench with opposite sign acting on the object. For notational convenience, the actual wrenches acting on the object will be denoted $\bar{h}_i$ in the sequel, so that

$$\bar{h}_i = -h_i \quad \text{and} \quad \bar{h}_i^d = -h_i^d. \tag{2.42}$$

This situation is illustrated in Fig. 2.2.
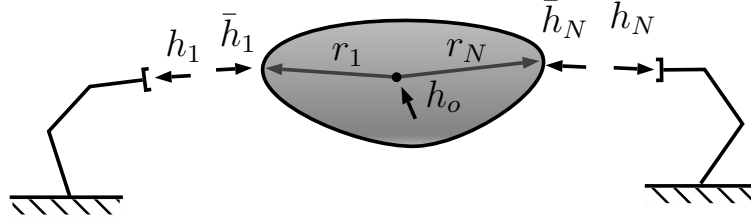
Fig. 2.2: Free-body diagram of the closed kinematic chain built by manipulators and object

To any wrench h_i acting on the end effector there is an opposed reaction $\bar{h}_i$ acting on the object. Note that the wrenches h_i are the end effector wrenches as potentially measurable by means of a wrist-mounted force/torque sensor (if available). However, in the sequel the primary interest is to find an analytical expression for the actual values of the interaction wrenches h_i. In view of any model-based (force feedback) control approach, this analytical expression for computing the h_i's is a prerequisite for a consistent analysis and control design.

While the h_i are a priori unknown, it is well known that once the h_i are known, the resulting object wrench h_o can be computed according to

$$h_o = G\bar{h} \tag{2.43}$$

with $\bar{h} = [\bar{h}_1, \ldots, \bar{h}_N]^T$. The grasp matrix G [44] incorporates explicitly the kinematic parameters defined via the constraints and are stacked into the parameter vector

$$r = \begin{pmatrix} r_1 \\ \ldots \\ r_N \end{pmatrix} \tag{2.44}$$

used in the definition of the grasp matrix

$$G = \begin{bmatrix} I_3 & 0_3 & \cdots & I_3 & 0_3 \\ S(r_1) & I_3 & \cdots & S(r_N) & I_3 \end{bmatrix}. \tag{2.45}$$

2.4.2 Gauss principle

This paragraph applies the Gauss principle to the combined system dynamics of manipulators and object in order to obtain an explicit expression for the interaction wrenches h_i. To this end, recall that the dynamics of the manipulators is imposed independently from each other through a control law given in the generic form (2.20), yielding an expression for h_i^Σ. The generic form of the object dynamics are given through (2.27) and determines h_o^Σ. Combining the dynamic equations of the end effectors and the object leads to the cooperative manipulator system representation

$$
\underbrace{\begin{bmatrix} M_o & & & \\ & M_1 & & \\ & & \ddots & \\ & & & M_N \end{bmatrix}}_{M'} \cdot \ddot{x}' = \underbrace{\begin{pmatrix} h_o^\Sigma \\ h_1^\Sigma \\ \vdots \\ h_N^\Sigma \end{pmatrix}}_{h'^\Sigma} + \underbrace{\begin{pmatrix} h_o \\ h_1 \\ \vdots \\ h_N \end{pmatrix}}_{h'}. \tag{2.46}
$$

Above representation admits the following interpretation. Since the stacked inertia matrix M' on the left-hand side of (2.46) is block-diagonal, the individual accelerations $\ddot{x}_o$ and $\ddot{x}_i$ of object and manipulators might appear decoupled. The wrenches h_o^Σ and h_i^Σ are clearly determined by the dynamics of object and manipulators and thus also independent from each other. However, the set of object and manipulator wrenches h_o and h_i is not independent from each other as pointed out earlier in (2.43). Moreover, as it is obvious from the previous section on the discussion on the kinematic constraints between end effectors and object, the individual accelerations of $\ddot{x}'$ are in fact not decoupled. Thus the only option for the coupled dynamics under the imposed kinematic constraints is that the vector h' adopts suitable values in order to render $\ddot{x}'$ compatible to the kinematic constraints (2.39).

The computation of the constraining wrench is a problem arising in the domain of constrained multi-body systems. In fact an explicit solution for h is presented in [45] given by

$$
h' = P'(b' - A'M'^{-1}h'^\Sigma) \tag{2.47}
$$

with $P' = M'^{\frac{1}{2}}(A'M'^{-\frac{1}{2}})^\dagger$ and $M' = \operatorname{diag}(M_o, M_1, \ldots, M_N)$. Given h' as above, the dynamics (2.46) can be interpreted as follows: the vector $h'^\Sigma := \left(h_o^\Sigma, h_1^\Sigma, \ldots, h_N^\Sigma\right)^T$ contains the wrenches resulting from the *local* system dynamics. The vector $h' := \left(h_o, h_1, \ldots, h_N\right)^T$ in turn results from the *global* interaction of all manipulators through the object. The vector h' thus adopts suitable values to render the accelerations $\ddot{x}$ on the left-hand side of (2.46) compatible to the constraint (2.39) at any time instant and for any given h'^Σ.

The derivation of h' is based on Gauss' principle of least constraint, which states that the acceleration of a constrained system is altered with respect to the acceleration of an equivalent unconstrained system such that the acceleration difference is minimal in the least-squares sense. The equivalent optimization problem is given by

$$
\min_{\ddot{x}'} \quad (\ddot{x}' - \ddot{x}'^\Sigma)^T M' (\ddot{x}' - \ddot{x}'^\Sigma) \tag{2.48}
$$
$$
\text{subject to} \quad A'\ddot{x}' = b'
$$

with $\ddot{x}'^\Sigma = M'^{-1}h'^\Sigma$ denoting the acceleration of the unconstrained system. The interpretation of the system dynamics (2.46) as the solution of a constrained optimization problem (2.48) admits interesting insights.

Arbitrary trajectories in terms of $x_i^d(t)$ may be specified *a priori* for each manipulator. The desired trajectories in combination with the desired end effector wrenches h_i^d determine unambiguously the virtual wrench vector h'^Σ as a function of the manipulator control laws. In case initially assigned trajectories are incompatible to the kinematically constrained

system, the emerging end effector wrenches h' render the system trajectory compatible to the imposed constraints by means of (2.47).

Discussion The cooperative manipulator dynamics (2.46) in combination with the Dirac structure represented by an explicit expression for the interaction wrenches h' in (2.47) constitutes for the first time a complete and physically consistent interaction model of the rigidly coupled manipulator system. Note that the vector h' in (2.46) contains the actual end effector wrenches h_1 to h_N as measurable by each manipulator by means of a wrist mounted force/torque sensor. The clear contribution of this modeling approach is that it provides a closed-form expression for *computing* the interaction wrenches instead of merely *measuring* them via force/torque sensors at the end effector. This is clearly a prerequisite for the consistent design of model-based force/torque controllers.

Example 1 (Load distribution). The following example illustrates the computation of the interaction wrenches as discussed previously and motivates simultaneously a more detailed analysis of the model as presented in the following chapters. Consider the following 1-dimensional cooperative manipulator scenario depicted in Fig. 2.3.
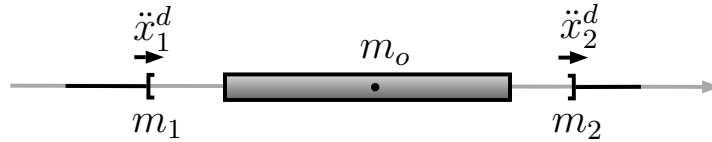
Fig. 2.3: Two cooperative manipulators handling a rigid object along one dimension

Two manipulators are coupled rigidly to a common object of mass m_o. In case of a simplified impedance control law (letting $K_i = D_i = 0$, i.e. only feed forward action), one has

$$h'^{\Sigma} = \begin{pmatrix} h_o^{\Sigma} \\ h_1^{\Sigma} \\ h_2^{\Sigma} \end{pmatrix} = \begin{pmatrix} 0 \\ m_1 \ddot{x}_1^d + \bar{h}_1^d \\ m_2 \ddot{x}_2^d + \bar{h}_2^d \end{pmatrix} \in \mathbb{R}^3 \tag{2.49}$$

The term $h_o^{\Sigma} \in \mathbb{R}$ is zero since the Coriolis term vanishes when manipulating along only one dimension. $h_1^{\Sigma} \in \mathbb{R}$ and $h_2^{\Sigma} \in \mathbb{R}$ contain the reduced impedance control law with feed forward acceleration term and desired forces $\bar{h}_1^d, \bar{h}_2^d \in \mathbb{R}$. Given a desired acceleration of the object $\ddot{x}_o^d \in \mathbb{R}$, a convenient choice for the manipulator setpoints is

$$\ddot{x}_1^d = \ddot{x}_2^d = \ddot{x}_o^d \tag{2.50}$$

and any distribution of the desired forces for $\alpha \in [0,1]$ which satisfies

$$\alpha \, \bar{h}_1^d + (1-\alpha) \, \bar{h}_2^d = h_o^d = m_o \ddot{x}_o^d. \tag{2.51}$$

In this example, the rigidity constraints impose $\ddot{x}_o = \ddot{x}_1 = \ddot{x}_2$, yielding

$$A' = \begin{bmatrix} 1 & -1 & 0 \\ 1 & 0 & -1 \end{bmatrix} \quad \text{and} \quad b' = \begin{pmatrix} 0 \\ 0 \end{pmatrix}. \tag{2.52}$$

It is now straightforward to compute the interaction wrenches. Explicit evaluation of (2.47) yields

$$h' = \begin{pmatrix} h_o \\ h_1 \\ h_2 \end{pmatrix} = \begin{pmatrix} m_o \ddot{x}_o^d \\ -\alpha \; h_o^d \\ -(1-\alpha) \; h_o^d \end{pmatrix}. \tag{2.53}$$

As expected, the object experiences the desired acceleration $\ddot{x}_o^d$ since $h_o = h_o^d = m_o \ddot{x}_o^d$. The end effector forces h_1 and h_2 depend on the actual implementation of the load distribution parameterized by α. However, one can still verify the validity of (2.43) since

$$h_o = -G \begin{pmatrix} h_1 \\ h_2 \end{pmatrix} \tag{2.54}$$

wherein the grasp matrix in this example is $G = \begin{bmatrix} 1 & 1 \end{bmatrix}$. Amongst others, this observation leads consequently to a more thorough analysis of potential load distributions for cooperative manipulation tasks.

Example 2 (Internal forces)**.** Note that in the previous example the setpoints for the desired motions (2.50) were compatible with the kinematic constraints in (2.52). In general, this might not always be the case. Consider in the following the modified motion setpoints of the manipulators according to

$$\ddot{x}_1^d = -\ddot{x}_2^d = \ddot{x}_{\text{int}}^d. \tag{2.55}$$

with an arbitrary value for $\ddot{x}_{\text{int}}^d \in \mathbb{R}$. Note that the desired accelerations of the two manipulators point in opposite direction, thus they tend to approach each other. In this example, it is further assumed that $m_1 = m_2 = m_{\text{int}}$, i.e. the two simplified impedance controllers feature the same gain. Analogue to the previous example, one has

$$h'^{\Sigma} = \begin{pmatrix} 0 \\ +m_{\text{int}}\ddot{x}_{\text{int}}^d \\ -m_{\text{int}}\ddot{x}_{\text{int}}^d \end{pmatrix} \in \mathbb{R}^3 \tag{2.56}$$

wherein the desired forces $\bar{h}_1^d$ and $\bar{h}_2^d$ are set to zero. Computation of the interaction wrenches in this example according to (2.47) yields

$$h' = \begin{pmatrix} h_o \\ h_1 \\ h_2 \end{pmatrix} = \begin{pmatrix} 0 \\ -m_{\text{int}}\ddot{x}_{\text{int}}^d \\ +m_{\text{int}}\ddot{x}_{\text{int}}^d \end{pmatrix}. \tag{2.57}$$

Since $h_o = 0$, the object remains at rest. Moreover, the end effector forces have the same magnitude but opposite signs. The result of this observation is that the object is subject to internal forces, namely a squeezing force of magnitude $m_{\text{int}}\ddot{x}_{\text{int}}^d$. The interaction wrenches as discussed in this chapter may thus contain motion-inducing components as well as internal wrench components. In the following chapter, a novel and more general approach to the characterization of internal wrenches is presented.

2.4.3 Comparison with previous approaches

The major difference of the presented modeling in this chapter with respect to existing approaches to the modeling of the cooperative dynamics in the literature is the focus on the task space dynamics only. In existing works, the cooperative dynamics are a mixture of joint and task space dynamics in the form of [34, Chapter 28, eq. (28.29)]

$$\begin{bmatrix} \Lambda(\xi) & 0 & J^T(\xi) \\ 0 & M_o(x_o) & -G \\ J(\xi) & -G^T & 0 \end{bmatrix} \begin{pmatrix} \ddot{\xi} \\ \ddot{x}_o \\ \lambda \end{pmatrix} = \begin{pmatrix} \tau - \Gamma \\ \dot{x}_o - C_o \\ b_\lambda \end{pmatrix} \tag{2.58}$$

with the stacked joint angle vector $\xi = (\xi_1^T, \dots, \xi_N^T)^T$, the stacked manipulator Jacobian $J = [J_1^T, \dots, J_N^T]^T$, the stacked joint space inertia matrix $\Lambda = \text{blockdiag}(\Lambda_1, \dots, \Lambda_N)$ and b_λ defined by

$$b_\lambda = [\frac{\partial(J\,\dot{\xi})}{\partial\xi}]\dot{\xi} - [\frac{\partial(G\,\dot{x}_o)}{\partial x_o}]\dot{x}_o. \tag{2.59}$$

In the cooperative dynamics model (2.58), λ contains the Lagrange multipliers associated to the kinematic constraint

$$\begin{bmatrix} J & -G^T \end{bmatrix} \begin{pmatrix} \dot{\xi} \\ \dot{x}_o \end{pmatrix} = 0. \tag{2.60}$$

Note that this constraint is a compact representation of the velocity constraints as presented in (2.31) and (2.35). In fact, under Assumption 2 (object and grasp rigidity), the Lagrange multipliers are equivalent to the end effector wrenches, i.e.

$$\lambda \equiv \begin{pmatrix} h_1 \\ \vdots \\ h_N \end{pmatrix} \tag{2.61}$$

but their computation is based on (2.59) and inversion of the matrix on the left-hand side of (2.58) which couples the variables $\ddot{\xi}$, $\ddot{x}_o$ and λ. Thus the effective value of λ can actually be computed by evaluating an expression which incorporates joint and task space quantities coupled through the kinematic constraint. As a consequence of the coupling between joint and task space, expression (2.59) in combination with (2.58) does not admit deeper insights on the origin and the characterization of the interaction wrenches. This is different for the expression of the end effector wrenches as provided in (2.47), where the dynamics of object and manipulators is projected onto the constrained manifold defined by the kinematic constraints. It is worth mentioning again that the right-hand side of (2.47) contains exclusively known task space quantities as e.g. the force/motion setpoints of the end effectors or the individual control gains but no joint space variables. Consequently, the analysis of the resulting end effector wrenches is greatly simplified (cf. the examples in the previous Section 2.4.2) which allows to focus on manipulator coordination strategies in task space as e.g. internal/external wrench control as described in the next chapter.

Summary and outlook

In this chapter a novel approach to the modeling of cooperative manipulator dynamics is introduced. The presented approach is characterized by a strict focus on the interaction effects of manipulators and object in task space. For computing the effective interaction wrenches between object and manipulators, the Gauss principle known from constrained multi-body systems is applied and the vital role of the imposed kinematic constraints is discussed. As an immediate result, an explicit closed-form expression for the interaction wrenches is derived.

The presented compact cooperative manipulator model in task space presents the basis for the subsequent analysis of control and coordination strategies. Moreover, it simplifies significantly the numerical simulation of multi-robot manipulation tasks since it transforms the initial model expressed as a differential algebraic equation (DAE) into an ordinary differential equation (ODE). This is clearly favorable in view of the reduced computational complexity in view of potential applications in real-time, model-based control algorithms.

3 Analysis of the cooperative multi-robot manipulation model

This chapter deals with the analysis of the dynamics of cooperative manipulators. Fundamental properties of the dynamic model presented in Chapter 2 are derived, which are relevant for the successful implementation of arbitrary manipulation tasks. The analysis includes a shift of paradigm for the computation of internal wrenches and is based on a novel, physically consistent definition of internal wrenches. Moreover, concise results on the stability of the interaction dynamics and model-based force/motion tracking are presented. A meaningful expression for the apparent dynamics of the object is derived when rigidly grasped by the manipulator ensemble. The chapter concludes with the analysis of the decoupling of internal/external wrench control schemes.

This chapter is structured as follows. First, the related work on load distribution and cooperative force/motion tracking is reviewed and open problems are discussed. Subsequently, an alternative definition and computation of internal wrenches based on the virtual work principle is presented in Section 3.1. As an immediate consequence of this definition, a more general approach to the load distribution problem is introduced in Section 3.2. A model-based force/motion tracking controller is presented in Section 3.3 and the apparent object dynamics is theoretically derived and experimentally evaluated in Section 3.4. Section 3.5 presents a robust stability result of the cooperative manipulator dynamics under inaccurate feedback linearization of the manipulators' joint space dynamics. Eventually, an internal wrench controller is proposed in Section 3.6 which provides a proper decoupling of internal and external wrench spaces consistent with the novel definition of internal wrenches presented in Section 3.1.

Related work and open problems

The related work on force/motion tracking in the robotics research is typically split into the two areas of internal/external wrench analysis and the cooperative control design. Therefore, the review of the related work is also divided into those two categories. As will become clear in the course of this chapter, the central link between both domains is given by the imposed kinematic constraints.

Internal wrench analysis and load distribution   The load distribution in robotic manipulation tasks is a particular input allocation problem [46], in which the redundant degrees of freedom for choosing the input can be given a meaningful interpretation in terms of motion-inducing components and internal wrenches applied to the object. A typical control goal in robotic manipulation tasks is the decoupled control of internal and external force/torque

components [47, 38, 48]. This topic has received quite some attention in the robotics literature. One of the first works addressing force control in a multi-manipulator setup is [49], resolving the load distribution problem by means of a linearly constrained quadratic optimization routine. A scalar weighting factor is introduced in order to balance between assigned end effector forces and torques, resulting in a weighted pseudoinverse for the load distribution problem. In [50] a definition of internal wrenches based on the principle of virtual work is provided without addressing the imposed kinematic constraints between object and manipulators. The authors of [51] claim that only a specific *non-squeezing* pseudoinverse avoids internal loading of the object. This particular load distribution is subsequently used for the analysis of interaction forces, i.e. the decomposition of manipulator forces/torques into internal and external components [52]. Recently, the authors of [53] challenged the result for the non-squeezing pseudoinverse in [51] and proposed to use the Moore-Penrose inverse instead. A common interpretation of internal loading is that the difference between two end effector forces projected onto their geometric connecting line does not vanish [52, 54]. However, it is not clear how to extend this concept in a meaningful way to describe internal torques. Beyond the scope of cooperative multi-robot manipulation, internal forces play a central role in the context of manipulation with multi-fingered robot hands [55]. A geometrically inspired definition of internal forces is presented in [56], trying to resolve inconsistencies occurring with the use of the pseudoinverse. An alternative characterization of internal forces is presented in [57] wherein the ensemble of manipulators is approximated as an articulated mechanism. Internal forces are interpreted as the actuator wrenches required to lock this mechanism. However, the influence of the applied end effector forces on the resulting torque is neglected. In summary, the complete characterization of internal forces *and* torques is still an open issue as well as suitable load distribution strategies that avoid internal wrenches applied to the object. The solution to the problem is essential for multi-robot manipulation. The need is particularly obvious in case of heterogeneous manipulators with different payload capacities, where the freedom to select a capacity compliant load distribution [58] is quintessential to solve the task.

Cooperative control design The control design for cooperative manipulation tasks is commonly performed in task space without explicitly addressing the coupling of the manipulator dynamics. Instead, the kinematic grasp parameters are used to compute the motion setpoints of the manipulators but no model for the resulting end effector wrenches and the resulting object trajectory is provided. Thus no conclusion of the system behavior under an infinitesimal disturbance of the manipulator coordination in task space is drawn. Based on the concept of impedance control [59], a cooperative control scheme realizing an apparent object impedance is proposed by the authors of [60] and [61]. A decentralized implementation of the object impedance scheme is presented in [62]. However, no expression for the resulting object impedance is provided. Recent publications on the control design for dexterous manipulation are either assuming quasi-static object manipulation [63] or specify the desired closed-loop behavior through *virtual* object dynamics [64] without explicit model of the interaction wrenches. Previous approaches to the force/motion control of cooperative manipulators [47, 38, 48] are not based on a complete model (i.e. including the end effector wrenches) of the interaction dynamics as presented in the previous Chap-

ter 2. As discussed previously, the cooperative dynamics can be written as an implicit port-Hamiltonian system [25]. In general the control design for implicit port-Hamiltonian systems is found to be non-trivial [65]. In [66] a differential geometric approach to the motion coordination of Lagrangian systems is presented which incorporates the kinematic constraints for the control synthesis, splitting the dynamics into a locked and a shape system. For the special case of two underactuated aerial manipulators a cooperative tracking control law based on an explicit internal force model is proposed very recently in [67]. In summary, there is currently no general methodology for the model-based control design for cooperative manipulators in task space which allows to analyze, derive and quantify relevant cooperative system properties such as robust stability or force/motion tracking.

3.1 Internal wrenches

This section focuses on the analysis of internal wrenches. Internal wrenches are end effector wrenches which do not contribute to the motion of the manipulated object but are sometimes required to achieve a stable grasp when grasp contacts are not rigid. A gentle squeezing of the object might be necessary to avoid slippage of the end effectors when contact points are subject to friction. However, in any manipulation scenario internal wrenches need to be limited to avoid damage of the object. Therefore, a consistent characterization of internal wrenches is mandatory.

3.1.1 Characterization of internal wrenches

Previously, internal wrenches were defined similarly in the area of cooperative manipulation [51] and grasping [68] as the components of the wrench vector h lying in the null space of the grasp matrix G. An alternative formulation of internal wrenches is proposed by means of the following definition.

Definition 1. *Internal wrenches are end effector wrenches for which the total virtual work is zero for any virtual displacement of the end effectors satisfying the kinematic constraints.*

This definition has some important consequences. One immediate observation is that internal wrenches do no work to the common object. That is, internal wrenches according to Definition 1 are not *motion-inducing* and are thus in line with the nomenclature in [51]. Note that in particular any wrench belonging to the null space of the grasp matrix G yields a total virtual work of zero for an arbitrary virtual displacement compatible with the constraints.

The most important difference of Definition 1 compared to previous definitions is that it is based on the kinematic constraints between the end effectors. The following theorem shows that the two formulations based on the virtual work principle and the null space of the grasp matrix are equivalent.

Theorem 1. *Under Assumption 2 and given a non-zero set of end effector wrenches h acting on the object, the following statements are equivalent:*

- *the wrenches h are internal according to Definition 1.*

- *the wrenches h belong to the null space of the grasp matrix G in* (2.45).

Proof. According to Definition 1, the virtual work of the set of internal wrenches h along the virtual end effector displacements δx compliant with the kinematic constraints is zero, i.e.

$$h^T \delta x = 0. \tag{3.1}$$

Given an infinitesimal displacement of the object δx_o, the infinitesimal displacement of the end effectors δx compliant to the kinematic constraints is obtained via (2.31) and (2.35), which can be rewritten as

$$\delta x = G^T \delta x_o. \tag{3.2}$$

Employing this fact in (3.1), one has

$$h^T \delta x = h^T G^T \delta x_o = (Gh)^T \delta x_o = 0, \tag{3.3}$$

Therefore, (3.3) holds for $Gh = 0_{6 \times 1}$. This means that the wrenches h are internal according to Definition 1 if and only if $h \in \mathrm{Ker}(G)$. □

This result illustrates that the virtual work principle is in accord with the previous definition of internal wrenches based on the null space of the grasp matrix. However, Definition 1 throws light on the significance of the kinematic constraints. Consideration of the kinematic constraint is crucial for the explicit computation of internal wrenches as discussed subsequently.

To this end, note that Definition 1 is consistent with the concept of constraining wrenches in the context of constrained multi-body systems [45]. It is well-known from Lagrangian mechanics that the total virtual work done by the constraining wrenches is zero. Internal wrenches can thus be interpreted as wrenches ensuring compliance of the manipulator motion to the imposed kinematic constraints.

3.1.2 Computation of internal wrenches

In the previous Chapter 2, the modeling of the cooperative manipulator system and the computation of the interaction wrenches is based on an augmented system description including the dynamics of manipulators *and* object. The computed *interaction wrenches h'* are the constraining wrenches for this augmented system as presented in (2.46), denoted by the apostrophe.

In this section, the constraining wrench formulation is again used for computing the *internal wrenches* h^{int}. This time, the constraining wrench are computed for the system incorporating only the dynamics of the manipulators *without* the object, yielding a physically consistent description of internal wrenches. This idea is illustrated in Fig. 3.1.
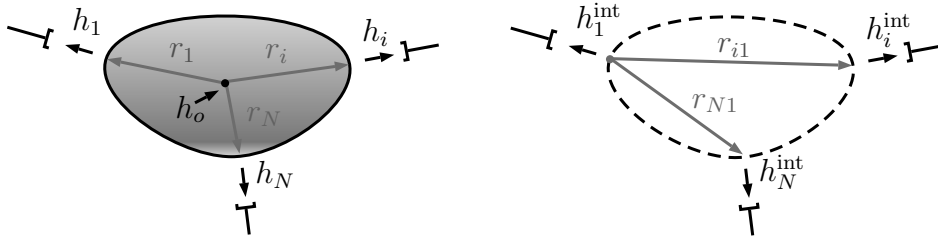
Fig. 3.1: Illustration of the constraining wrenches for the system of manipulators *plus* object and for the system of manipulators *without* object

On the left-hand side of Fig. 3.1 the system of manipulators *and* object is depicted. Computation of the constraining wrench for this system yields an expression for the wrench acting on the object h_o and the end effector wrenches h_i. Consequently, the end effector wrenches h_i comprehend the inertial effects related to the object dynamics. On the right-hand side of Fig. 3.1, the reduced system consisting of the manipulators only is depicted. Note that the relative kinematics between the end effectors is uniquely determined by means of the relative grasp parameters

$$\Delta r_{ij} = r_i - r_j \tag{3.4}$$

$\forall i \in \{1, \dots, N\} \backslash \{j\}$ for an arbitrary choice of $j \in \{1, \dots, N\}$. In Fig. 3.1, the case for $j = 1$ is depicted. The constraining wrench for the system of end effectors without object is identified with the internal wrenches as discussed in the sequel. It is intuitively clear that the internal wrenches h^{int} should not depend on the actual object dynamics. In fact, it is shown subsequently that internal wrenches depend exclusively on the motion setpoints of the end effector ensemble.

In order to quantify the internal wrenches arising in a cooperative manipulation task, reconsider the term h_i^x in (2.22) representing the motion controller of a single end effector. Alternatively, one can reformulate (2.22) on acceleration level by multiplying with M_i^{-1} from the left, yielding

$$\ddot{x}_i^x = \ddot{x}_i^d - M_i^{-1}\{D_i[\dot{x}_i - \dot{x}_i^d] + h_i^K(x_i, x_i^d)\}. \tag{3.5}$$

In case that no tracking error exists, i.e. $x_i(t) = x_i^d(t)$, the acceleration of the motion controller $\ddot{x}_i^x$ coincides with the desired acceleration $\ddot{x}_i^d$. Simultaneously, this means that the (virtual) spring and damper of this end effector are in rest position. In general however, the contributions from spring and damping elements need to be considered, too. The focus is now put on the case that the action of the motion controller is not compatible with the kinematic constraints. Such a situation is depicted in Fig. 3.2.

The set of the $\ddot{x}_i^x$ do not necessarily have to respect the kinematic constraints as depicted on the right-hand side of Fig. 3.2. However, the constraining wrenches h_i^{int} render the *actual* end effector accelerations $\ddot{x}_i$ compatible with the imposed constraints as depicted on the left-hand side of Fig. 3.2. This observation links the computation of internal wrenches closely to the kinematics of the cooperative manipulator system.

Fig. 3.2: Illustration of internal wrenches in a multi-robot manipulation task. The actual motion of the manipulators $\ddot{x}$ is the superposition of their motion controller acceleration $\ddot{x}^x$ and the interaction in terms of the internal wrenches h^{int}.

In order to quantify the constraining wrenches, the kinematic constraints in (2.32) and (2.36) are reformulated in matrix form as

$$A\ddot{x} = b \tag{3.6}$$

by letting $\ddot{x} = (\ddot{x}_1^T, \ldots, \ddot{x}_N^T)^T$, the matrix $A \in \mathbb{R}^{6(N-1) \times 6N}$

$$
A = \begin{bmatrix}
-I_3 & S(\Delta r_{21}) & I_3 & 0_3 & & & \\
0_3 & -I_3 & 0_3 & I_3 & & & \\
\vdots & \vdots & & & \ddots & & \\
-I_3 & S(\Delta r_{N1}) & & & & I_3 & 0_3 \\
0_3 & -I_3 & & & & 0_3 & I_3
\end{bmatrix}, \tag{3.7}
$$

with the relative grasp positions Δr_{ji} as in (3.4) and the vector $b \in \mathbb{R}^{6(N-1)}$ incorporating the centripetal terms

$$
b = \begin{pmatrix}
S(\omega_2)S(\omega_2)\Delta r_{21} \\
0_{3\times 1} \\
\ldots \\
S(\omega_N)S(\omega_N)\Delta r_{N1} \\
0_{3\times 1}
\end{pmatrix}. \tag{3.8}
$$

An explicit expression for the internal wrenches in the sense of Definition 1, result from a projection of the motion controller accelerations $\ddot{x}^x$ onto the kinematic constraints [45] according to

$$h^{\text{int}} = M^{\frac{1}{2}}(AM^{-\frac{1}{2}})^{\dagger}(b - A\ddot{x}^x) \tag{3.9}$$

with the matrix $M = \text{diag}(M_1, \ldots, M_N)$ incorporating the apparent inertia of the robotic end effectors in task-space. In fact, the kinematic error $e = b - A\ddot{x}^x$ indicates if the desired end effector accelerations $\ddot{x}^x$ violate the imposed kinematic constraint (3.6). Moreover, the constraining wrench h^{int} vanishes whenever the commanded acceleration of the manipulators is compatible with the kinematic constraints.

It remains to demonstrate that the internal wrenches computed according to (3.9) are in compliance with Definition 1. To this end, the following intermediate result is helpful.

Lemma 1. *Under Assumption 2, an equivalent expression for the internal wrenches* (3.9) *is given by*

$$h^{int} = A^T (AM^{-1}A^T)^{-1}(b - A\ddot{x}^x). \tag{3.10}$$

Proof. The proof is based on an explicit computation of the Moore-Penrose inverse $(AM^{-\frac{1}{2}})^\dagger$ in (3.9). Note that the Moore-Penrose inverse of a matrix X with full row rank is explicitly given by $X^\dagger = X^*(XX^*)^{-1}$ wherein X^* denotes the conjugate transpose of X. It is straightforward to show that A has full row rank since the kinematic constraints are (by construction) linearly independent. Moreover, M is square, symmetric and positive definite by construction and has consequently full rank. The same properties hold for $M^{-\frac{1}{2}}$. Thus it follows that [69, p. 88, (3.121)]

$$\mathrm{rank}(AM^{-\frac{1}{2}}) = \mathrm{rank}(A), \tag{3.11}$$

i.e. $AM^{-\frac{1}{2}}$ has full row rank. Explicit computation of $(AM^{-\frac{1}{2}})^\dagger$ and substitution in (3.9) yields immediately the result (3.10).

$\square$

Based on the interaction wrench formulation (3.10), the next fundamental result on internal wrenches is derived.

Theorem 2. *Under Assumption 2, the wrenches h^{int} given by* (3.10) *are internal according to Definition 1.*

Proof. In order to prove that h^{int} are internal wrenches in the sense of Definition 1, according to Theorem 1, it is sufficient to show that $h^{\mathrm{int}} \in \mathrm{Ker}(G)$. To this end, it can be shown that

$$\mathrm{Im}(A^T) \equiv \mathrm{Ker}(G) \tag{3.12}$$

which follows from combining

(i) the dimensions of $\mathrm{Im}(A^T)$ and $\mathrm{Ker}(G)$ coincide, since $\dim(\mathrm{Im}(A^T)) = 6(N-1)$ and by applying the rank-nullity theorem of linear algebra one has $\dim(\mathrm{Ker}(G)) = 6N - \dim(\mathrm{Im}(G)) = 6N - 6 = 6(N-1)$

(ii) the matrix product GA^T vanishes. Substitution of G in (2.45) and A^T in (3.7) yields

$$G\,A^T = \begin{bmatrix} \cdots & -I_3 + I_3 & 0_3 & \cdots \\ \cdots & -S(r_1) + S(\Delta r_{1j}) + S(r_j) & -I_3 + I_3 & \cdots \end{bmatrix} = 0_{6\times 6(N-1)}. \tag{3.13}$$

By definition in (3.4), $\Delta r_{1j} = r_1 - r_j$, and consequently $S(\Delta r_{1j}) = S(r_1) - S(r_j)$. Thus all elements of the matrix product GA^T are zero.

Given (3.12), it is now straightforward to verify that

$$G \, h^{\text{int}} = \underbrace{G \, A^T}_{0_{6 \times 6(N-1)}} (AM^{-1}A^T)^{-1}(b - A\ddot{x}^x) = 0_{6 \times 1} \tag{3.14}$$

and thus $h^{\text{int}} \in \text{Ker}(G)$. □

The computation of the internal wrenches as performed by means of (3.10) clearly constitutes a shift of paradigm for the analysis and computation of internal wrenches. This new perspective links the analysis of internal wrenches closely to the kinematic constraints imposed to the end effectors.

3.1.3 Comparison with previous approaches

Previously, the computation of internal wrenches was performed via a decomposition of the manipulator wrenches without incorporating the end effector kinematics. This former approach depends implicitly on a specific load distribution in terms of a generalized inverse of the grasp matrix G^+. This becomes clear as the internal wrench components are computed e.g. in [52] via

$$h^{\text{int}} = (I_{6N \times 6N} - G^+ G)h, \tag{3.15}$$

which is based on a particular wrench distribution G^+. Alternatively, one could also reformulate this approach as $h^{\text{int}} = h - h^{\text{ext}}$ with $h^{\text{ext}} = G^+ Gh$. As will be detailed in the next section of this chapter, there is no unique generalized inverse G^+ allowing a conclusion on the internal components. Thus the previous approach in (3.15) for computing the internal wrenches is in fact assuming a particular distribution for the external end effector wrenches h^{ext} and is computing the internal components h^{int} subsequently.

A more general and physically consistent characterization of internal wrenches results from incorporating the end effector kinematics by means of $\ddot{x}^x$ for computing the internal components h^{int} as presented in (3.10).

Remark (Internal stress) In continuum mechanics, internal stress is defined as the contact force between neighboring particles inside a solid body. In the scope of the analysis of cooperating manipulators one is not interested in the actual stress distribution *inside* the commonly manipulated object - internal stress occurs even when manipulating a rigid object with a single end effector and can thus not be avoided.

3.2 Load distribution

With the physically consistent characterization of internal wrenches according to Definition 1 in the previous section, the focus is now shifted on the load distribution in cooperative manipulation tasks. The load distribution allocates suitable force and torque setpoints to an ensemble of manipulators in order to implement a desired action on the manipulated object. Mathematically, this is equivalent to finding an inverse expression for the grasp

matrix G in (2.43). More precisely, given a desired wrench applied to the object h_o^d, one would like to resolve the intrinsic redundancy in

$$\begin{pmatrix} \bar{h}_1^d \\ \vdots \\ \bar{h}_N^d \end{pmatrix} = G^+ h_o^d \tag{3.16}$$

by means of a suitably parameterized generalized inverse G^+. In particular, one is interested in finding all load distributions which are free of internal wrenches according to Definition 1. This leads to the major result of this section.

Theorem 3. *Under Assumption 2, the load distribution given by*

$$G_M^+ = \begin{bmatrix} m_1^*[m_o^*]^{-1}I_3 & m_1^*[J_o^*]^{-1}S(r_1)^T \\ 0_3 & J_1^*[J_o^*]^{-1} \\ \vdots & \vdots \\ m_N^*[m_o^*]^{-1}I_3 & m_N^*[J_o^*]^{-1}S(r_N)^T \\ 0_3 & J_N^*[J_o^*]^{-1} \end{bmatrix} \tag{3.17}$$

for some positive-definite weighting coefficients $m_i^* \in \mathbb{R}$ and $J_i^* \in \mathbb{R}^{3\times3}$ with

$$m_o^* = \sum_i m_i^* \tag{3.18}$$

$$J_o^* = \sum_i J_i^* + \sum_i S(r_i)m_i^*S(r_i)^T, \tag{3.19}$$

and

$$\sum_i r_i m_i^* = 0_{3\times1} \tag{3.20}$$

is free of internal wrenches applied to the object according to Definition 1.

Proof. The proof is based on a particular parameterization of the generalized inverse of the grasp matrix. This parameterization appears naturally when considering the dynamics of a *virtual* end effector system subject to the kinematic constraints and allows to give these parameters the meaning of virtual masses and inertias. With h_o^d in hand, one readily computes the resulting virtual acceleration $\ddot{x}_o^*$ which the object would experience if it had the mass m_o^* and inertia J_o^* under the assumption that only the desired wrench h_o^d was acting on the object. This is done by inverting

$$\begin{bmatrix} m_o^*I_3 & 0_3 \\ 0_3 & J_o^* \end{bmatrix} \ddot{x}_o^* = h_o^d. \tag{3.21}$$

With this virtual object acceleration $\ddot{x}_o^*$ it is possible to conclude on the (virtual) acceleration of the attached end effectors $\ddot{x}_i^*$ by employing the kinematic constraints (2.32) and (2.36). By assigning now virtual inertias m_i^* and J_i^* to the i-th end effector, it is straightforward to compute the required wrench $\bar{h}_i^d$ inducing the virtual end effector acceleration

$\ddot{x}_i^*$ according to

$$\bar{h}_i^d = \begin{bmatrix} m_i^* I_3 & 0_3 \\ 0_3 & J_i^* \end{bmatrix} \ddot{x}_i^*. \tag{3.22}$$

So far, all occurring virtual inertias and thus the individual manipulator wrenches $\bar{h}_i^d$ are undetermined. However, any admissible load distribution should satisfy (2.43), i.e. $h_o^d = G\bar{h}^d$ being equivalent to the individual conditions on the desired object force $f_o^d = \sum_i \bar{f}_i^d$ and the desired object torque $t_o^d = \sum_i \bar{t}_i^d + \sum_i r_i \times \bar{f}_i^d$. Substituting (3.21) and (3.22) for the force components and employing (2.32) leads to

$$m_o^* \ddot{p}_o^* = \sum_i m_i^* \left[\ddot{p}_o^* + \dot{\omega}_o^* \times r_i + \omega_o^* \times (\omega_o^* \times r_i) \right] . \tag{3.23}$$

Comparing the coefficients of $\ddot{p}_o^*$ immediately yields $m_o^* = \sum_i m_i^*$. Since $\dot{\omega}_o^*$ (and ω_o^*) can take arbitrary values, the virtual masses need to respect $\sum_i r_i m_i^* = 0_{3\times 1}$ in order to cancel the terms involving $\dot{\omega}_o^*$ and ω_o^* in (3.23). Considering the torque components in (2.43) and again substituting (3.21) and (3.22) combined with (2.32) and (2.36) one has

$$J_o^* \dot{\omega}_o^* = \sum_i J_i^* \dot{\omega}_o^* + \sum_i r_i \times m_i^* [\ddot{p}_o^* + \dot{\omega}_o^* \times r_i + \omega_o^* \times (\omega_o^* \times r_i)]. \tag{3.24}$$

Comparing coefficients yields $J_o^* = \sum_i J_i^* + \sum_i S(r_i) m_i^* S(r_i)^T$ wherein the cross-product is expressed in terms of skew-symmetric matrices. The term involving $\ddot{p}_o^*$ on the right-hand side of (3.24) vanishes (since $\sum_i r_i m_i^* = 0_{3\times 1}$) so that only the additional term $\sum_i r_i \times m_i^* [\omega_o^* \times (\omega_o^* \times r_i)]$ remains. Recall that (3.21) determines solely a *virtual* object acceleration due to h_o^d at a specific time instant but no information about the object's virtual velocity is available. In order to obtain an admissible load distribution satisfying (2.43), a convenient choice is thus $\omega_o^* = 0_{3\times 1}$ which eliminates the impact of the virtual product of inertia-like term. Note that this does not mean that the manipulated (physical) object needs to be at rest since $\ddot{x}_o^*$ is in general different from the object's *actual* acceleration (and velocity). The choice for the object's virtual velocity $\omega_o^* = 0_{3\times 1}$ is arbitrary and simply ensures that at one specific time instant and a given h_o^d, an admissible set of end effector wrenches $\bar{h}_i^d$ is computed - completely independent from the actual object dynamics. By construction, the total virtual work done by the end effector wrenches is non-zero for any virtual displacement satisfying the constraints. The load distribution is thus free of internal wrenches according to Definition 1.

$\square$

Note that the weighting coefficients m_i^* and J_i^* (and consequently m_o^* and J_o^*) do have the meaning of inertial parameters but they are abstract parameters. They are exclusively used to parameterize the generalized inverse G_M^+ for the purpose of load distribution but they do not characterize the inertial properties of the manipulated object. A particular choice of these weighting coefficients leads to an explicit expression for the Moore-Penrose inverse of the grasp matrix.

Corollary 1. *An equal distribution of the manipulator weights according to $m_i^* = 1$ and $J_i^* = I_3$ yields*

$$G^\dagger = \frac{1}{N} \begin{bmatrix} I_3 & \bar{J}^{-1} S(r_1)^T \\ 0_3 & \bar{J}^{-1} \\ \vdots & \vdots \\ I_3 & \bar{J}^{-1} S(r_N)^T \\ 0_3 & \bar{J}^{-1} \end{bmatrix} \tag{3.25}$$

with $\bar{J} = I_3 + \frac{1}{N} \sum_i S(r_i) S(r_i)^T$ and (3.25) being equivalent to the Moore-Penrose inverse of G.

Proof. The Moore-Penrose inverse of a matrix might be interpreted as the solution to a quadratic programming problem with equality constraint. Thus the load distribution problem is reformulated as

$$\min_{h^d} \|\bar{h}^d\|^2. \tag{3.26}$$
$$\text{s.t.} \quad h_o^d = G\bar{h}^d$$

An explicit, analytical solution to this optimization problem can be obtained by computing the Schur complement

$$\bar{S} := GG^T = N \begin{bmatrix} I_3 & 0_3 \\ 0_3 & I_3 + \frac{1}{N} \sum_i S(r_i) S(r_i)^T \end{bmatrix} \tag{3.27}$$

which is used for computing the desired mapping

$$\bar{h}^d = G^T \bar{S}^{-1} h_o^d. \tag{3.28}$$

By definition the Moore-Penrose inverse is equivalent to the solution of the minimization problem (3.26) such that

$$G^\dagger = G^T \bar{S}^{-1}. \tag{3.29}$$

Straightforward computation of $G^T \bar{S}^{-1}$ reveals equivalence of this expression to (3.25). $\square$

Clearly, there exist not a single load distribution free of internal wrenches but a set of load distributions avoiding application of internal wrenches to the object. This is in line with the observations from the previous Example 1 in Chapter 2, where the interaction wrenches required to manipulate the object were balanced between two end effectors while avoiding entirely internal wrenches. A more detailed discussion of the load distribution presented in Theorem 3 and its implications is given in the subsequent examples.

Example 3 (Heterogeneous load distribution)**.** In this example, a heterogeneous load distribution is analyzed and the non-squeezing property is further stressed. To this end, consider the one-dimensional multi-robot manipulation example depicted in Fig. 3.3, wherein two manipulators cooperatively move an object in the horizontal direction.
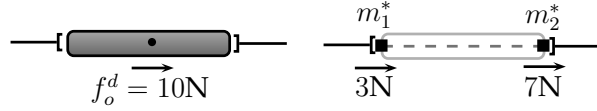
Fig. 3.3: Two cooperating manipulators moving a rigid object in one dimension.

The force distribution indicated at the right-hand side of Fig. 3.3 results obviously in the desired object force f_o^d. The relevant question is if the load distribution contains internal forces applied to the object. In contrast to previous results [51, 52, 53] it becomes obvious that in this case there is not necessarily an internal wrench applied to the object: Both end effector forces contribute entirely to the desired motion of the object and thus no internal wrench is present. Existing criteria [51, 53] for the analysis of internal wrenches yield an internal force component of $\pm 2N$ for the force distribution in Fig. 3.3. This is due to the fact that a specific (an equal) distribution of manipulator forces is assumed implicitly by using e.g. $G^\dagger$ for the computation of internal and external wrenches by means of (3.15). By letting $m_1^* = 3$kg and $m_2^* = 7$kg in (3.17), the force distribution indicated in Fig. 3.3 is obtained. Note that this one-dimensional example is equivalent to manipulating a point mass and condition (3.20) is trivially met through choosing $r_1 = r_2 = 0_{3 \times 1}$ for any values of m_1^* and m_2^*. By considering an infinitesimal displacement of the end effectors along the horizontal axis it becomes obvious that the total virtual work done is non-zero and the load distribution is free of internal wrenches.

For the current example this means that no internal wrenches are applied to the object as long as both manipulators agree and move with a common desired acceleration $\ddot{x}_o^d$ while applying the indicated end effector forces. In order to conclude consistently on the existence of internal wrenches, the end effector kinematics need to be evaluated by means of (3.9). This observation is in contrast to the results in [51, 52] where the difference in the applied force of two manipulators projected onto their connecting line was used to conclude on internal loading.

Example 4 (Balancing for load distribution). This example stresses further that there exists no unique load distribution free of internal wrenches. Consider the multi-robot manipulation setup depicted in Fig. 3.4.
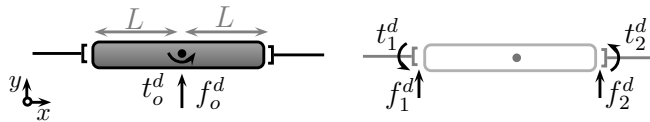
Fig. 3.4: Load distribution example for two cooperating manipulators.

This time a desired torque about the axis perpendicular to the paper plane is implemented, i.e. only $t_{o,z}^d = \tau$ in the desired object wrench h_o^d. The load distribution according to the Moore-Penrose inverse $G^\dagger$ in (3.25) gives for $\tau = 1$Nm and $L = 1$m

$$\bar{f}_{1,y}^d = -\bar{f}_{2,y}^d = -\frac{1}{4}\text{N} \quad , \quad t_{1,z}^d = t_{2,z}^d = \frac{1}{4}\text{Nm}. \tag{3.30}$$

The choice of $m_i^* = 4$ and $J_i^* = I_3$ for the load distribution by means of G_M^+ in (3.17) gives

$$\bar{f}_{1,y}^d = -\bar{f}_{2,y}^d = -\frac{4}{10}\text{N} \quad , \quad t_{1,z}^d = t_{2,z}^d = \frac{1}{10}\text{Nm}. \tag{3.31}$$

The load distribution obtained by the modified, non-unitary weights yields a wrench distribution which demands a smaller torque to be applied by the robotic end effectors but leads to an equivalent object wrench. The ratio between the resulting inertial parameters m_o^* and J_o^* in (3.18) and (3.19) can be used to tune the amount of the resulting object torque t_o^d that is either produced by end effector forces $\bar{f}_i^d$ acting over a lever r_i, or by direct application of the end effector torques $\bar{t}_i^d$. It is worth noticing that the wrench distribution (3.31) does not induce internal wrenches at the object. As a limit case for $J_i^* \to 0_3$, the desired object torque t_o^d is exclusively produced by the desired end effector forces $\bar{f}_i^d$ and the allocated end effector torques are zero, i.e. $\bar{t}_i^d = 0_{3\times1}$.

3.3 Cooperative force/motion tracking

Based on the previous discussion on internal wrenches and load distributions, a fundamental result on force/motion tracking for the cooperative manipulator ensemble is presented in this section . With the desired motion of the object $\dot{x}_o^d$ in hand, the desired motion of the end effectors $\dot{x}_i^d$ is unambiguously determined by the following relation

$$\dot{x}^d = G^T \dot{x}_o^d, \tag{3.32}$$

with $\dot{x}^d = [(\dot{x}_1^d)^T, \ldots, (\dot{x}_N^d)^T]^T$ which is essentially a reformulation of the kinematic constraints presented in (2.32) and (2.36) at velocity level.

Remark (Motion setpoint computation) Based on $\dot{x}_i^d$, each manipulator is able to compute $\ddot{x}_i^d$ and x_i^d in its local end effector frame by proper derivation/integration of the desired velocity. Equivalently, the desired trajectory x_i^d can locally be computed by double integration of $\ddot{x}_i^d$.

Combining the kinematic coordination (3.32) with any suitable load distribution according to (3.17) achieves cooperative force/motion tracking as stated in the following theorem.

Theorem 4. *Consider the object dynamics (2.25) without disturbance $\tilde{h}_o = 0_{6\times1}$ and ideal feedback linearization $\tilde{h}_i = 0_{6\times1}$ in (2.11). Further assume that the object's inertia M_o and the grasp matrix G are known and that Assumptions 1 and 2 hold. Then the combined dynamic and kinematic coordination strategies in (3.16) and (3.32) achieve tracking, i.e.*

$$h_o(t) \equiv h_o^d(t) \quad and \quad \dot{x}_o(t) \equiv \dot{x}_o^d(t) \tag{3.33}$$

for the cooperative manipulation task without applying internal wrenches according to Definition 1.

Proof. Ideal kinematic coordination of the manipulators according to (3.32) means that $\forall i : x_i(t) = x_i^d(t)$ which implies $\dot{x}_i = \dot{x}_i^d$ and $\ddot{x}_i = \ddot{x}_i^d$ in compliance with the kinematic constraints by construction. Using this fact in (2.11) (or in any other force/motion control

scheme) one has immediately $h_i = h_i^d$ and $\bar{h}_i = \bar{h}_i^d$ respectively. Combining (2.43) and (3.16) leads to an explicit expression for the object wrench h_o in (2.25) as

$$h_o = GG_M^+ h_o^d. \tag{3.34}$$

By definition GG_M^+ is the identity matrix. Substituting this result in the object dynamics (2.25) and choosing $h_o^d = M_o \ddot{x}_o^d + C_o(x_o^d, \dot{x}_o^d) \dot{x}_o^d$ yields $\ddot{x}_o(t) = \ddot{x}_o^d(t)$ and thus $x_o(t) = x_o^d(t)$ for $x_o^d(0) = x_o(0)$ and $\dot{x}_o^d(0) = \dot{x}_o(0)$. No internal wrenches are applied to the object since the desired motion of the manipulators is by construction compatible to the kinematic constraints. Mathematically, this can be verified by employing $\ddot{x}'^x = \ddot{x}^d$ in (3.9) from which follows $h'_{\text{int}} = 0_{6 \times 1}$. $\qquad\square$

This result gives insight to the fundamental characteristics of a cooperative manipulation task. In general it is not sufficient to choose a suitable load distribution strategy for the manipulator ensemble but the effective end effector motions need to be kinematically compatible to the imposed constraints, too. The control strategy of Theorem 4 achieves tracking and is essentially an inverse dynamics controller for the interaction dynamics model as given through (2.46) and (2.47) with respect to the manipulated object. The corresponding block scheme is depicted in Fig. 3.5.
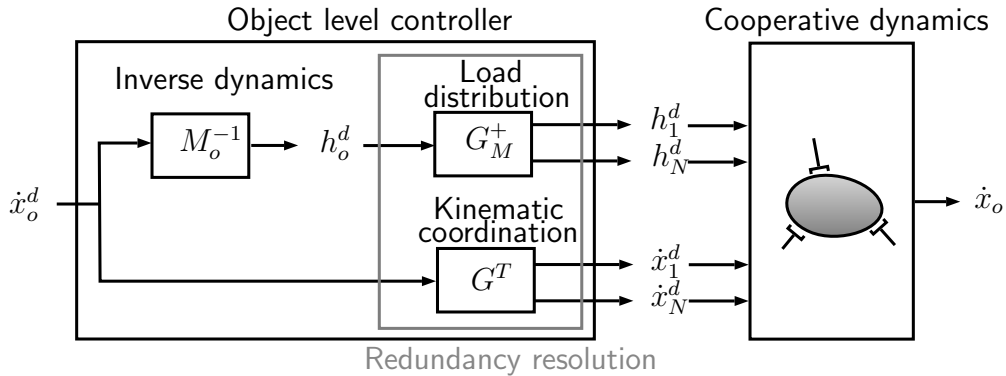
Fig. 3.5: Block scheme representation of controller and plant dynamics for cooperative force/motion tracking

From the desired object motion $\dot{x}_o^d$, the desired object wrench h_o^d is computed by means of the (inverse) dynamics given in (2.25). The load distribution allocates suitable end effector wrenches h_i^d while the kinematic coordination computes suitable motion setpoints for the individual manipulators. In this context, the coordination strategies (3.16) and (3.32) can be interpreted as a dynamically consistent redundancy resolution for the manipulator ensemble. The actual manipulator and object dynamics are contained in the *Cooperative dynamics* block as described in Chapter 2, i.e. in particular the system representation (2.46) and (2.47).

3.4 Apparent object dynamics

In this section the apparent object dynamics with respect to a disturbing wrench is derived. This behavior is particularly relevant whenever contact with the environment occurs during

the manipulation task. In case of impedance controlled end effectors, it turns out that the object behavior can again be characterized by an equivalent impedance in the form of (2.11) if the manipulators compensate the object's inertial effects.

Theorem 5. *Consider the impedance controlled end effector dynamics (2.11) with ideal feedback linearization, i.e. $\tilde{h}_i = 0_{6\times 1}$, and assume the manipulator ensemble to compensate the gravity force of the object, i.e. $h_o^d = h_g$ in (3.16) and with h_g from (2.26). Assume further that Assumptions 1 and 2 hold. Then the apparent dynamics of the cooperative manipulator system with respect to a disturbance $\tilde{h}_o$ in (2.25) is given by*

$$\mathcal{M}\ddot{x}_o + \mathcal{D}\dot{x}_o + h_o^K(x_o, x_o^d) + \mathcal{C}_o\dot{x}_o = \tilde{h}_o. \tag{3.35}$$

The apparent inertia $\mathcal{M}$, damping $\mathcal{D}$ and stiffness h_o^K are

$$\mathcal{M} = \begin{bmatrix} (m_o + \sum_i m_i)I_3 & \sum_i m_i S^T(r_i) \\ \sum_i S(r_i)m_i & \mathcal{J} \end{bmatrix} \tag{3.36}$$

with $\mathcal{J} := J_o + \sum_i J_i + \sum_i S(r_i)[m_i I_3]S^T(r_i)$,

$$\mathcal{D} = \begin{bmatrix} (\sum_i d_i)I_3 & \sum_i d_i S^T(r_i) \\ \sum_i S(r_i)d_i & \sum_i \delta_i + \sum_i S(r_i)[d_i I_3]S^T(r_i) \end{bmatrix} \tag{3.37}$$

and

$$h_o^K(x_o, x_o^d) = \sum_{i=1}^N \{ \begin{bmatrix} k_i I_3 & 0_3 \\ \Xi_i & \kappa_i' I_3 \end{bmatrix} \begin{pmatrix} \Delta p_o \\ \Delta \epsilon_o \end{pmatrix} \} \tag{3.38}$$

with the coupling terms $\Xi_i \in \mathbb{R}^{3\times 3}$ defined by $\Xi_i := S^T(r_i)k_i$. For an infinitesimal twist displacement of the object δx_o about x_o^d in (3.38) one has $h_o^K = \mathcal{K}\,\delta x_o$ with

$$\mathcal{K} = \sum_{i=1}^N \begin{bmatrix} k_i I_3 & 0 \\ \Xi_i & S^T(r_i)[k_i I_3]S(r_i) + \kappa_i I_3 \end{bmatrix}. \tag{3.39}$$

Among all possible representations, one particular factorization of the Coriolis-centrifugal matrix $\mathcal{C}_o$ for the cooperative dynamics can be computed via

$$\mathcal{C}_o\dot{x}_o = \dot{\mathcal{M}} - \frac{1}{2}\frac{\partial}{\partial x_o}\left(\dot{x}_o^T \mathcal{M} \dot{x}_o\right). \tag{3.40}$$

Proof. The apparent inertia of the object $\mathcal{M}$ is computed by considering the kinetic energy of the overall system being equivalent to the sum of the kinetic energy of the subsystems

$$T = T_o(\dot{x}_o) + \sum_{i=1}^N T_i(\dot{x}_i). \tag{3.41}$$

By employing the constraint (2.31) in (3.41) one has

$$T = \dot{x}_o^T \mathcal{M} \dot{x}_o \tag{3.42}$$

yielding the expression for $\mathcal{M}$ in (3.36). Similar to the kinetic energy, the potential energy

of the augmented system can be used to conclude on the apparent stiffness of the object $\mathcal{K}$. The potential energy of the overall system is the sum of the potential energy of the subsystems, i.e.

$$U = U_o(x_o) + \sum_{i=1}^{N} U_i(x_i). \tag{3.43}$$

The potential energy U_i depends implicitly on the desired pose of the i-th end effector x_i^d since it is equivalent to the elastic energy stored in a tensioned spring between the points x_i and x_i^d with stiffness k_i/κ_i. The desired end effector pose is chosen to coincide with the initial end effector pose resulting in zero preload of all springs. By considering an arbitrary object equilibrium pose

$$\bar{x}_o = \begin{pmatrix} \bar{p}_o \\ \bar{q}_o \end{pmatrix} = \text{const.} \tag{3.44}$$

the desired end effector pose can be derived from the kinematic constraints

$$x_i^d = \begin{pmatrix} p_i^d \\ q_i^d \end{pmatrix} = \begin{pmatrix} \bar{p}_o +^w R_o(\bar{q}_o)^o r_i \\ \bar{q}_o * \delta q_i \end{pmatrix}. \tag{3.45}$$

It is worth noticing that the relative rotation of the object w.r.t. its equilibrium

$$\Delta q_o = q_o * (\bar{q}_o)^{-1} \tag{3.46}$$

is equivalent to the relative rotation of the attached end effectors w.r.t. their equilibrium pose, i.e. $\Delta q_i = \Delta q_o$. Thus the potential energy of the individual end effector U_i in (3.63) can conveniently be written as a function of the object coordinates x_o according to

$$U_i(x_o) = \frac{1}{2} \Delta p_i^T [k_i I_3] \Delta p_i \ + \ 2 \Delta \epsilon_o^T [\kappa_i I_3] \Delta \epsilon_o. \tag{3.47}$$

In order to conclude on the apparent stiffness of the object, one needs to investigate the forces arising from the potential energy. Taking the partial derivative of the potential energy U in (3.43) w.r.t. the object coordinates x_o yields

$$\frac{\partial U}{\partial x_o} = h_g + h_o^K(x_o) \tag{3.48}$$

with the gravitational force h_g presented in (2.26) and $h_o^K(x_o)$ as given in (3.36).

With the expressions for the kinetic and potential energy in (3.41) and (3.43) one readily derives the system's equation of motion by applying Lagrangian mechanics

$$\mathcal{M}\ddot{x}_o + \mathcal{C}_o \dot{x}_o + h_o^K(x_o) + h_g = h^* \tag{3.49}$$

wherein h^* is a generalized, non-conservative wrench acting on the object and $\mathcal{C}_o$ is the Coriolis-centrifugal matrix [70] associated to $\mathcal{M}$. For isotropic inertial parameters m_i and J_i the corresponding elements of $\mathcal{M}$ do *not* depend on the generalized coordinate x_o and the associated Christoffel symbols are thus zero. In this particular case one has $\mathcal{C}_o = C_o$ as in (2.26). The term h^* in (3.49) turns out to be of the form

$$h^* = -\mathcal{D}\dot{x}_o + h_o + \tilde{h}_o \tag{3.50}$$

with $\mathcal{D}$ given in (3.37). The expression for h^* can be derived by substituting (2.43) in the object dynamics (2.25) and replacing h_i by the impedance control law in (2.11). This yields

$$\mathcal{M}\ddot{x}_o + \mathcal{C}_o\dot{x}_o + \mathcal{D}\dot{x}_o + h_o^K(x_o) + h_g = h_o^d + \tilde{h}_o. \tag{3.51}$$

from which (3.35) follows immediately by letting $h_o^d = h_g$.

$\square$

This result has a straightforward interpretation in terms of a mechanical equivalent. The effective object inertia M_o is augmented by attaching rigidly the individual manipulator inertias M_i to the respective grasp points x_i. Additionally, for each manipulator a spring-damper element defined through the parameters K_i and D_i is attached at each grasp point with the remote suspension point located at the manipulators' desired pose x_i^d. This is illustrated in Fig. 3.6.
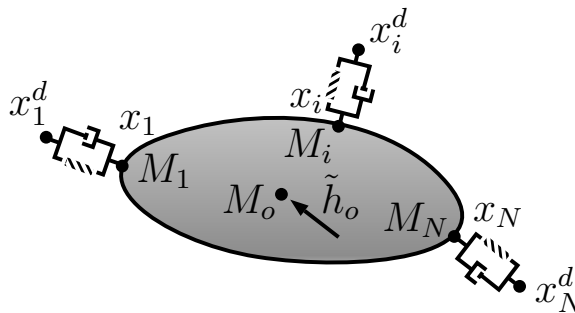
Fig. 3.6: Illustration of the apparent object dynamics as a parallel connection of mass-spring-damper elements

The apparent damping and stiffness of the object results from a parallel connection of the individual spring-damper elements. Note that the apparent end effector inertias M_i appear as if attached rigidly to the object at the grasp point x_i, not at the desired manipulator pose x_i^d. Furthermore, the analytic expressions for $\mathcal{M}, \mathcal{D}$ and $\mathcal{K}$ in Theorem 5 constitute the fundamental equations for the impedance synthesis in multi-robot cooperative manipulation tasks. Their significance is illustrated by the following example.

Example 5 (Apparent object stiffness). Consider two manipulators with $k_1 = k_2 = 100\frac{\text{N}}{\text{m}}$, $\kappa_1 = \kappa_2 = 100\frac{\text{Nm}}{\text{rad}}$ and ${}^o r_{1/2} = \pm(1, 0, 0)^T\text{m}$. According to (3.39), the apparent translational stiffness of the object is isotropic and simply the parallel connection of k_1 and k_2 yielding $200\frac{\text{N}}{\text{m}}$. The rotational stiffness is the parallel connection of κ_1 and κ_2 plus the contribution from the translational stiffness yielding $(200, 400, 400)^T\frac{\text{Nm}}{\text{rad}}$ for infinitesimal rotations about the object axes. Even in case of a symmetric manipulator setup, the apparent stiffness of the object is non-isotropic. However, due to the symmetry the coupling term $\sum_i \Xi_i$ between translational and rotational motion is zero.

The preceding observation for a symmetric setup of the manipulator system can further be generalized.

Corollary 2. *Let the values of m_i, d_i and k_i in (3.36), (3.37) and (3.38) respectively be homogeneous*

$$\forall i \neq j: \ m_i = m_j, \ d_i = d_j, \ k_i = k_j \tag{3.52}$$

and the grasp geometrically symmetric, that is $\sum_i r_i = 0_{3 \times 1}$. Then the translational and rotational object motion of the cooperative system (3.35) subject to a disturbance $\tilde{h}_o$ is decoupled, i.e. the matrices $\mathcal{M}$, $\mathcal{D}$ and $\mathcal{K}$ are block-diagonal.

Proof. It is straightforward to verify that the matrices $\mathcal{M}$, $\mathcal{D}$ and $\mathcal{K}$ are block-diagonal with zero off-diagonal matrices 0_3 by considering (3.36), (3.37) and (3.39) while employing (3.52) and exploiting the linearity of the skew-symmetric operator $S(\cdot)$ for $\sum_i r_i = 0_{3 \times 1}$. $\square$

In the symmetric setup under consideration both the *center of stiffness* and the *center of compliance* [71] coincide with the origin of the object frame $\{o\}$, yielding perfect decoupling of translational and rotational behavior. Consider yet another practically motivated example.

Example 6 (Impedance synthesis). Assume that the apparent impedance of the cooperative manipulator system is to be tuned to exhibit critical damping. By considering the entries of $\mathcal{M}$, $\mathcal{D}$ and $\mathcal{K}$ in Theorem 5 it is obvious that the rotational impedance parameters involve the translational impedance parameters *and* the grasp kinematics in terms of r_i. Thus the impedance synthesis needs to incorporate the actual grasp geometry. An independent design of rotational and translational impedance leads in general not to the desired target impedance.

3.4.1 Experimental evaluation

The conducted experimental study focuses on the evaluation of the apparent dynamics of the cooperative manipulator system presented in Theorem 5. To this end, the wrench $\tilde{h}_o$ and the object pose x_o in a cooperative manipulator setup is measured and a system identification is performed subsequently in order to estimate the parameters $\mathcal{M}$, $\mathcal{D}$ and $\mathcal{K}$.

Experimental setup

The experimental setup involving two anthropomorphic manipulators with 7 degrees of freedom and wrist-mounted force/torque sensors is depicted in Fig. 3.7.

Both end effectors are rigidly grasping an aluminum beam with a quadratic profile and 1.5mm edge length. The overall length of the beam is 1m. A JR3 67M25 6-dimensional force/torque sensor is attached to the center of the beam and an auxiliary handle is mounted on the opposite side of the sensor, enabling the measurement of the externally applied wrench $\tilde{h}_o$. The force/torque signal is filtered by a low-pass filter with 500Hz cutoff frequency. Simultaneously, the object is equipped with optical markers in order to track its pose x_o via a Qualisys Motion Capture System. The object coordinate frame $\{o\}$ coincides with the center of mass and is indicated by means of red arrows in Fig. 3.7. The overall mass of the object is $m_o = 1.75$kg and its moment of inertia about the x-axis is $J_{o,x} \approx 0.055$kgm^2.
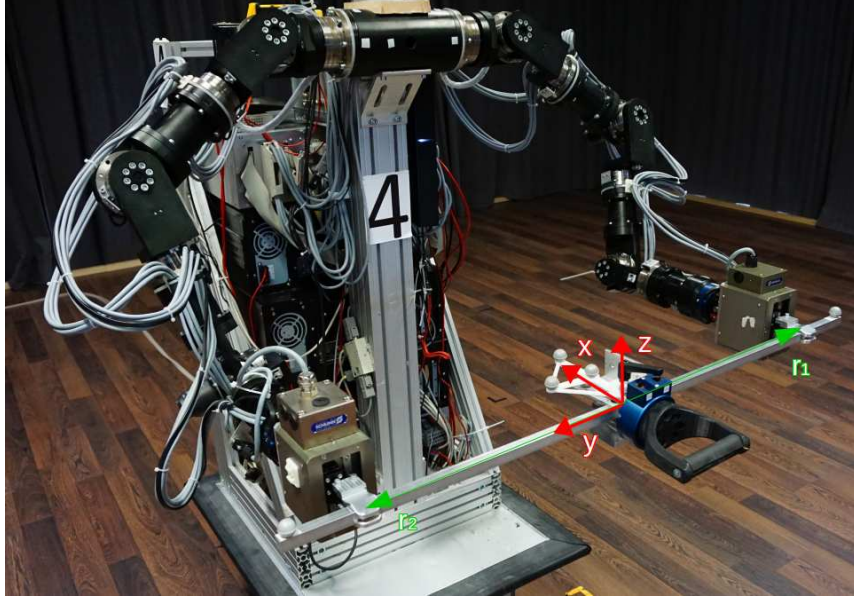
Fig. 3.7: Experimental setup with two robotic manipulators and force/torque sensor for measuring the externally applied wrench $\tilde{h}_o$

The manipulators are controlled individually by an impedance control scheme according to (2.11) with a sampling time of $T_s = 1$ms, wherein the desired wrench is set to zero, i.e. $h_i^d = 0_{6 \times 1}$ and a constant desired end effector pose, i.e. $x_i^d = $ const., such that $r_1 = (0.0, -0.40, 0.0)^T$m and $r_2 = (0.0, +0.40, 0.0)^T$m. The impedance control parameters for both manipulators are $m_i = 10$kg, $d_i = 180\frac{\text{Ns}}{\text{m}}$, $k_i = 300\frac{\text{N}}{\text{m}}$ for the translational behavior and $J_i = I_3 \cdot 0.5$kgm^2, $\delta_i = 10$Nm$\frac{\text{rad}}{\text{s}}$, $\kappa_i = 50\frac{\text{Nm}}{\text{rad}}$ for the rotational behavior.

Translational dynamics

The apparent translational dynamics in x-direction derived from (3.35) can be written as

$$m_o^* \, \ddot{p}_x + d_o^* \, \dot{p}_x + k_o^* \, p_x = \tilde{f}_x \tag{3.53}$$

with the object's position in x-direction $p_x \in \mathbb{R}$, the applied force in x-direction $\tilde{f}_x \in \mathbb{R}$ and the translational impedance parameters

$$m_o^* = 21.75\text{kg}, \quad d_o^* = 360\frac{\text{Ns}}{\text{m}}, \quad k_o^* = 600\frac{\text{N}}{\text{m}} \tag{3.54}$$

extracted from the matrices $\mathcal{M}$, $\mathcal{D}$ and $\mathcal{K}$ in Theorem 5. The applied force $\tilde{f}_x$ and the position p_x are plotted in Fig. 3.8.

Based on the reduced dynamical model (3.53) and the input/output data given by $\tilde{f}_x / p_x$, a system identification is performed. Estimates of the scalar parameters m_o^*, d_o^* and k_o^* are obtained using the linear grey-box model estimation method (`greyest`) of the Matlab System Identification Toolbox. The estimates are

$$\hat{m}_o^* = 21.5\text{kg}, \quad \hat{d}_o^* = 384\frac{\text{Ns}}{\text{m}}, \quad \hat{k}_o^* = 630\frac{\text{N}}{\text{m}}. \tag{3.55}$$
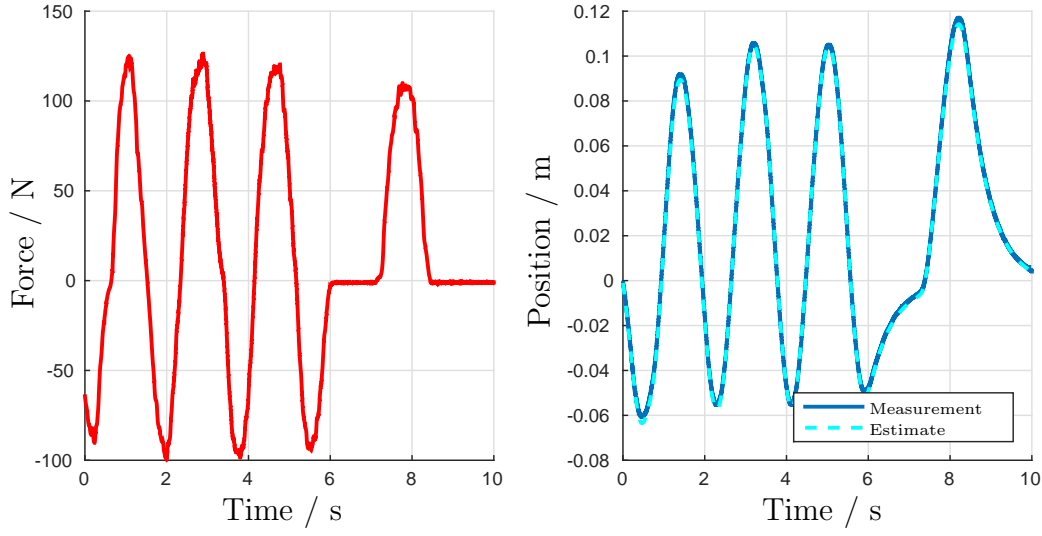
Fig. 3.8: Externally applied force and resulting position in x-direction

The identified model parameters correspond very well to their nominal values as indicated in (3.54). The model output for the input depicted on the left-hand side of Fig. 3.8 and the estimated parameters (3.55) is illustrated by the dashed line on the right-hand side of Fig. 3.8, yielding a mean squared error $\|\hat{p}_x - p_x\|^2$ of $3.86 \cdot 10^{-6} \text{m}^2$ for a recording interval of 45s. Estimated and measured values coincide well and prove consistency of the presented approach.

Rotational dynamics

The apparent rotational dynamics about the object's z-axis derived from (3.35) can be written as

$$J_{o,z}^* \, \ddot{\varphi}_z + d_o^* \, \dot{\varphi}_z + k_o^* \, \varphi_z = \tilde{t}_z \tag{3.56}$$

with the object's orientation about the x-axis $\varphi_x \in \mathbb{R}$, the applied torque about the x-axis $\tilde{t}_x \in \mathbb{R}$ and the rotational impedance parameters

$$J_{o,z}^* = 4.255 \text{kgm}^2, \quad \delta_{o,z}^* = 77.6 \text{Nm} \frac{\text{rad}}{\text{s}}, \quad \kappa_{o,z}^* = 196 \frac{\text{Nm}}{\text{rad}}. \tag{3.57}$$

The applied torque $\tilde{t}_z$ and the resulting orientation φ_z are plotted in Fig. 3.9.

The estimates for the rotational dynamics in (3.56) are

$$\hat{J}_{o,z}^* = 4.652 \text{kgm}^2, \quad \hat{\delta}_{o,z}^* = 84 \text{Nm} \frac{\text{rad}}{\text{s}}, \quad \hat{\kappa}_{o,z}^* = 170 \frac{\text{Nm}}{\text{rad}}. \tag{3.58}$$

The identified rotational impedance parameters approximate their nominal values well. The most significant divergence is observed for the rotational stiffness. The identified value $\hat{\kappa}_{o,z}^*$ is slightly smaller than predicted. This result is attributed to a finite stiffness of the mechanical arrangement whereas an ideal rigid structure is assumed for computing $\kappa_{o,z}^*$. The model output for the estimated parameters is illustrated by the dashed line on the
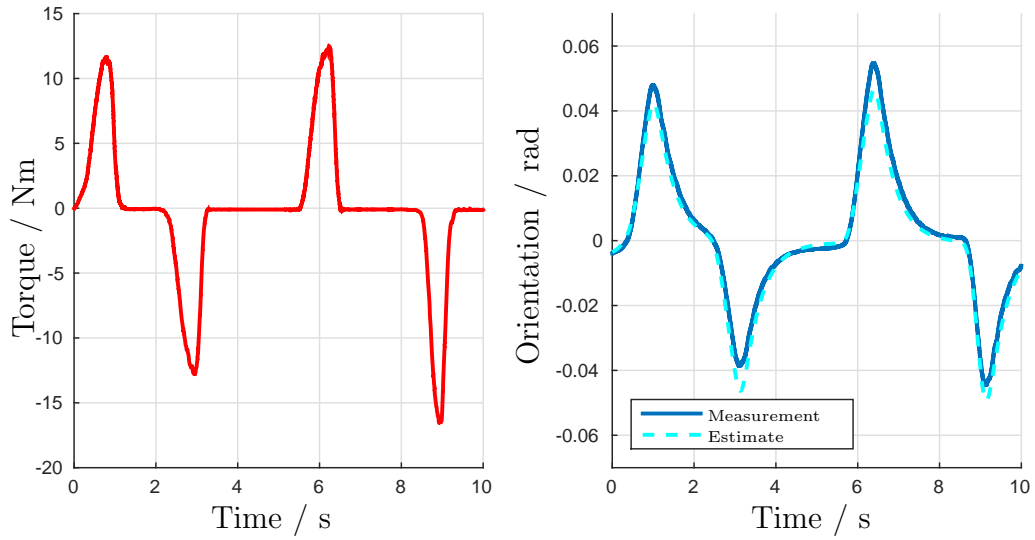
Fig. 3.9: Externally applied torque and resulting orientation about the z-axis

right-hand side of Fig. 3.9, yielding a mean squared error $\|\hat{\varphi}_x - \varphi_x\|^2$ of $2.46 \cdot 10^{-5} \mathrm{rad}^2$ for a recording interval of 60s.

Dynamics in SE(3)

For the identification of the impedance parameters in $SE(3)$ the (linearized) dynamics of the cooperating manipulators are used as presented in (3.83). For the manipulator setup under consideration the object impedance parameters are

$$
\begin{aligned}
\mathcal{M}^* &= [21.75 \mathrm{kg} \cdot I_3, 0_3; 0_3, \mathrm{diag}([4.255, 1, 4.255]) \mathrm{kgm}^2] \\
\mathcal{D}^* &= [360 \frac{\mathrm{Ns}}{\mathrm{m}}, 0_3; 0_3, \mathrm{diag}([78, 20, 78]) \mathrm{Nm} \frac{\mathrm{rad}}{\mathrm{s}}] \\
\mathcal{K}^* &= [600 \frac{\mathrm{N}}{\mathrm{m}}, 0_3; 0_3, \mathrm{diag}([196, 100, 196]) \frac{\mathrm{Nm}}{\mathrm{rad}}].
\end{aligned}
\tag{3.59}
$$

The wrench $\tilde{h}_o$ applied to the object and the resulting object pose δx_o are plotted in Fig. 3.10.

The estimates of the object impedance parameters in (3.83) are

$$
\begin{aligned}
\hat{\mathcal{M}}^* &= [25.8 \mathrm{kg} \cdot I_3, 0_3; 0_3, \mathrm{diag}([2.8, 0.45, 2.8]) \mathrm{kgm}^2] \\
\hat{\mathcal{D}}^* &= [485 \frac{\mathrm{Ns}}{\mathrm{m}}, 0_3; 0_3, \mathrm{diag}([73, 19, 73]) \mathrm{Nm} \frac{\mathrm{rad}}{\mathrm{s}}] \\
\hat{\mathcal{K}}^* &= [820 \frac{\mathrm{N}}{\mathrm{m}}, 0_3; 0_3, \mathrm{diag}([148, 78, 148]) \frac{\mathrm{Nm}}{\mathrm{rad}}].
\end{aligned}
\tag{3.60}
$$

The estimated values provide a satisfactory approximation of the nominal impedance parameters. The most significant divergence is observed for the estimates of the rotational
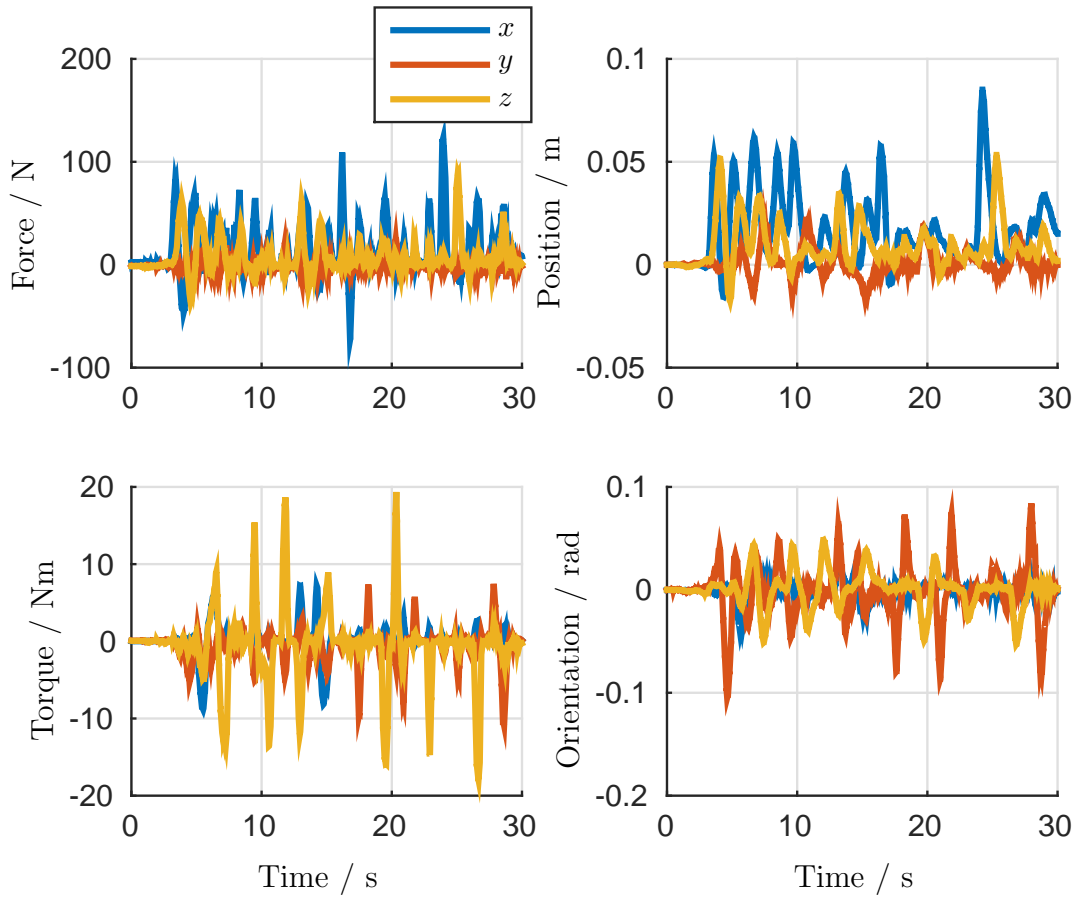
Fig. 3.10: Applied object wrench $\tilde{h}_o$ and resulting object pose δx_o in $SE(3)$

inertia, yielding too small values. This observation is explained through a comparatively low excitation of the rotational motion in combination with the finite structural stiffness of the object. However, the rotational damping is perfectly identified. The translational parameters match satisfactory. Moreover, the experimental study shows clearly the relevance of the coupling between the translational and rotational impedance parameters for the apparent object impedance.

3.5 Stability of the cooperative manipulator system

In this section a formal stability analysis of the cooperative manipulator system is provided. First, strict output passivity of the interaction dynamics is shown. To this end, the notation of passivity is introduced. A system is said to be output strictly passive [72, p. 236] if there exists a positive semidefinite storage function V and a positive definite function $y^T \rho(y)$ such that

$$u^T y \geq \dot{V} + y^T \rho(y) \tag{3.61}$$

for $y \neq 0$.

The kinetic and potential energy of the object defined in (2.24) and the equivalent energy of the i-th manipulator

$$T_i = \frac{1}{2}\dot{x}_i^T M_i \dot{x}_i \tag{3.62}$$

$$U_i = \frac{1}{2}\Delta p_i^T [k_i I]\Delta p_i + 2\Delta \epsilon_i^T [\kappa_i I]\Delta \epsilon_i \tag{3.63}$$

are used in the storage function for the cooperative system

$$V = T_o + U_o + \sum_i \{T_i + U_i\}. \tag{3.64}$$

This leads to the following intermediate result.

Lemma 2. *Assume that the manipulators compensate the gravity force of the object by letting $h_o^d = h_g$ in (3.16) and (2.26), respectively. Then, under Assumption 2, the system of object and manipulators (3.35) is strictly output passive with respect to the input $u = \tilde{h}_o$ and the output $y = \dot{x}_o$ with the storage function V in (3.64).*

Proof. The computation of the time derivative of (3.64) yields

$$\dot{V} = \dot{x}_o^T \mathcal{M}\ddot{x}_o + \frac{1}{2}\dot{x}_o^T \dot{\mathcal{M}}\dot{x}_o + \sum_{i=1}^{N}\{\Delta \dot{p}_i^T f_i^K + \Delta \omega_i^T t_i^K\}. \tag{3.65}$$

By substituting (3.51) in (3.65), one has

$$
\begin{aligned}
\dot{V} =\ & \dot{x}_o^T \left[h_o^d - h_g + \tilde{h}_o - h_o^K(x_o) - \mathcal{D}\dot{x}_o - \mathcal{C}_o\dot{x}_o \right] \\
& + \frac{1}{2}\dot{x}_o^T \dot{\mathcal{M}}\dot{x}_o \\
& + \sum_{i=1}^{N}\{(\dot{p}_o^T + [\omega_o \times r_i]^T)f_i^K + \omega_o^T t_i^K\}.
\end{aligned}
\tag{3.66}
$$

Letting $h_o^d = h_g$ and using the fact that $\dot{x}_o^T[\dot{\mathcal{M}} - 2\mathcal{C}_o]\dot{x}_o = 0$ (cf. [73]) yields

$$
\begin{aligned}
\dot{V} =\ & \dot{x}_o^T \tilde{h}_o - \dot{x}_o^T \mathcal{D}\dot{x}_o - \dot{x}_o^T h_o^K(x_o) \\
& + \sum_{i=1}^{N}\{(\dot{p}_o^T + [\omega_o \times r_i]^T)f_i^K + \omega_o^T t_i^K\}.
\end{aligned}
\tag{3.67}
$$

Employing (3.38) for $h_o^K(x_o)$ and rewriting the sum in terms of a dot product with $\dot{x}_o$ cancels out the last two terms in (3.67) and eventually yields

$$\dot{V} = \dot{x}_o^T \tilde{h}_o - \dot{x}_o^T \mathcal{D}\dot{x}_o < \dot{x}_o^T \tilde{h}_o \tag{3.68}$$

and thus $\rho(y) = \mathcal{D}y$ in (3.61). It is straightforward to show that the damping matrix $\mathcal{D}$ given in (3.37) is positive definite which concludes the proof. $\qquad\square$

This result is a direct consequence of the passivity property of the subsystems, i.e. the rigid body dynamics and the closed-loop manipulator dynamics and is readily expressed in terms of end effector wrenches/velocities.

Corollary 3. *The system of object and manipulators* (3.35) *with the storage function V in* (3.64) *is strictly output passive with respect to the input/output combination $u = \tilde{h}_i$ and $y = \dot{x}_i$ for any $i \in \{1, \ldots, N\}$.*

Proof. Choosing $u = \tilde{h}_i$ and $y = \dot{x}_i$ as input/output signals is equivalent to a change of the coordinate system preserving the passivity property presented in Lemma 2. By employing (2.31) and $\omega_o = \omega_i$ for computing $\dot{x}_i$ and transforming the wrench $\tilde{h}_o$ to an equivalent wrench $\tilde{h}_i$ one has

$$\dot{x}_i = \begin{bmatrix} I_3 & S^T(r_i) \\ 0_3 & I_3 \end{bmatrix} \dot{x}_o \quad \text{and} \quad \tilde{h}_i = \begin{bmatrix} I_3 & 0_3 \\ S^T(r_i) & I_3 \end{bmatrix} \tilde{h}_o. \tag{3.69}$$

It is now straightforward to verify that $\dot{x}_o^T \tilde{h}_o = \dot{x}_i^T \tilde{h}_i$ from which follows $\dot{V} < \dot{x}_i^T \tilde{h}_i$. $\qquad\square$

Based on this passivity characterization, one readily derives stability of the cooperative manipulator system.

Theorem 6. *Under Assumptions 1 and 2, the cooperative manipulator system* (3.35) *is asymptotically stable about*

$$x_o = x_o^d = const. \tag{3.70}$$

for $\tilde{h}_o = 0_{6 \times 1}$ in (2.25) *and $\tilde{h}_i = 0_{6 \times 1}$ in* (2.11). *Moreover, when interacting with a passive environment, i.e. the relation between $\dot{x}_o$ and $\tilde{h}_o$ is described by a strictly passive map [72, Def. 6.3], the cooperative manipulator system remains stable.*

Proof. As stated in Lemma 2, the system of object and manipulators (3.35) is strictly output passive. The feedback interconnection of the cooperative dynamics and the passive environment is strictly passive with input $\tilde{h}_o$ and output $\dot{x}_o$. In order to conclude on stability, it is required to show that the system (3.35) is zero-state detectable. Here it is shown that the system is zero-state observable which implies that it is also zero-state detectable. Consider the output $y = \dot{x}_o = 0_{6 \times 1}$. It follows immediately that $\ddot{x}_o = 0_{6 \times 1}$. Employing this and $\tilde{h}_o = 0_{6 \times 1}$ in (3.35) one has $h_o^K(x_o, x_o^d) = 0_{6 \times 1}$, which can only hold true if $\Delta p_o \equiv \Delta\epsilon_o \equiv 0_{3 \times 1}$ in (3.38). Hence the system (3.35) is zero-state observable for the error state $\Delta x = (\Delta p_o^T, \Delta\varepsilon_o^T)^T$. Asymptotic stability of the cooperative manipulator system without disturbances follows immediately from application of Lemma 6.7. Stability of the manipulators in contact with a strictly passive environment follows by Theorem 6.3 in [72]. $\qquad\square$

Above result shows that the rigidly coupled manipulators interact in such a way that the overall system remains stable if no additional disturbance is present. For the relevant case when the system is subject to non-ideal feedback linearization and externally applied wrenches the following result is presented.

Lemma 3. *Consider the (non-ideal) joint space feedback linearization control law (2.5) with $\hat{\Lambda}_i \neq \Lambda$ and $\hat{\Gamma}_i \neq \Gamma_i$ and the robust tracking controller [34, (8.77)]*

$$\mu_i = \ddot{\xi}_i^d + K_{D,i}\dot{\tilde{\xi}}_i + K_{P,i}\tilde{\xi} + w_i. \tag{3.71}$$

incorporating the uncertainty compensation term

$$w_i = \frac{\rho_i}{\|u_i\|}u_i \tag{3.72}$$

with

$$u_i = D_i^T Q_i \begin{pmatrix} \tilde{\xi}_i \\ \dot{\tilde{\xi}}_i \end{pmatrix}, \tag{3.73}$$

$D_i = [0_{n_i}; I_{n_i}]$ and any positive definite $Q_i \in \mathbb{R}^{2n_i \times 2n_i}$. Assume further that [34, (8.72) through (8.74)]

$$\sup \|\ddot{\xi}_i^d\| < \alpha_{\xi_i} < \infty \qquad \forall \ddot{\xi}_i^d \tag{3.74}$$

$$\|I_{n_i} - \Lambda_i^{-1}\hat{\Lambda}_i\| \leq \alpha_{\Lambda_i} \leq 1 \qquad \forall \xi_i \tag{3.75}$$

$$\|\hat{\Gamma}_i - \Gamma_i\| \leq \alpha_{\Gamma_i} < \infty \qquad \forall \xi_i, \dot{\xi}_i. \tag{3.76}$$

and that the robotic manipulator is sufficiently far from singular joint configurations. Then the equivalent disturbance in task space $\tilde{h}_i$ due to non-ideal feedback linearization of the i-th manipulator is uniformly bounded.

Proof. The proof starts with discussing the assumptions taken in this Lemma and follow the argumentation presented in [34, pp. 334]. Assumption (3.74) is practically always satisfied since any desired trajectory of the object (and consequently of the attached manipulators) should not require infinite acceleration. Assumption (3.75) concerns the boundedness of the inertia matrix. Given a lower and upper bound of Λ_i, there exists a proper choice for $\hat{\Lambda}_i$ which satisfies (3.75), yielding $\alpha_{\Lambda_i} = 0$ in case of $\hat{\Lambda}_i = \Lambda_i$. Finally, assumption (3.76) puts a bound on the Coriolis error term. This last assumption is most restrictive, in the sense that unbounded joint velocities may arise for an unstable system, leading to an arbitrary large error. However, due to physical actuation limits of the robotic manipulator, the joint space velocities will remain bounded and consequently an appropriate α_{Γ_i} in (3.76) can eventually be found.

In order to show boundedness of the disturbance from non-ideal feedback linearization, an expression for the emerging disturbance in joint space is derived. Employing (2.5) and (2.7) in the manipulator dynamic (2.4) and solving for $\ddot{x}_i$ yields

$$\ddot{\xi}_i = \mu_i - \eta_i \tag{3.77}$$

with the error term

$$\eta_i = (I_{n_i} - \Lambda_i^{-1}\hat{\Lambda}_i)\mu_i - \Lambda_i^{-1}(\hat{\Gamma}_i - \Gamma_i). \tag{3.78}$$

Choosing

$$\rho_i \geq \|\hat{\Gamma}_i - \Gamma_i\| \quad \forall \xi_i, \dot{\xi}_i, \ddot{\xi}_i^d \tag{3.79}$$

for the sliding gain ensures convergence of the error system trajectories to zero. Given the assumptions (3.74), (3.75) and (3.75), the signal η_i can be shown to be (uniformly) bounded [34, (8.86)]. Thus the resulting disturbance in joint space $\tilde{\tau}_i$ in (2.4) becomes

$$\tilde{\tau}_i = \Lambda_i \eta_i. \tag{3.80}$$

Consequently, $\tilde{\tau}_i$ is bounded since the inertia matrix Λ_i is a positive definite matrix with upper and lower limited norm.

The equivalent disturbance at the end effector can be computed by

$$\tilde{h}_i = \bar{J}_i^T(\xi_i) \, \tilde{\tau}_i \tag{3.81}$$

with the generalized inverse $\bar{J}_i$ of the Jacobian matrix corresponding to the solution that minimizes the manipulator's instantaneous kinetic energy [35]

$$\bar{J}_i = \Lambda_i^{-1}(\xi_i) \, J_i^T(\xi_i) \, M_i^\Lambda(\xi_i) \tag{3.82}$$

and $M_i^\Lambda(\xi_i)$ as in (2.10). As long as the manipulator does not reach a singular configuration, $\bar{J}_i$ is a continuous mapping and hence bounded. Thus the equivalent disturbance at the end effector $\tilde{h}_i$ is bounded. $\qquad\square$

With the previous intermediate result on the boundedness of the disturbance terms due to non-ideal feedback linearization the main result of this section concerning the robust stability of the cooperative manipulator dynamics is presented next.

Theorem 7. *Assume that the external disturbance on the object $\tilde{h}_o$ in (2.25) and the disturbance due to non-ideal feedback linearization of the manipulators $\tilde{h}_i$ in (2.11) are uniformly bounded and that Assumption 2 holds. Then x_o in (3.35) is uniformly ultimately bounded about $x_o^d = const.$*

Proof. The net wrench about the object's center of mass $\tilde{h}_o^\Sigma$ due to the disturbances $\tilde{h}_o$ and $\tilde{h} = [\tilde{h}_1^T, \ldots, \tilde{h}_N^T]^T$ is given by $\tilde{h}_o^\Sigma = G\tilde{h} + \tilde{h}_o$. Since the $\tilde{h}_i$'s and $\tilde{h}_o$ are bounded, $\tilde{h}_o^\Sigma$ is bounded, too. Linearization of the interaction dynamics (3.35) about an arbitrary equilibrium pose $\bar{x}_o$ yields

$$\mathcal{M}\delta\ddot{x}_o + \mathcal{D}\delta\dot{x}_o + \mathcal{K}\delta x_o = \tilde{h}_o^\Sigma. \tag{3.83}$$

It is obvious that $\mathcal{M}$ and $\mathcal{D}$ are symmetric and positive definite while $\mathcal{K}$ is in general *asymmetric*. $\mathcal{K}$ is positive definite, too, since all eigenvalues of the summand matrices in (3.39) are the eigenvalues of the block matrices (k_i and $\kappa_i + \|r_i\|^2 k_i$ respectively) on the diagonal. As discussed in [71, Theorem 2], the stiffness matrix $\mathcal{K}$ can always be brought into symmetric form by an appropriate change of coordinates. In fact the linearized system (3.83) can be diagonalized by means of a real congruence transformation if and only if $\mathcal{M}^{-1}\mathcal{D}$ commutates with $\mathcal{M}^{-1}\mathcal{K}$ [74]. Explicit computation reveals $\mathcal{D}\mathcal{M}^{-1}\mathcal{K} = \mathcal{K}\mathcal{M}^{-1}\mathcal{D}$. Thus there exists a transformation which decouples the dynamics (3.83) into six independent second order ODEs. Since $\mathcal{M}$, $\mathcal{D}$ and $\mathcal{K}$ are positive definite, the diagonal elements

(corresponding to the eigenvalues of the matrices) are all positive, yielding (exponential) stability of the linearized system. Furthermore, under mild assumptions [34, (8.70) through (8.74)] it can be shown that the joint space disturbances arising from non-ideal feedback linearization are bounded which leads to bounded disturbances $\tilde{h}_i$ in task space by employing the generalized inverse of the Jacobian [35] for the mapping between joint and task space. Boundedness of $\tilde{h}_o$ and $\tilde{h}_i$ and exponential stability of the linearized dynamics (3.83) yields (local) stability of the interaction dynamics (3.35) by applying Lemma 9.2 in [72]. □

This result is of prior relevance for the practical implementation of cooperative manipulation tasks. It proofs robustness of the interaction dynamics to small (bounded) perturbations arising e.g. from imperfect feedback linearization or contact with the environment. Implicitly, the robustness property has been used for the successful implementation of cooperative manipulation schemes in the past but no explicit and formal verification was presented so far incorporating the Dirac structure in the interaction model.

3.6 Internal wrench control

In the previous sections of this chapter, a novel characterization of internal wrenches is presented by means of Definition 1. Based on this definition, all load distributions free of internal wrenches are derived in Section 3.2 and a force/motion tracking controller avoiding application of internal wrenches is presented in Section 3.3. In this section, the focus is put on a basic internal wrench controller suitable for the implementation of a desired internal wrench.

Recalling that internal wrenches according to Definition 1 are equivalently characterized by belonging to the null space of the grasp matrix and employing relation (3.12), i.e. that the null space of the grasp matrix G is identical to the range space of the constraint matrix A^T, the following proposition is presented.

Proposition 1. *The desired internal wrench $h^{int,d} \in \mathbb{R}^{6N \times 1}$ must satisfy $h^{int,d} \in Ker(G)$ or equivalently $h^{int,d} \in Im(A^T)$. Thus one can write*

$$h^{int,d} = A^T z \tag{3.84}$$

for a suitable vector $z \in \mathbb{R}^{6(N-1) \times 1}$.

The vector z selects columns of the constraint matrix A^T and thus determines in which direction internal wrenches are applied. This is illustrated by the following example.

Example 7 (Desired internal wrench parameterization)**.** Reconsider the setup in Fig. 2.3 with two robotic end effectors manipulating an object along one dimension. In this case, the constraint matrix becomes

$$A^T = \begin{bmatrix} 1 \\ -1 \end{bmatrix} \tag{3.85}$$

and $z \in \mathbb{R}$ is a scalar which determines whether the manipulators squeeze ($z > 0$) or pull the object apart ($z < 0$). In this simple example, there is obviously just one potential direction for the application of an internal wrench, i.e.

$$h^{\text{int},d} = \begin{pmatrix} +z \\ -z \end{pmatrix}. \tag{3.86}$$

In order to implement the desired internal wrench $h^{\text{int},d}$ given by (3.84), the following result is of relevance.

Theorem 8. *Assume that the grasp matrix G is known and that the kinematic coordination is implemented cooperatively by means of (3.32), i.e. the initial manipulator motion is compliant to the kinematic constraints. Then, under Assumption 2, the extended motion control law*

$$h^{\mathcal{X}} = h^x - h^{int,d} \tag{3.87}$$

with the kinematic controller h^x from (2.22) and the desired internal wrench $h^{int,d}$ from (3.84) makes the actual internal wrench h^{int} coincide with its desired value. Moreover, any $h^{int,d}$ according to (3.84) does not interfere with the apparent (external) object dynamics (3.35).

Proof. The proof is based on explicit computation of the emerging internal wrench h^{int} as presented in (3.10), i.e.

$$h^{\text{int}} = A^T (A M^{-1} A^T)^{-1} (b - A \ddot{x}^{\mathcal{X}}). \tag{3.88}$$

Note that in the expression above, the commanded acceleration of the extended motion control law $\ddot{x}^{\mathcal{X}}$ is used, resulting from

$$\ddot{x}^{\mathcal{X}} = M^{-1} h^{\mathcal{X}}. \tag{3.89}$$

Moreover, one has $\ddot{x}^{\mathcal{X}} = M^{-1}(h^x - h^{\text{int},d}) = \ddot{x}^x - M^{-1} h^{\text{int},d}$ by employing (3.5). Substituting this in (3.88) yields

$$h^{\text{int}} = A^T (A M^{-1} A^T)^{-1} (b - A \ddot{x}^x + A M^{-1} h^{\text{int},d}). \tag{3.90}$$

Since the commanded acceleration of the initial motion controller $\ddot{x}^x$ are compatible to the kinematic constraints by construction, it is straightforward to verify by explicit computation that $b - A \ddot{x}^x = 0_{6(N-1) \times 1}$. Employing this fact in (3.90) and exploiting (3.84) leads to

$$h^{\text{int}} = A^T (A M^{-1} A^T)^{-1} (A M^{-1} A^T) z, \tag{3.91}$$

in which $(A M^{-1} A^T)^{-1} (A M^{-1} A^T)$ cancels out such that

$$h^{\text{int}} = A^T z = h^{\text{int},d}. \tag{3.92}$$

Since $h^{\text{int}} \in \text{Ker}(G)$, the dynamics of the object with respect to an external disturbance $\tilde{h}_o$ as e.g. in (3.35) remains unchanged. $\qquad \square$

The extended motion control law (3.87) incorporates the individual impedance control laws for the external dynamics h^x and a feed forward action for the internal wrench implementation $h^{\text{int},d}$. This simple approach points out that internal wrench control is closely related to the kinematics and can be achieved by appropriate shaping of the feed forward motion signals. Obviously, in view of the robustness with respect to disturbances more sophisticated control approaches such as an internal wrench PI controller might be favorable. However, any additional wrench for internal wrench control should still belong to $\text{Im}(A^T)$ according to (3.84) in order to guarantee proper, physically consistent decoupling of the internal and external wrench space.

Summary and outlook

In this chapter the cooperative manipulator model is systematically analyzed and relevant properties for the model-based control design are discussed. Robust stability of the manipulators with respect to inaccuracies in the individual feedback linearization loop and external disturbances is derived. A shift of paradigm for the decomposition of internal/external wrenches based on the principle of virtual work is introduced. An immediate consequence is that it is in general not possible to conclude on the presence of internal wrenches by simply analyzing the manipulator wrenches itself. A consistent analysis of internal wrenches needs to incorporate the end effector kinematics, too.

The results of this chapter present the fundamentals for model-based control design in cooperative manipulation tasks. Based on the employed comprehensive model it is possible to compute dynamically consistent feedforward control signals for cooperative force/motion tracking. This becomes particularly obvious for internal wrench control tasks, where the feedforward terms are given by suitably shaped *kinematic* setpoints for the end effectors whereas previous model-free control schemes depend on the feedback of the force/torque measurements. This insight highlights again the vital role of the kinematics for the control and coordination of the multi-robot manipulator system.

The result that the constrained cooperative manipulator dynamics maintain the passivity property as derived in Section 3.5 is the missing complement to the numerous passivity-based control schemes for cooperative manipulation proposed in the literature. The passivity formalism presents simultaneously a promising concept for the stability analysis in more complex setups.

4 Adaptive control for cooperative multi-robot manipulation

This chapter deals with the cooperative manipulator control problem when no global coordinate frame for the multi-robot coordination is available. This situation arises whenever the multi-robot team has no access to a global localization system or when only inaccurate measurements of the relative kinematics between the manipulators are at hand. As a consequence, the kinematic grasp parameters employed in the manipulation task model are biased and counteract the manipulation task objective. The resulting coordination problem without global coordinate frame is reformulated as a robust force/motion tracking problem under uncertain kinematic grasp parameters. An adaptive control scheme for planar cooperative force/velocity manipulation tasks is presented which is evaluated in a numerical simulation at the end of this chapter.

This chapter is structured as follows. First, the related work on cooperative manipulation tasks under uncertain kinematic parameters is reviewed and open problems are discussed. Section 4.1 introduces and motivates the problem of manipulator coordination without global coordinate frame. In Section 4.3 analytical conditions on the manipulator motion are derived for which the uncertain kinematic parameters can be identified. Section 4.2 formulates a general robust force/motion control problem under uncertain kinematic grasp parameters. In Section 4.4 an adaptive control law for planar, force/velocity manipulation tasks is proposed which guarantees robust tracking under uncertain grasp parameters in a simplified setting.

Related work and open problems

Only few works in the robotics literature address the problem of kinematic uncertainties in the control design for cooperative manipulator systems. In [75] an adaptive controller is presented dealing with uncertain kinematic parameters of a single robot in a motion tracking task. An adaptive control scheme for two cooperating manipulators with geometric uncertainties in the closed kinematic loop is presented in [76]. A least squares approach is used to identify the rigid transformation between the manipulators' end effector frames. While minimizing the actuator torques, the actual contact force is not addressed in the resulting control scheme. The work in [77] deals with the modeling and the control design for a single manipulator operating an uncertain kinematic mechanism. Although cooperative manipulators handling a common object are frequently subject to kinematic uncertainties, the consequences on position and force tracking are widely unexplored. The authors of [78] solve the planar object attitude manipulation problem taking into account the distributed coordinate knowledge of the individual agents for computing the rotation centroid. In the area of formation control, the work in [79] describes the severe impact of biased measure-

ments of the relative kinematics on the formation dynamics. For cooperative manipulation tasks, the effect of biased kinematic grasp parameters resulting in undesired interaction forces is discussed and experimentally evaluated in [80]. In summary, the cooperative force/motion tracking problem under uncertain kinematic grasp parameters is a relevant but yet disregarded topic.

4.1 Kinematic coordination without global coordinate system

This section motivates the problem of achieving kinematic coordination of cooperating manipulators when no global coordinate frame is available. As detailed in the previous chapters, typical manipulation task objectives, such as tracking of a desired object trajectory or implementing internal/external wrench control, require exact knowledge of the kinematic grasp parameters as e.g. incorporated in the grasp matrix G in (2.45) or the constraint matrix A in (3.7). However, these crucial parameters are not accurately available when the ensemble of autonomous robotic manipulators has no access to a global coordinate frame. This situation is illustrated in Fig. 4.1.
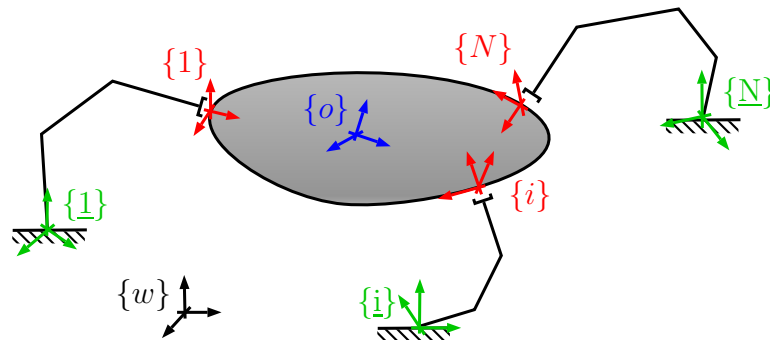
Fig. 4.1: Illustration of the local coordinate frames employed by the robotic manipulators for the cooperative manipulation task

In order to determine the kinematic grasp parameters, the position of a single end effector $\{i\}$ is usually expressed in the object-fixed coordinate system $\{o\}$. That is the translational grasp parameter $^o r_i$ is a vector expressed in the frame $\{o\}$ pointing to the origin of frame $\{i\}$. But this approach requires that both frames $\{o\}$ and $\{i\}$ can be localized in a common global coordinate system $\{w\}$ for computing $^o r_i$. The requirement to have access to such a global coordinate frame for object and manipulator localization is clearly restrictive in view of potential application scenarios as described in Chapter 1. Note further that the manipulators and the object form a closed kinematic chain which is properly defined and independent of any global frame $\{w\}$. This chain is uniquely described by the end effector frames $\{i\}$, the manipulator base frames $\{\underline{i}\}$ as depicted in Fig. 4.1 and the kinematic transformations between those frames as detailed in the sequel.

Manipulator kinematics

All robotic manipulators feature commonly a base frame, denoted $\{\underline{i}\}$ for the i-th manipulator, and a coordinate frame rigidly attached to the end effector denoted $\{i\}$. The kinematic transformation between those two frames is determined by means of the forward kinematics involving the individual joint angles as presented in (2.1).

Assumption 3 (Accurate kinematic manipulator calibration)**.** *The individual manipulators are kinematically calibrated, i.e. the forward kinematic transform, representing the rigid transformation between the base frame $\{\underline{i}\}$ and end effector frame $\{i\}$ for the i-th manipulator, is accurate.*

This assumption is considered valid in view of the vast variety of kinematic calibration methods for robotic manipulators [81]. Thus each manipulator has accurate information about its own end effector pose, twist and acceleration in its proper base frame denoted $\underline{i}x_i$, $\underline{i}\dot{x}_i$ and $\underline{i}\ddot{x}_i$, respectively. Note that with $\underline{i}x_i$ in hand, it is straightforward to transform all local quantities (twist, acceleration, wrench) from the base to the end effector frame.

Grasp kinematics

The grasp parameters, as e.g. incorporated in the grasp matrix G (2.45), might be interpreted as the rigid transformation between the object frame $\{o\}$ and the end effector frames of the robotic manipulators $\{1\}$ to $\{N\}$. To be precise, one needs additionally to specify in which coordinate frame the stacked translational grasp parameter vector r as introduced in (2.44) is expressed. Usually r is expressed in the body-fixed object frame $\{o\}$ since in this frame the grasp points remain constant, i.e.

$$^{o}r = \begin{pmatrix} ^{o}r_1 \\ \vdots \\ ^{o}r_N \end{pmatrix} = \text{const.} \tag{4.1}$$

But the actual grasp also determines the mutual orientation of object and end effector frames. As discussed in Chapter 2, the relative orientation between object and manipulators as introduced in (2.33) remains constant, too, yielding

$$^{o}\delta q = \begin{pmatrix} ^{o}\delta q_1 \\ \vdots \\ ^{o}\delta q_N \end{pmatrix} = \text{const.} \tag{4.2}$$

In fact the representation of the grasp kinematics in terms of (4.1) and (4.2) is redundant since the choice of the object frame $\{o\}$ is a priori arbitrary. If not stated otherwise, the object frame is assumed to be located in the object's physical center of mass and its axes aligned with its principle axes of inertia. This choice eliminates the intrinsic redundancy contained in the kinematic grasp parameters.

In case a global coordinate frame (as e.g. the inertial world frame $\{w\}$ in Fig. 4.1) *is* available, the individual pose coordinates of manipulators and object is expressed in this frame and the relative grasp kinematics is readily computed. This means at the same time,

that either the end effector frame or the base frame of each manipulator can be located in this global frame (e.g. by means of an optical tracking system, GPS sensing or laser scanner). The computation of the relative kinematics depends obviously on the accuracy of the employed sensing system.

However, in case such a sensing system is *not* available, there is no other option than estimating the grasp kinematics. Consequently, only estimates of the relative displacement and orientation between object and manipulators $^o\hat{r}$ and $^o\delta\hat{q}$ are at hand.

Instead of estimating the relative end effector pose, i.e. the kinematic transformation between two end effector frames, one might also estimate the relative pose of the base frames. Depending on the available sensing equipment, the relative base pose is estimated through some localization algorithm [82, 83]. Typically, an accuracy of a few centimeters/degrees is reached, which - depending on the actual distance of the manipulators - can sum up to even more significant errors in the relative end effector pose. Therefore, biased estimates of the grasp geometry need to be addressed in the cooperative control scheme.

Cooperative control scheme without global coordinate system

Before presenting the extended coordination scheme incorporating the estimates of the grasp kinematics, the following assumptions are made.

Assumption 4 (Desired object trajectory)**.** *The desired trajectory for the object $x_o^d(t)$ as e.g. provided by a motion planner is smooth.*

Assumption 5 (Object tracking)**.** *The current pose of the object $x_o(t)$ is measurable by means of a suitable sensing system.*

Above assumptions are crucial for the implementation of an object-centered control scheme. Smoothness of the desired object trajectory is easily guaranteed through application of an appropriate filter. Sensing of the actual object pose x_o is required in order to transform the desired object motion x_o^d into the body-fixed coordinate frame $\{o\}$. Tracking of x_o might be realized e.g. by visual object tracking. Under Assumption 5, it is possible to compute the desired object acceleration $^o\ddot{x}_o^d$ (expressed in the body-fixed frame $\{o\}$).

Given the estimates of the grasp geometry $^o\hat{r}$ and $^o\delta\hat{q}$, the resulting block scheme is illustrated in Fig. 4.2.

The estimate $\hat{r}$ of the translational grasp geometry is employed for computing the desired end effector wrenches and achieving kinematic coordination. Note that this computation is carried out in the object frame $\{o\}$ since also $^o\ddot{x}_o^d$ is specified in this frame. Subsequently, the desired wrench $^oh_i^d$ and acceleration vector $^o\ddot{x}_i^d$ need to be converted to the respective end effector frame $\{i\}$. This is achieved by means of the stacked block-diagonal rotation matrix

$$\mathcal{R}(\delta q) = \begin{bmatrix} R(\delta q_1) & 0_3 \\ 0_3 & R(\delta q_1) \\ & & \ddots \\ & & & R(\delta q_1) & 0_3 \\ & & & 0_3 & R(\delta q_1) \end{bmatrix} \tag{4.3}$$

**Fig. 4.2:** Extended block scheme representation of the cooperative control system

with the 3×3 rotation matrix $R \in SO(3)$ parameterized by a unit quaternion $q = (\eta, \epsilon^T)^T$ according to

$$R(q) = (\eta^2 - \epsilon^T \epsilon)I_3 + 2\epsilon\epsilon^T - 2\eta S(\epsilon). \tag{4.4}$$

The effective change of coordinates yields the manipulator force/motion setpoints expressed in their individual end effector frame. Note that the cooperative dynamics block on the right-hand side of Fig. 4.2 contains the individual manipulator control schemes (which are usually implemented to accept setpoints such as force/motion commands expressed in the end effector frame). The effective interaction behavior is again based on the actual grasp parameters r and δq. For convenience, the cooperative dynamics as presented in Chapter 2 are in turn expressed in the inertial world frame $\{w\}$. However, any other suitable frame might be chosen. From a pure control perspective, the cooperative dynamics block in Fig. 4.2 is equivalent to the plant model and the object level controller is a particular control scheme. Under Assumption 4 it is straightforward to implement an additional control block addressing the potential object tracking error between $\ddot{x}_o^d$ and $\ddot{x}_o$. Force/motion tracking as proposed in Section 3.3 holds obviously just in case $\hat{r} = r$ and $\delta\hat{q} = \delta q$. This is illustrated by means of the following example.

Example 8 (Biased kinematic grasp parameter)**.** Consider a planar manipulation task in which two manipulators rotate a rigid bar of length L counter-clockwise. This situation is depicted in Fig. 4.3.

At time instant t_o, the manipulators grasp the bar and are at rest. Assume in the following that the manipulators have only a biased estimate of their relative displacement $\hat{L} < L$. As soon as the manipulators perform a counter-clockwise rotation of the object, the desired trajectories of the manipulators will describe a segment of a circle (black lines in Fig. 4.3) which lies inside of the circle described by the edges of the bar (gray circle in Fig. 4.3). It is straightforward to verify that internal wrenches are applied to the object, i.e. in fact the manipulators squeeze the object. Moreover, for $\hat{L} < L$ the actual rotation of the object is inferior to the desired rotation, resulting in a (negative) orientation error. The converse situation (pulling the object apart, positive tracking error) is encountered for $\hat{L} > L$.
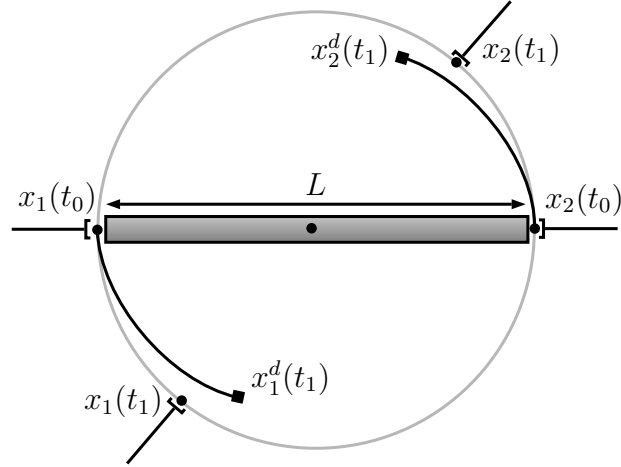
Fig. 4.3: Two planar manipulators with biased grasp parameter $\hat{L} < L$ rotate a rigid bar counter-clockwise

The previous example highlights that the identification of the actual kinematic grasp parameters is a prerequisite for cooperative force/motion tracking. This observation is formalized in the following section.

4.2 Adaptive control for uncertain kinematic grasp parameters

This section deals with the control design for the cooperative manipulator system subject to uncertainty in the kinematic grasp parameters. Before discussing potential control design approaches, the general problem setting is formulated.

Problem formulation   Find a control law for the cooperative manipulator dynamics (2.46) which achieves tracking of the desired object trajectory

$$x_o(t) \rightarrow x_o^d(t) \tag{4.5}$$

and tracking of the desired internal end effector wrenches

$$h^{\mathrm{int}}(t) \rightarrow h^{\mathrm{int},d}(t) \tag{4.6}$$

for $t \rightarrow \infty$ and some initially biased estimates of the kinematic grasp parameters

$$\hat{r}(t=0) \neq r \quad \text{and} \quad \delta\hat{q}(t=0) \neq \delta q. \tag{4.7}$$

The problem stated above is clearly a robust force/motion tracking problem. The stability analysis for this kind of control problem is typically involved - even in case of constrained *single* manipulators [84, 85]. In the cooperative manipulator case under consideration, there are additional challenges which require a novel approach to the analysis and the design of an adaptive control law.

Based on the cooperative force/motion tracking scheme in Section 3.3 and the internal wrench control law as proposed in Section 3.6, the implementation of an adaptive, self-tuning controller appears convenient. The resulting block scheme is illustrated in Fig. 4.4.
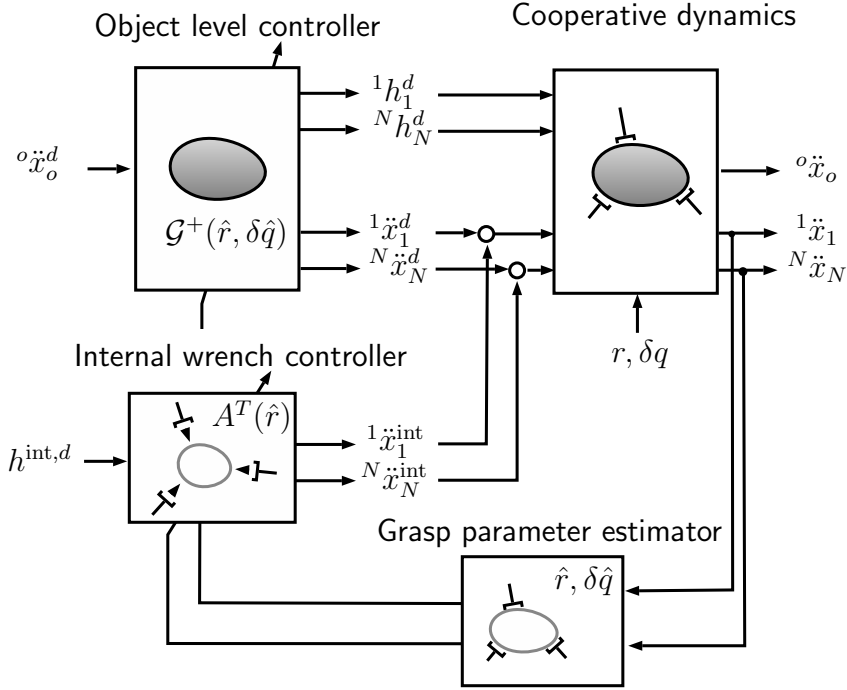
Fig. 4.4: Block scheme representation of the adaptive control law for robust force/motion tracking

In the adaptive, self-tuning control scheme, the object level controller and the internal wrench controller employ the kinematic grasp parameter estimates $\hat{r}$ and $\delta\hat{q}$. Simultaneously, the estimates are updated continuously based on the motion signals as measured by the robotic manipulators. The stability analysis for the depicted control scheme is involved due to several reasons, which are detailed in the sequel.

- Considering the pure motion tracking objective (4.5), one can analogous to (3.34) find an explicit expression for the effectively applied object wrench, which in case of uncertain kinematic grasp parameters becomes

$$h_o = \mathcal{G}(r, \delta q)\, \mathcal{G}^+(\hat{r}, \delta\hat{q})\, h_o^d \tag{4.8}$$

with the augmented grasp matrix

$$\mathcal{G}(r, \delta q) = G(r)\, \mathcal{R}^T(\delta q) \tag{4.9}$$

incorporating the change of coordinates between object and end effector frames in terms of the stacked rotation matrix $\mathcal{R}(\delta q)$ as in (4.3). It is obvious that

$$\mathcal{G}^+(r, \delta q) = \mathcal{R}(\delta q)\, G^+(r). \tag{4.10}$$

Looking again at (4.8), the matrix product can be split into

$$\mathcal{G}(r, \delta q) \, \mathcal{G}^+(\hat{r}, \delta\hat{q}) = I_6 + \mathcal{U}(\tilde{r}, \delta\tilde{q}) \tag{4.11}$$

with the nonlinear matrix expression $\mathcal{U} \in \mathbb{R}^{6\times6}$ incorporating the dependency on the parameter error. Obviously $\mathcal{U} \to 0_6$ for $\hat{r} \to r$ and $\delta\hat{q} \to \delta q$. The matrix $\mathcal{U}$ contains in fact an explicit coupling between translational and rotational estimation errors. The *nonlinear parameter dependency* of $\mathcal{U}$ on $\tilde{r}$ and $\delta\tilde{q}$ requires sophisticated, non-classical tools for the stability analysis of the adaptive controller.

- The force tracking objective (4.6) requires necessarily the computation of the internal wrenches as presented in (3.10). However, this computation is again based on the estimates of the grasp geometry, i.e.

$$\hat{h}^{\text{int}} = \hat{A}^T(\hat{A}M^{-1}\hat{A}^T)^{-1}(\hat{b} - \hat{A}\mathcal{R}^T(\delta\hat{q})\ddot{x}^x) \tag{4.12}$$

with $\hat{A} = A(\hat{r})$ and $\hat{b} = b(\hat{r})$ as defined in (3.7) and (3.8) respectively. Consequently, the computed internal wrenches $\hat{h}^{\text{int}}$ might actually contain components which are not in the null space of the grasp matrix $G(r)$ representing the actual grasp geometry. In turn, it is also possible that the allocated external wrenches

$$\hat{h}^{\text{ext}} = \mathcal{G}^+(\hat{r}, \delta\hat{q}) \, h_o^d \tag{4.13}$$

based on the grasp geometry estimates do contain internal components when implemented by the cooperative manipulator system with the kinematic grasp parameters r and δq. This initial but yet undesired *coupling between internal and external wrench spaces* requires the implementation of additional dynamics for the (feed forward) internal wrench controller as presented in (3.87) in order to compensate for this disturbance. The stability analysis of the interacting internal/external wrench control laws during the transient of $\hat{r} \to r$ and $\delta\hat{q} \to \delta q$ is not straightforward.

- For the purpose of *pose tracking* as in (4.5), the self-tuning control scheme in Fig. 4.4 needs to be augmented by an additional control loop handling the pose error. In its current form, the block scheme represents a pure feed forward motion controller. The additional dynamics of the pose controller and its potential interaction with the internal wrench controller needs to be considered in the stability analysis, too.

- Beyond the pure stability analysis, the *closed-loop parameter identifiability* needs to be investigated separately. Descriptively speaking this means that the actual object motion $x_o(t)$ has to satisfy the persistent excitation condition (4.15) and (4.23) under continuous adaptation of the parameter estimates. In general it is not sufficient that the desired motion $x_o^d(t)$ meets the persistent excitation requirement. In [15] it is shown that singular trajectories exist in which compliance of the desired motion to the persistent excitation condition does not necessarily admit a proper parameter identification.

The points above sketch the complexity of a comprehensive stability analysis for robust force/motion tracking. A core criterion for the proper functionality of adaptive control laws is the identifiability of the parameters which is discussed in the next section.

4.3 Identifiability of the kinematic grasp parameters

In this section conditions are derived under which the kinematic grasp parameters can be identified by the manipulator ensemble. Since there is no global coordinate frame providing direct measurements of object pose x_o and end effector poses x_i, the parameter identification needs to be based on locally available measurements. Typically, each manipulator has access to its end effector velocity ${}^i\dot{x}_i$ expressed in the respective end effector frame. Under Assumption 5, it is also possible to compute the current object velocity ${}^o\dot{x}_o$ in the body-fixed frame $\{o\}$.

4.3.1 Identifiability of the relative orientation in $SE(3)$

Recall that the kinematic constraint (2.35) enforced the object and end effectors to have equal angular velocities. Expressing this equation in the local coordinate frames yields

$$ {}^i\omega_i = R(\delta q_i) \, {}^o\omega_o. \tag{4.14} $$

Clearly, given the available measurements ${}^i\omega_i$ and ${}^o\omega_o$ one would like to identify the mutual orientation of object and end effector, parameterized by the unit quaternion δq_i. This problem, being equivalent to an attitude determination using vector observations, was formulated for the first time by Wahba [86]. Subsequently, different algorithms based on the unit quaternion representation were proposed addressing this problem, such as e.g. QUEST, the q-method or nonlinear observer approaches (see [87] for a recent survey). The authors of [76] employed the q-method for estimating the relative orientation between two robotic end effectors. Moreover, convergence of the estimate to the actual orientation is guaranteed only if the velocity signal satisfies the *persistent excitation* condition.

Proposition 2. *The object's angular velocity ω_o is persistently exciting for the identification of the relative orientation error $\delta\tilde{q}_i = \delta q_i^{-1} * \delta\hat{q}_i$ if the direction of the angular velocity does not remain constant, i.e.*

$$ \dot{\omega}_o \notin Im(\omega_o). \tag{4.15} $$

Proof. Substituting the estimate $\delta\hat{q}_i$ in (4.14) yields the prediction

$$ {}^i\hat{\omega}_i = R(\delta\hat{q}_i) \, {}^o\omega_o. \tag{4.16} $$

Unfortunately, the right-hand side of (4.16) is not linear in the parameter estimate $\delta\hat{q}_i$. However, while employing the fact that $R(\delta\hat{q}_i) = R(\delta\tilde{q}_i)R(\delta q_i)$ with the parameter error defined as $\delta\tilde{q}_i = \delta q_i^{-1} * \delta\hat{q}_i$, the prediction error becomes

$$ {}^i\tilde{\omega}_i = {}^i\hat{\omega}_i - {}^i\omega_i = [R(\delta\hat{q}_i) - R(\delta q_i)] \, {}^o\omega_o = [R(\delta\tilde{q}_i) - I_3] \underbrace{R(\delta q_i) \, {}^o\omega_o}_{{}^i\omega_o}. \tag{4.17} $$

In order to obtain an expression linear in the parameter error, the rotation matrix $R(\delta\tilde{q}_i)$ is linearized using the corresponding roll-pitch-yaw angles $\Theta_i = (\phi_i, \theta_i, \psi_i)^T$. Thus one has [37]

$$R(\delta\tilde{q}_i) \approx R(\tilde{\Theta}_i) = \begin{bmatrix} 1 & \tilde{\psi}_i & -\tilde{\theta}_i \\ -\tilde{\psi}_i & 1 & \tilde{\phi}_i \\ \tilde{\theta}_i & -\tilde{\psi}_i & 1 \end{bmatrix} = I_3 - S(\tilde{\Theta}_i). \qquad (4.18)$$

Substituting this result in the prediction error yields immediately

$$^i\tilde{\omega}_i = -S(\tilde{\Theta}_i)^i\omega_o = S(^i\omega_o)\tilde{\Theta}_i \qquad (4.19)$$

from which the regressor matrix is identified with the skew-symmetric matrix $S(^i\omega_o)$. Thus the object's angular velocity is persistently exciting (cf. Appendix A) if

$$\int_t^{t+\Delta T} S^T(\omega_o)S(\omega_o)dr \qquad (4.20)$$

is uniformly positive definite. Consider two subsequent time intervals of length ΔT starting at t_1 and t_2 in which the angular velocity of the object $\omega_o(t_1)$ and $\omega_o(t_2)$ remains constant. For those two time intervals, the integral becomes

$$\left[S^T(\omega_o(t_1))S(\omega_o(t_1)) + S^T(\omega_o(t_2))S(\omega_o(t_2))\right]\Delta T. \qquad (4.21)$$

With the property of skew-symmetric matrices that $S(\cdot) = -S(\cdot)^T$ one has $\text{Im}(S(\omega_o)) = \text{Im}(S^T(\omega_o))$. It is straightforward to verify that the image of $S(\omega_o)$ is spanned by the plane orthogonal to ω_o. Thus the matrix sum in (4.21) has full rank whenever $\omega_o(t_1)$ and $\omega_o(t_2)$ are not collinear. For $\Delta T \to 0$ this means that the object's angular acceleration is not collinear with its current angular velocity.

Remark (Region of validity) Due to the linearization in (4.18), the result as derived in its present form has (in a strict sense) only local validity. Taking into account the algebraic properties of rotation matrices, it is possible to prove that the presented persistent excitation condition (4.15) holds globally [88]. $\qquad\qquad\square$

Under the persistent excitation condition in Proposition 2, any attitude estimation algorithm (cf. [87]) can be employed for finding the relative orientation between object and end effector frame. Consequently, with the convergence of $^o\delta\hat{q}_i \to^o \delta q_i$, it becomes possible to transform local quantities in the manipulator frames to a common coordinate frame as e.g. in the object frame $\{o\}$ and carry out further computations such as the estimation of the relative displacement.

4.3.2 Identifiability of the relative displacement in $SE(3)$

Given the converging estimates of the relative orientations as discussed in the previous subsection, one is now interested in eliminating the error in the translational parameters $\hat{r}_i$. To this end, consider again the kinematic constraint (2.32) expressed in the object frame $\{o\}$

$$^o\ddot{p}_i =^o \ddot{p}_o +^o \dot{\omega}_o \times^o r_i +^o \omega_o \times (^o\omega_o \times^o r_i). \tag{4.22}$$

Alternatively, one can use the kinematic constraint (2.31) formulated in terms of the involved velocities instead of the rigid body accelerations. However, above representation is particularly illustrative in view of the following result.

Proposition 3. *The object's angular velocity ω_o is persistently exciting for the identification of the relative displacement error $\tilde{r}_i = \hat{r}_i - r_i$ if the direction of the angular velocity does not remain constant, i.e.*

$$\dot{\omega}_o \notin Im(\omega_o). \tag{4.23}$$

Proof. For the relative displacement identification the analysis of the persistent excitation condition is less involved since the model (4.22) is already linear in the unknown parameter r_i. Thus the prediction based on the estimate $\hat{r}_i$ is

$$^o\hat{\ddot{p}}_i =^o \ddot{p}_o +^o \dot{\omega}_o \times^o \hat{r}_i +^o \omega_o \times (^o\omega_o \times^o \hat{r}_i), \tag{4.24}$$

from which the prediction error is readily computed according to

$$^o\tilde{\ddot{p}}_i =^o \hat{\ddot{p}}_i -^o \ddot{p}_i = \underbrace{[S(^o\dot{\omega}_o) + S(^o\omega_o)S(^o\omega_o)]}_{W_{\hat{r}_i}(\omega_o,\dot{\omega}_o)} \, ^o\tilde{r}_i. \tag{4.25}$$

The matrix $W_{\hat{r}_i}(\omega_o, \dot{\omega}_o)$ on the right-hand side of above expression is the regressor matrix for the relative displacement estimation. The regressor has full rank if and only if $\dot{\omega}_o \notin Im(\omega_o)$ and thus satisfying the persistent excitation condition (A.12) since consequently $W_{\hat{r}_i}^T W_{\hat{r}_i}$ has full rank, too.

$\square$

It turns out that the persistency of excitation condition for the identification of relative orientation (4.15) and relative displacement (4.23) are identical. Note that in practice one would therefore ensure that the input is persistently exciting, i.e. $\dot{\omega}_o \notin Im(\omega_o)$, and implement a cascaded estimation of $\delta\hat{q}_i$ and $\hat{r}_i$.

4.3.3 Identification of the kinematic grasp parameters in $SE(2)$

A relevant special case occurs when the robotic end effectors are manipulating an object in the plane. Obviously, the persistent excitation conditions (4.15) and (4.23) cannot be satisfied anymore since the object pose is limited to the oriented plane $SE(2)$. Thus the only available axis of rotation is the one orthogonal to the plane and hence $\dot{\omega}_o \in Im(\omega_o)$. However, it is still possible to identify the kinematic grasp parameters as described by the following result.

Proposition 4. *The object motion in the oriented plane $SE(2)$*

$$\dot{x}_o = \begin{pmatrix} \dot{p}_o \\ \omega_o \end{pmatrix} \in se(2) \tag{4.26}$$

with $\dot{p}_o \in \mathbb{R}^2$ and $\omega_o \in \mathbb{R}$ is persistently exciting for the identification of the kinematic grasp error

$$\tilde{\Theta}_i = \begin{pmatrix} \tilde{r}_i \\ \tilde{\varphi}_i \end{pmatrix} \tag{4.27}$$

with $\tilde{r}_i \in \mathbb{R}^2$ and $\tilde{\varphi}_i \in \mathbb{R}$, if the angular velocity is not constant, i.e.

$$\dot{\omega}_o \neq 0 \tag{4.28}$$

and the object twist does not remain collinear, i.e.

$$\begin{bmatrix} \dot{p}_o(t_1) \\ \omega_o(t_1) \end{bmatrix} \notin span \begin{bmatrix} \dot{p}_o(t_2) \\ \omega_o(t_2) \end{bmatrix} \tag{4.29}$$

for two subsequent time instants t_1 and t_2.

Proof. Choose the model output as

$$^i\dot{p}_i = R(\varphi_i)[^o\dot{p}_o +^o \omega_o s(^o r_i)] \tag{4.30}$$

with the matrix operator

$$s(r_i) = \begin{bmatrix} 0 & -1 \\ 1 & 0 \end{bmatrix} r_i \tag{4.31}$$

performing a rotation of $+90$ degree with the vector r_i and the rotation matrix

$$R(\varphi_i) = \begin{bmatrix} \cos(\varphi_i) & -\sin(\varphi_i) \\ \sin(\varphi_i) & \cos(\varphi_i) \end{bmatrix} \in SO(2). \tag{4.32}$$

Note that φ_i is the orientation of the i-th end effector frame $\{i\}$ with respect to the object frame $\{o\}$. The output sensitivity with respect to the kinematic grasp parameters is

$$\frac{\partial\ ^i\dot{p}_i}{\partial\ \Theta_i} = \left[\bar{R}(\varphi_i)^o\omega_o, \quad \bar{R}(\varphi_i)[^o\dot{p}_o +^o \omega_o s(^o r_i)] \right] \tag{4.33}$$

with the modified rotation matrix $\bar{R}(\varphi_i) = R(\varphi_i - \frac{\pi}{2})$. The sensitivity matrix for two output observations at two distinct time instants t_1 and t_2 is

$$\mathcal{S}(t_1, t_2) = \begin{bmatrix} \bar{R}\omega_o(t_1), & \bar{R}[\dot{p}_o(t_1) + \omega_o(t_1)s(r_i)] \\ \bar{R}\omega_o(t_2), & \bar{R}[\dot{p}_o(t_2) + \omega_o(t_2)s(r_i)] \end{bmatrix} = \begin{bmatrix} \bar{R}\omega_o(t_1), & \bar{R}\bar{v}_1 \\ \bar{R}\omega_o(t_2), & \bar{R}\bar{v}_2 \end{bmatrix}. \tag{4.34}$$

After multiplication of $\mathcal{S}$ with $\bar{R}^T$ from the left and performing elementary matrix operations one has

$$\mathcal{S}(t_1, t_2) \simeq \begin{bmatrix} I_2\omega_o(t_1) & \bar{v}_1 \\ 0_2 & \omega_o(t_1)\bar{v}_2 - \omega_o(t_2)\bar{v}_1 \end{bmatrix} \tag{4.35}$$

which has full rank if $\omega_o(t_1)\bar{v}_2 - \omega_o(t_2)\bar{v}_1 \neq 0_{2\times 1}$.

Reformulation of this latter inequality yields

$$\underbrace{\begin{bmatrix} I_2\omega_o(t_1) & -\dot{p}_o(t_1) \end{bmatrix}}_{Q} \begin{pmatrix} \dot{p}_o(t_2) \\ \omega_o(t_2) \end{pmatrix} \neq 0_{2\times 1}, \tag{4.36}$$

wherein all quantities are expressed in the object frame and the leading superscript is omitted for brevity of notation. The null space of the matrix Q is

$$\mathrm{Ker}(Q) = \mathrm{span}\begin{pmatrix} \dot{p}_o(t_1) \\ \omega_o(t_1) \end{pmatrix} \tag{4.37}$$

which means that the sensitivity matrix $\mathcal{S}$ has full rank whenever

$$\begin{bmatrix} \dot{p}_o(t_1) \\ \omega_o(t_1) \end{bmatrix} \notin \mathrm{span}\begin{bmatrix} \dot{p}_o(t_2) \\ \omega_o(t_2) \end{bmatrix}. \tag{4.38}$$

$\square$

This result is particularly interesting since conditions (4.28) and (4.29) admit a combined identification of orientation *and* displacement error based on the translational velocities ${}^i\dot{p}_i$ and ${}^o\dot{p}_o$. Evaluation of the angular velocities in $SE(2)$ provides no additional information since the measured angular velocity is simply a scalar with the same value in all local coordinate frames. With respect to the previous results for $SE(3)$ it is worth mentioning that in $SE(2)$ a *non-zero* translational velocity of the object $\dot{p}_o$ is required for proper identification of the grasp kinematics.

4.4 Adaptive control for cooperative manipulation in $SE(2)$

In view of the evident complexity of the general adaptive control problem formulated in Section 4.2, a simplified setting is considered in the sequel for which stability of the control law and convergence of the parameter estimates is studied in detail. A concise stability analysis for an adaptive control law needs to address the interplay between system dynamics, controller and parameter estimators in order to *guarantee* robust tracking performance. To this end, the manipulation task under study is reduced in dimensionality and conducted in the oriented plane $SE(2)$.

Remark (Reduced dimensionality)   In this section, the pose coordinates of object and end effectors are $x_o, x_i \in SE(2)$ with the assigned twist vectors $\dot{x}_o, \dot{x}_i \in se(2)$. The object and manipulator wrenches are $h_o, h_i \in se^T(2)$.

In order to further simplify the setting under consideration, the coupling effects between internal and external wrenches are eliminated through the following assumption.

Assumption 6 (Kinematic approximation)**.** *The wrench required to manipulate the object remains small such that*

$$h_o \approx 0_{3\times 1}. \tag{4.39}$$

This assumption eliminates the object's inertial forces and thus the entire load distribution problem from the robust tracking task. As an immediate consequence of Assumption 6, the resulting manipulator forces are exclusively internal and satisfy

$$\sum_{i=1}^{N} f_i = 0_{2\times 1}. \tag{4.40}$$

Note that the ability to compensate the object's gravitational force is unaffected in case gravity acts orthogonal to the plane.

4.4.1 Gauss principle for cooperative force/velocity manipulation tasks

An alternative interpretation of Assumption 6 is that with $h_o \approx 0_{3\times 1}$, the object acceleration $\ddot{x}_o$ needs to remain small, too. This implication leads to models for manipulation scenarios based exclusively on force, position and velocity signals while neglecting the acceleration. This simplified modeling approach appeared convenient for the design of adaptive control laws in manipulation tasks [15, 77, 78]. The Gauss principle as presented in Section 2.4.2 can be readily applied for the modeling of force/velocity manipulation tasks and presents a general and unifying framework for constrained manipulation tasks.

In order to derive the modified Gauss principle for pure force/velocity manipulation tasks, consider the following general, second-order manipulator model

$$M_i \ddot{x}_i = w_i \tag{4.41}$$

with the positive definite task space inertia matrix $M_i \in \mathbb{R}^{3\times 3}$, the end effector acceleration $\ddot{x}_i \in \mathbb{R}^3$ and the control input $w_i \in \mathbb{R}^3$. Choosing the control law

$$w_i = \hat{M}_i \ddot{x}_i + K_{i,c}(\dot{x}_i^r - \dot{x}_i) \tag{4.42}$$

with the positive definite control gain $K_{i,c} \in \mathbb{R}^{3\times 3}$ allows to track a reference velocity $\dot{x}_i^r$ which is typically composed of a desired (feed forward) velocity $\dot{x}_i^d$ and a force feedback term, incorporating the end effector wrench h_i according to

$$\dot{x}_i^r = \dot{x}_i^d + C_i h_i \tag{4.43}$$

with the positive definite end effector compliance $C_i \in \mathbb{R}^{3\times 3}$. Letting now $K_{i,c} \to \infty$ enforces

$$\dot{x}_i = \dot{x}_i^r. \tag{4.44}$$

Thus the stacked system of manipulators can be rewritten as

$$
\begin{bmatrix} C_1^{-1} & & \\ & \ddots & \\ & & C_N^{-1} \end{bmatrix} \underbrace{}_{C^{-1}} \begin{pmatrix} \dot{x}_1 \\ \vdots \\ \dot{x}_N \end{pmatrix} = \begin{pmatrix} C_1^{-1}\dot{x}_1^d \\ \vdots \\ C_1^{-1}\dot{x}_N^d \end{pmatrix} + \begin{pmatrix} h_1 \\ \vdots \\ h_N \end{pmatrix} \tag{4.45}
$$

which has the same structure as the stacked system dynamics (2.46). Therefore, the end effector wrenches h_i are computed by employing the Gauss principle for the modified system with the inertia matrix C^{-1} and the kinematic constraints expressed on the velocity level, i.e.

$$
A\,\dot{x} = b \tag{4.46}
$$

with

$$
A = \begin{bmatrix} I_2 & -s(r_1) & -I_2 & s(r_2) & & & \\ 0_{1\times 2} & 1 & 0_{1\times 2} & -1 & & & \\ \vdots & \vdots & & & \ddots & & \\ I_2 & -s(r_1) & & & & -I_2 & s(r_N) \\ 0_{1\times 2} & 1 & & & & 0_{1\times 2} & -1 \end{bmatrix} \quad \text{and} \quad b = 0_{3(N-1)\times 1}, \tag{4.47}
$$

yielding

$$
h = A^T(ACA^T)^{-1}(b - A\dot{x}^d). \tag{4.48}
$$

Note that neither the object wrench h_o nor the object pose and velocity appear explicitly in the force/velocity representation. However, the origin of the grasp vectors r_i defines also the origin of the object frame $\{o\}$, which for consistency should coincide with the equivalent center of mass of the end effector ensemble satisfying

$$
\sum_{i=1}^{N} C_i^{-1} r_i = 0_{2\times 1}. \tag{4.49}
$$

The resulting block scheme of the force/velocity manipulator model is depicted in Fig. 4.5.
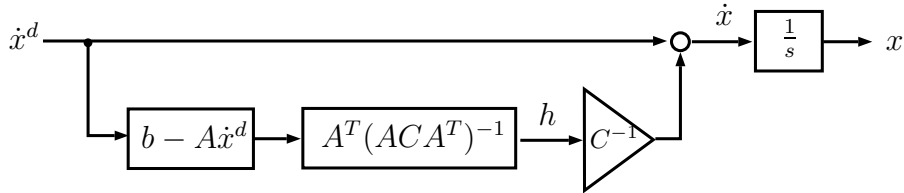
Fig. 4.5: Block scheme representation of the force/velocity cooperative manipulator model

The actual manipulator velocities $\dot{x}$ are the sum of the desired (feed forward) velocities $\dot{x}^d$ and the feedback term $C^{-1}h$, which results from a projection of the desired velocities $\dot{x}^d$ on the kinematic constraints contained in the matrix A. The actual system

dynamics are represented by a single integrator element with the manipulator poses x as output.

4.4.2 Kinematic controller

The desired velocities of the individual end effectors are computed as follows. Without loss of generality, the orientation of the object frame $\{o\}$ is assumed to coincide with the orientation of the end effector frame $\{1\}$ such that

$$
{}^1\dot{x}_1^d \;\equiv\; {}^o\dot{x}_o^d = \begin{pmatrix} {}^o\dot{p}_o^d \\ \omega_o \end{pmatrix}. \tag{4.50}
$$

Given the desired velocity for object, the desired velocity for the j-th manipulator in coordinate frame $\{j\}$ for $j \in \{2, \ldots, N\}$ is computed according to

$$
{}^j\dot{x}_j^d = \begin{pmatrix} R(\hat{\varphi}_{1j})[{}^1\dot{p}_o^d - \omega_o s(\hat{r}_{1j})] \\ \omega_o \end{pmatrix}, \tag{4.51}
$$

based on the kinematic grasp estimates $\hat{\varphi}_{1j}$ and $\hat{r}_{1j}$ for the relative orientation and displacement, respectively. The desired velocity expressed in the object frame $\{o\}$ (or equivalently in the end effector frame $\{1\}$) is

$$
{}^1\dot{x}_j^d = \begin{pmatrix} R(\tilde{\varphi}_{1j})[{}^1\dot{p}_o^d - \omega_o s(\hat{r}_{1j})] \\ \omega_o \end{pmatrix} \tag{4.52}
$$

which depends explicitly on the relative orientation estimation error $\tilde{\varphi}_{1j}$. By projecting the stacked desired velocities ${}^1\dot{x}^d$ on the kinematic constraints, the kinematic error is

$$
e = b - A\,{}^o\dot{x}^d = \begin{pmatrix} [I_2 - R(\tilde{\varphi}_{12})]{}^o\dot{p}_o^d + [R(\tilde{\varphi}_{12})s(\hat{r}_{12}) - s(r_{12})]\omega_o \\ 0 \\ \vdots \\ [I_2 - R(\tilde{\varphi}_{1N})]{}^o\dot{p}_o^d + [R(\tilde{\varphi}_{1N})s(\hat{r}_{1N}) - s(r_{1N})]\omega_o \\ 0 \end{pmatrix}. \tag{4.53}
$$

It is straightforward to verify that the kinematic error e, and consequently also h in (4.48), vanishes for $\tilde{\varphi}_{1j} \to 0$ and $\tilde{r}_{1j} \to 0_{2 \times 1}$.

4.4.3 Robust force/velocity tracking

Based on the previous modeling of the force/velocity dynamics for cooperative manipulation tasks, in this subsection an adaptive controller addressing uncertain kinematic grasp parameters in $SE(2)$ is presented.

Theorem 9. *Under the Assumptions 1, 2, 3, 4, 5 and 6, the kinematic object level controller (4.50) and (4.51) and the kinematic manipulator control law (4.43) achieve robust force/velocity tracking for the cooperative manipulator system (4.45), i.e.*

$$\dot{x}_o(t) \to \dot{x}_o^d(t) \quad and \quad h(t) \to h^{int,d}(t) \tag{4.54}$$

under some initially biased translational grasp parameter estimates

$$\hat{r}(t = 0) \neq r \tag{4.55}$$

and some sufficiently small orientation errors, i.e.

$$\hat{\varphi}(t = 0) \approx \varphi \tag{4.56}$$

for $t \to \infty$ and the kinematic grasp parameter estimators

$$\dot{\hat{\varphi}} = -K_\varphi W_\varphi^T \left(-\sum_{j=2}^{N} \{R(\hat{\varphi}_{1j})^j f_j\} -^1 f_1 \right) \tag{4.57}$$

with

$$W_\varphi = \begin{bmatrix} s(^2 f_2) & \cdots & s(^N f_N) \end{bmatrix} \tag{4.58}$$

and

$$\dot{\hat{r}} = -K_r \, W_r^T \begin{pmatrix} ^1\dot{p}_o + \omega_o s(\hat{r}_{12}) - R(\tilde{\varphi}_{12})^2 \dot{p}_2 \\ \vdots \\ ^1\dot{p}_o + \omega_o s(\hat{r}_{1N}) - R(\tilde{\varphi}_{1N})^N \dot{p}_N \end{pmatrix} \tag{4.59}$$

with

$$W_r = \begin{bmatrix} 0 & -\omega_o & & & \\ \omega_o & 0 & & & \\ & & \ddots & & \\ & & & 0 & -\omega_o \\ & & & \omega_o & 0 \end{bmatrix} \tag{4.60}$$

and the positive definite estimation gain matrices $K_\varphi \in \mathbb{R}^{(N-1)\times(N-1)}$ and $K_r \in \mathbb{R}^{2(N-1)\times 2(N-1)}$, if the initial orientation errors $\|\tilde{\varphi}\| = \|\hat{\varphi} - \varphi\|$ are small and the regressor matrices W_φ and W_r in (4.77) and (4.60) respectively fulfill the persistent excitation condition (A.12).

Proof. Without loss of generality, it is assumed for the proof that $h^{\text{int},d}(t) \equiv 0_{3N\times 1}$. Nev-

ertheless it is possible to choose $h^{\text{int},d}(t) = A^T(\hat{r})z(t)$ with $z(t) \neq 0$ according to (3.84) by adding an appropriate velocity vector $\dot{x}^{\text{int},d} = Ch^{\text{int},d}$ to the desired velocity $\dot{x}^d$. For the illustrative case of $h^{\text{int},d}(t) \equiv 0_{3N \times 1}$ it becomes obvious by rewriting (4.45) as

$$C^{-1}(\dot{x} - \dot{x}^d) = h \tag{4.61}$$

that force/velocity tracking is achieved for $h = 0_{3N \times 1}$. Since h as presented in (4.48) results from a projection of the desired velocities $\dot{x}^d$ onto the actual kinematic constraints incorporated in A, tracking is achieved if and only if the kinematic grasp parameter estimates match the actual grasp parameters, i.e. $\dot{x}^d \in \ker(A)$. As a matter of fact, the only dynamics relevant to the force/velocity tracking objective stems from the parameter estimators.

Remark (Uniqueness of the kinematic grasp parameters) Assumption 6 eliminates the object's inertial effects and thus the significance of the object's center of mass. The grasp parameters are hence uniquely determined by the *relative kinematics* between the individual end effectors (excluding the object)

$$\hat{r} = \begin{pmatrix} \hat{r}_{12} \\ \vdots \\ \hat{r}_{1N} \end{pmatrix} \quad \text{and} \quad \hat{\varphi} = \begin{pmatrix} \hat{\varphi}_{12} \\ \vdots \\ \hat{\varphi}_{1N} \end{pmatrix}, \tag{4.62}$$

expressed with respect to end effector $\{1\}$. It is possible to express the set of grasp parameters with respect to any other arbitrary coordinate frame when using this frame for the kinematic controller as described in Section 4.4.2.

The parameter estimation model for the relative orientation is based on (4.40) while expressing the locally available end effector forces $^i f_i$ with respect to frame $\{1\}$, i.e.

$$\sum_{i=1}^{N} R(^1\varphi_i)^i f_i = 0_{2 \times 1}. \tag{4.63}$$

wherein $\varphi_{1i} \in \mathbb{R}$ is the actual relative orientation between the end effector frames $\{1\}$ and $\{i\}$. Since trivially $\varphi_{11} = 0$ and thus $R(\varphi_{11}) = I_2$, one can rewrite

$$^1 f_1 = -\sum_{i=2}^{N} R(\varphi_{1i})^i f_i \tag{4.64}$$

and analogous for the orientation estimates

$$^1 \hat{f}_1 = -\sum_{i=2}^{N} R(\hat{\varphi}_{1i})^i f_i. \tag{4.65}$$

One has further

$$^1 \hat{f}_1 - {}^1 f_1 = \sum_{j=2}^{N} [{}^j f_j, \ s({}^j f_j)] \begin{pmatrix} \cos(\hat{\varphi}_{1j}) - \cos(\varphi_{1j}) \\ \sin(\hat{\varphi}_{1j}) - \sin(\varphi_{1j}) \end{pmatrix} \tag{4.66}$$

which is, for small orientation errors $\hat{\varphi}_{1j} \approx \varphi_{1j}$, linear in $\tilde{\varphi}$, i.e.

$$^1\hat{f}_1 - {}^1 f_1 \approx \sum_{j=2}^{N} [{}^j f_j, \ s({}^j f_j)] \begin{pmatrix} 0 \\ \tilde{\varphi}_{1j} \end{pmatrix} = W_\varphi \ \tilde{\varphi}. \tag{4.67}$$

The translational parameter estimator is based on a prediction model incorporating the kinematic velocity constraints (2.31), i.e.

$$^j\dot{p}_j = {}^j\dot{p}_o + \omega_o s(r_{1j}) \quad \text{and} \quad {}^j\hat{\dot{p}}_j = {}^j\dot{p}_o + \omega_o s(\hat{r}_{1j}) \tag{4.68}$$

which is obviously linear in the translational grasp parameters $\hat{r}$.

Remark (Orientation error convergence) Convergence of $\tilde{\varphi}_{1j} \to 0$ ensures that the measured end effector forces sum up to zero, i.e. $\sum_i f_i = 0_{2\times1}$. However, this does not imply that the end effector forces vanish since one still has $f_i \neq 0_{2\times1}$ for an translational parameter estimation error $\tilde{r}_i \neq 0_{2\times1}$.

Consider now the Lyapunov function candidate

$$V = \frac{1}{2} \left(\tilde{\varphi}^T \tilde{\varphi} + \tilde{r}^T \tilde{r} \right). \tag{4.69}$$

Straightforward computation of the time derivative yields

$$\dot{V} = -\tilde{\varphi}^T K_\varphi(\hat{\varphi}) W_\varphi^T W_\varphi \tilde{\varphi} - \tilde{r}^T K_r W_r^T W_r \tilde{r} \leq 0. \tag{4.70}$$

Convergence of $\dot{V} \to 0$ and consequently $\tilde{\varphi} \to 0_{(N-1)\times1}$ and $\tilde{r} \to 0_{2(N-1)\times1}$ follows immediately by employing the persistent excitation property of the regressor matrices W_φ and W_r and by invoking standard arguments for convergence analysis [89, Theorem 4.3.2] by deriving boundedness of $\ddot{V}$ given the boundedness of $\dot{x}_o^d$ and its derivative in case the estimators for $\hat{\varphi}$ and $\hat{r}$ are decoupled.

As visible in (4.59), the translational parameter estimator depends on the orientation errors $\tilde{\varphi}_{1j}$. Put differently, the translational estimator is subject to a disturbance stemming from the orientation error since the two estimators are cascaded. Given the persistent excitation property of the regressor matrices, the gradient estimators for $\hat{u}$ and $\hat{r}$ guarantee exponential convergence of the estimation error to zero in the unperturbed case [89, Theorem 4.3.2]. The cascaded estimator incorporating the rotational estimates for the translational parameter estimation can be analyzed by means of the stability theory for perturbed systems. The induced perturbation on the translational parameter estimator due to $R(\tilde{\varphi}_{1j}) \neq I_2$ in (4.59) is vanishing since for $\tilde{\varphi}_{1j} \to 0$ one has $R(\tilde{\varphi}_{1j}) \to I_2$ exponentially. Moreover, by an appropriate bound on $\|p_o^d\|$ it is possible to find for any $\tilde{\varphi}_{1j}$ a suitable $\gamma_j > 0$ such that

$$\|^1\dot{p}_o - R(\tilde{\varphi}_{1j})^j\dot{p}_j\| < \gamma_j \ \|\tilde{\varphi}_{1j}\|, \tag{4.71}$$

by employing e.g. the Frobenius norm or the 2-norm [90]. With this bound for the vanishing perturbation and the exponential convergence of the unperturbed system, Lemma 9.1 in [72] guarantees exponential convergence of the perturbed translational estimation error

to zero. □

This theorem generalizes a previous result for planar cooperative force/velocity manipulation tasks under uncertain kinematic grasp parameter involving two manipulators [15] to the case of $N > 2$ manipulators. Moreover, it is possible to extend the result in Theorem 9 to larger initial orientation errors $\tilde{\varphi}$ by exploiting the geometry of the 1-sphere $\mathbb{S}^1$, a 1-dimensional manifold representing the orientation of a rigid body in the plane.

4.4.4 Reparameterization of the relative orientation

The persistent challenge in the analysis of adaptive control laws incorporating rotational parameters such as the relative grasp orientation is that those parameters appear nonlinearly in the prediction models. In $SE(2)$ the orientation of a rigid body, such as the i-th end effector, is uniquely determined by a scalar value, namely the angle of rotation $\varphi_i \in \mathbb{S}^1$. Moreover, each φ_i can be identified unambiguously with a unit vector $u_i \in \mathbb{R}^2$ given by

$$u_i = \begin{bmatrix} \cos(\varphi_i) \\ \sin(\varphi_i) \end{bmatrix}. \tag{4.72}$$

Based on the unit vector representation, it is possible to reparameterize any two-dimensional rotation matrix in (4.32) as

$$R(\varphi_i) = \begin{bmatrix} u_i, & s(u_i) \end{bmatrix} \tag{4.73}$$

with the matrix operator $s(\cdot)$ defined in (4.31). Thus it is possible to reformulate the prediction model output as

$$^1f_1 = -\sum_{i=2}^{N} R(\varphi_{1i})^i f_i \tag{4.74}$$

$$= -\sum_{i=2}^{N} [u_{1i}, \ s(u_{1i})] \ ^i f_i \tag{4.75}$$

$$= -\sum_{i=2}^{N} [^i f_i, \ s(^i f_i)] \ u_{1i}. \tag{4.76}$$

Rewriting the sum as matrix multiplication yields

$$^1f_1 = -\underbrace{[^2f_2, \ s(^2f_2), \ \dots, \ ^Nf_N, \ s(^Nf_N)]}_{W_u} \underbrace{\begin{pmatrix} u_{12} \\ \dots \\ u_{1N} \end{pmatrix}}_{u} \tag{4.77}$$

which is clearly linear in the stacked unit vectors u. Moreover, W_u is a regressor incorporating only known quantities, namely the end effector forces expressed in the individual end effector frames.

The resulting parameter update law based on the unit vector representation is given by

$$\dot{\hat{u}} = -K_u \, \mathcal{P}(\hat{u}) \, W_u^T \, \left(W_u \, \hat{u} \, - \, {}^1f_1\right) \tag{4.78}$$

with W_u as in (4.77) and the projection matrix

$$\mathcal{P}(\hat{u}) = \begin{bmatrix} I_2 - \hat{u}_{12}^T \hat{u}_{12} & & \\ & \ddots & \\ & & I_2 - \hat{u}_{1N}^T \hat{u}_{1N} \end{bmatrix} \tag{4.79}$$

which ensures that the computed gradient of the parameter update law points in the direction spanned by the tangent plane of $\hat{u}$. The orientation error dynamics becomes

$$\frac{d}{dt}[\hat{u}^T \hat{u}] = -\tilde{u}^T K_u \mathcal{P}(\hat{u}) W_u^T W_u \tilde{u} \tag{4.80}$$

for which it remains to verify that the projection matrix $\mathcal{P}(\hat{u})$ in (4.78) does not alter the convergence properties of the gradient algorithm.

A prerequisite for ensuring the convergence properties of the projected gradient algorithm with classical tools is that the projected parameter set is bounded and convex. The orientation error $\tilde{\varphi}_{1j} \in \mathbb{S}^1$ belong to the spherical group which is not bounded nor convex. The group $\mathbb{S}^1$ can be visualized as a circle in the plane and is depicted in Fig. 4.6.
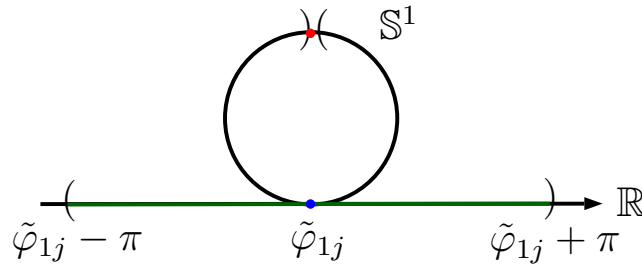
Fig. 4.6: Illustration of the parameterization of the 1-sphere $\mathbb{S}^1$

Any element $\tilde{\varphi}_{1j} \in \mathbb{S}^1$ as depicted by the blue dot in Fig. 4.6 can however be mapped to a segment of $\mathbb{R}$ (depicted by the green line) when excluding the opposing element (depicted in the figure by the red dot). Clearly, the open interval $(\tilde{\varphi}_{1j} - \pi, \tilde{\varphi}_{1j} + \pi)$ is bounded and convex. Moreover, the mapping (4.72) can be interpreted as isomorphism between this line interval and its corresponding unit vector representation. In this regard, the presented projected gradient algorithm (4.78) is expected to provide almost global convergence of $\tilde{\varphi}_{1j} \to 0$ for $|\tilde{\varphi}_{1j}| < \pi$ according to [89, Theorem 4.4.1] and W_u fulfilling the persistent excitation criterion.

Discussion For a concise analysis of the transient and the resulting convergence properties of the projected gradient algorithm, a more detailed study of the employed isomorphism (4.72) in the context of classical projected gradient algorithms such as [89, Theorem 4.4.1] is required. The unit vector representation enables to rewrite the parameter model equation linear in the orientation error. However, the chosen unit vector representation is not minimal. Therefore, the matrix $\mathcal{P}$ realizes a projection of arbitrary vectors in $\mathbb{R}^2$ (generated by the gradient algorithm), to the unit circle. In this regard, the involved projection does

not limit the range of the orientation error itself but ensures that the chosen orientation parameterization remains conform to the unit norm requirement.

4.4.5 Numerical results

The adaptive control law proposed in Theorem 9 is illustrated in the sequel by means of a numerical example. To this end, consider the following planar manipulation setup with $N = 3$ manipulators depicted in Fig. 4.7.
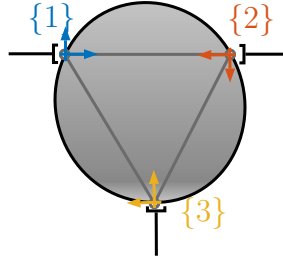
Fig. 4.7: Illustration of the kinematic grasp parameters for a planar manipulation task with $N = 3$ manipulators

In this example the kinematic grasp parameters are

$$^1r_{12} = \begin{pmatrix} 1.0 \\ 0.0 \end{pmatrix} \text{m} \quad , \quad \varphi_{12} = \pi \text{ rad} \tag{4.81}$$

for manipulator $\{2\}$ and

$$^1r_{13} = \begin{pmatrix} 0.5 \\ -0.8600 \end{pmatrix} \text{m} \quad , \quad \varphi_{13} = \frac{\pi}{2} \text{ rad} \tag{4.82}$$

for manipulator $\{3\}$. The grasp parameter estimates are chosen as

$$^1\hat{r}_{12} = \begin{pmatrix} 1.0 \\ 0.0 \end{pmatrix} \text{m} \quad , \quad \varphi_{12} = \pi \text{ rad} \tag{4.83}$$

and

$$^1\hat{r}_{13} = \begin{pmatrix} 0.5 \\ -1.0 \end{pmatrix} \text{m} \quad , \quad \varphi_{13} = \frac{\pi}{2} + 0.3 \text{ rad}. \tag{4.84}$$

This choice means that only the kinematic grasp parameter estimates of manipulator $\{3\}$ are biased.

Initially, the pose of the object (and by definition equivalent to the pose of manipulator $\{1\}$) is set to

$$x_o(t_0) = x_1(t_0) = \begin{pmatrix} 0.0\text{m} \\ 0.0\text{m} \\ 0.0 \text{ rad} \end{pmatrix}. \tag{4.85}$$

In this example, the desired velocity for the object is imposed by choosing a constant value of

$$\dot{x}_o^d = \frac{x_o^d}{T_{\text{sim}}} \tag{4.86}$$

with

$$x_o^d = \begin{pmatrix} 2.0\text{m} \\ 1.0\text{m} \\ \frac{\pi}{2}\text{ rad} \end{pmatrix} \quad \text{and} \quad T_{\text{sim}} = 10\text{s}. \tag{4.87}$$

In case of unbiased kinematic grasp parameters, this choice of $\dot{x}_o^d$ (expressed in the world frame $\{w\}$) should transport the object within the simulation period T_{sim} to its goal pose x_o^d. The compliance of the end effectors is set to

$$C_i = \begin{bmatrix} 0.01\frac{\text{Ns}}{\text{m}}\ I_2 & 0_{2\times 1} \\ 0_{1\times 2} & 0.01\frac{\text{Nms}}{\text{rad}} \end{bmatrix} \tag{4.88}$$

for all $i = \{1, 2, 3\}$.

Cooperative manipulation task without parameter adaptation   The resulting trajectory of the manipulator ensemble for constant but biased parameter estimates according to (4.81) through (4.84) is illustrated in Fig. 4.8.
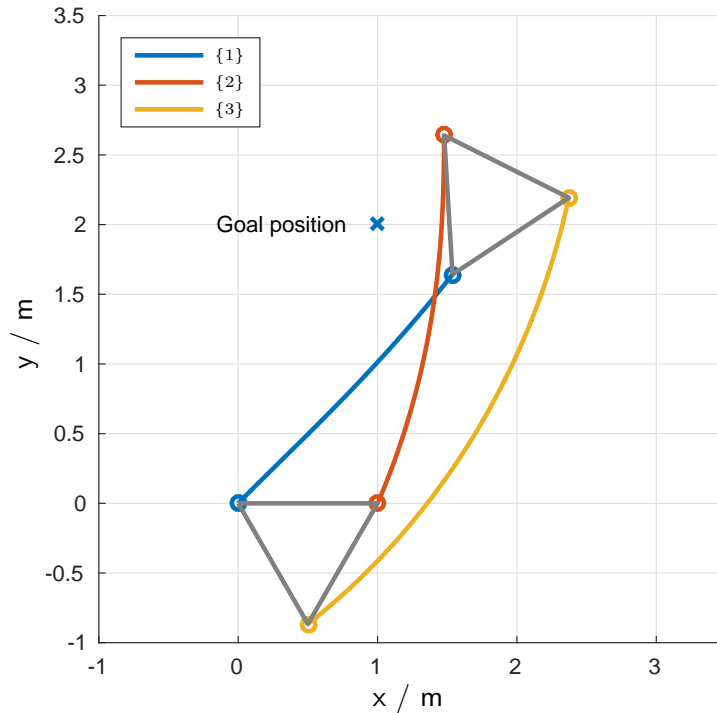
Fig. 4.8: Trajectory of the end effectors during the cooperative manipulation task

First note that the end effector poses are compliant to the kinematic constraints through-

out the entire manipulation task execution. This is visualized for the initial and final pose of the ensemble by means of the gray triangular in Fig. 4.8. However, the object does not reach its goal position - the small blue circle indicating the position of end effector {1} should be located at $p_o^d = (1.0, 2.0)^T$ m. It is also visible in Fig. 4.8 that the effective rotation of the object is greater than $\varphi_o^d = \frac{\pi}{2}$. The emerging end effector forces are plotted in Fig. 4.9.
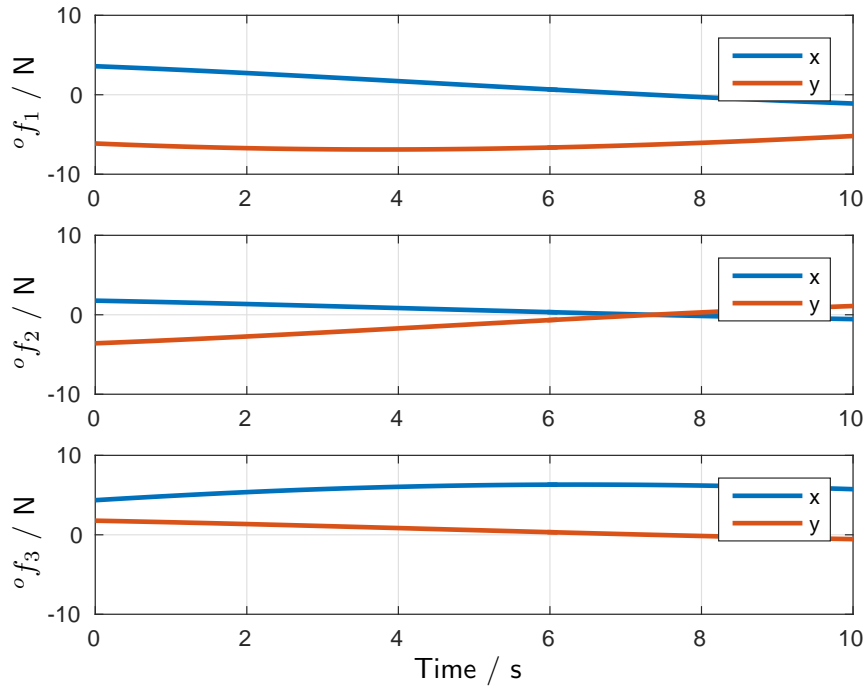

Fig. 4.9: End effector forces during the cooperative manipulation task without parameter adaptation

The end effector forces are all non-zero and do not match the desired end effector forces. It is worth noticing that although only the kinematic grasp parameter of end effector {3} are biased, the end effector force of manipulator {2} is non-zero, too. This observation illustrates the intrinsic all-to-all interaction in cooperative manipulation tasks. Obviously this holds also true for the error propagation under biased kinematic grasp parameters. Therefore, an accurate estimate of the kinematic grasp parameters is of prior relevance.

Cooperative manipulation task with parameter adaptation The robust tracking controller as presented in Theorem 9 and the relative orientation estimate as proposed in (4.78) is employed for the cooperative manipulation task example for $N = 3$ and biased kinematic grasp parameters as given by (4.81) through (4.84). The parameter adaptation gains for the simulation are set to

$$K_u = 10 \ I_6 \quad \text{and} \quad K_r = 100 \ I_6. \tag{4.89}$$

The time plot of the estimation error for the cooperative manipulation task under consideration is depicted in Fig. 4.10.
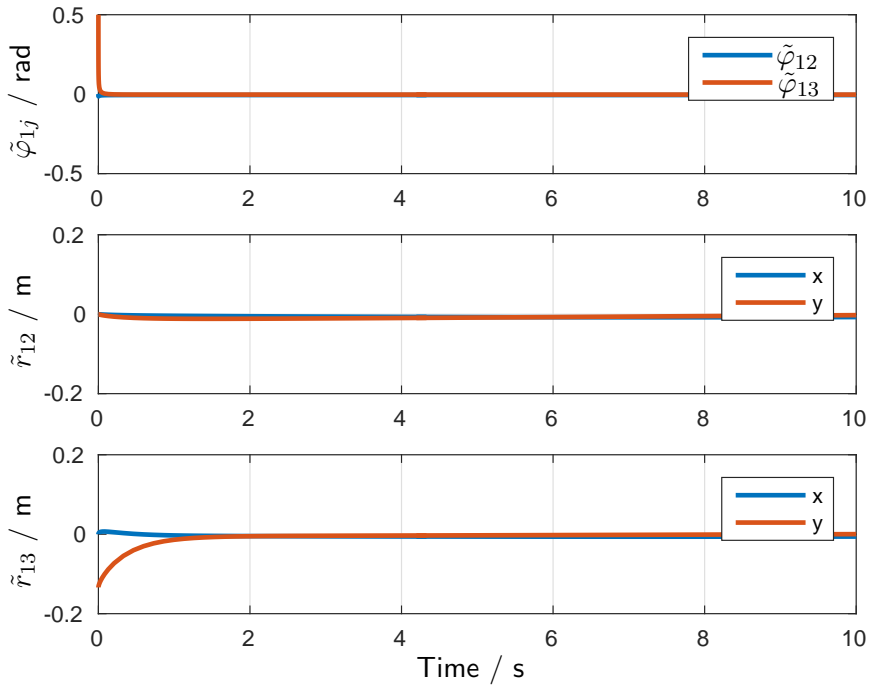
Fig. 4.10: Parameter estimation error during the cooperative manipulation task

In the top plot of Fig. 4.10 it is visible that the orientation error $\tilde{\varphi}_{13}$ drops quickly from its initial value +0.5rad to zero. The initially unbiased translational estimation error $\tilde{r}_{12}$ depicted in the plot in the middle of the figure undergoes just a slight initial perturbation due to a non-zero orientation error but remains close to zero throughout the whole manipulation task. The translational error $\tilde{r}_{13}$ illustrated in the bottom plot of Fig. 4.10 converges within a period of approximately 1.5s to zero. As an immediate consequence of the convergence of the estimation error to zero, one expects the manipulator forces to approach zero, too. The manipulator forces for the cooperative manipulation task with parameter estimation is depicted in Fig. 4.11.

As expected, all manipulator forces tend to zero. This highlights and stresses the relevance of having precise estimates of the relative end effector orientation. This is particularly true for pure translational motion tasks. The greater the desired angular motion of the manipulator ensemble, the greater will be the impact of biased translational parameter estimates. As a further consequence of converging parameter errors, the resulting tracking error of the manipulator ensemble also decreases as depicted in Fig. 4.12.

The object approaches its goal pose this time much closer - the small blue circle indicating the position of end effector $\{1\}$ should be located at $p_o^d = (1.0, 2.0)^T$m. The remaining pose error is in fact too small to be visible from Fig. 4.12. Note that no additional pose tracking controller is used and only the desired feed forward object twist in combination with the adaptive parameter estimation minimize the resulting pose error very efficiently. This again proves the relevance of having accurate estimates for the kinematic grasp parameters at hand.
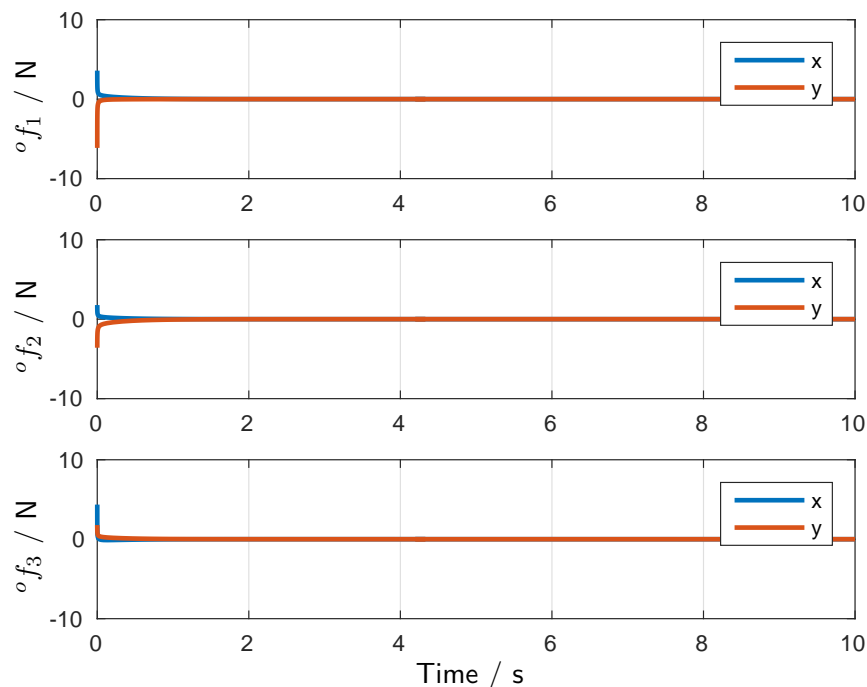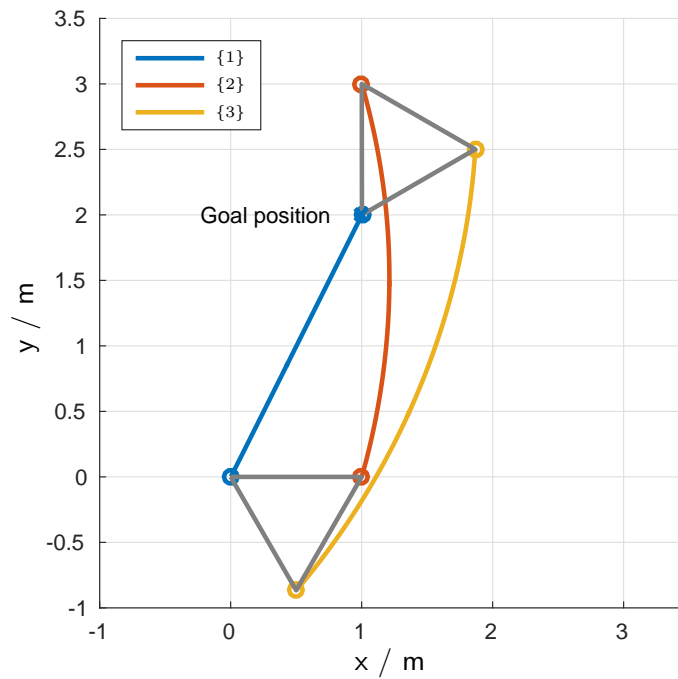
Fig. 4.11: End effector forces during the cooperative manipulation task with parameter adaptation

Summary and outlook

This chapter motivates and describes the challenges encountered in cooperative manipulation tasks for the relevant case when no global coordinate frame is available for the multi-robot coordination. The resulting coordination problem is reformulated as a robust force/motion tracking problem under uncertain kinematic grasp parameters and an adaptive control scheme is presented which solves this control problem for a planar and quasi-static manipulation task. Numerical results are provided which illustrate the impact of uncertain kinematic parameters on the force/motion tracking task. Moreover, the efficiency of the proposed adaptive controller is evaluated in simulation, too.

The findings in this chapter do not present an extensive solution to the proposed general robust force/motion tracking problem. The results should be read as a rudimentary attempt towards a conceptual approach for dealing with uncertain kinematic parameters in manipulation tasks by combining techniques from physical system modeling, control design and parameter identification. In view of the proposed identifiability criterion for planar manipulation tasks, it appears that more generalized parameter estimators might be found by addressing the identification of a rigid transformation, i.e. joined estimation of translational and rotational grasp parameters. This observation leads consequently to methods and tools from differential geometry, which comprise the core characteristics of the configuration and parameter space $SE(3)$ as a manifold. The parameter estimation problem might thus potentially be reformulated as an optimization problem on manifolds, aiming for global parameter convergence, an improved convergence compared to the cas-

Fig. 4.12: Trajectory of the end effectors during the cooperative manipulation task with parameter adaptation

caded estimation of translation/rotation parameters and a characterization of the error dynamics in the framework of the passivity formalism.

5 Conclusions

The increasingly autonomous character of robotic manipulator systems creates an entire set of novel challenges regarding an efficient team coordination during the cooperative manipulation tasks. In the future, cooperative manipulation tasks will not be limited to dedicated laboratory environments but they will become an indispensable part of industrial manufacturing, delivery logistics and remotely supervised missions such as search and rescue, space exploration or underwater operations. While the benefits of using a team of robots are obvious, the actual success of cooperating manipulators in all these different domains will depend on one crucial factor: the ability to maintain and exploit the robots' autonomous features while integrating them by means of distributed coordination and control algorithms for performing the manipulation task. Thus each robot is able to contribute best as possible to the common task, given the individual sensing and actuation capabilities. Moreover, the cooperative manipulator ensemble remains autonomous and eventually outperforms conventional single and centralized manipulator systems in view of the achievable redundancy, its modularity and the resulting online reconfigurability. This thesis contributes to this endeavor by conducting a systematic analysis of the cooperative manipulation dynamics and addressing some of the encountered challenges when targeting distributed control architectures.

Summary of contributions

The main achievement of Chapter 2 is the novel characterization of the cooperative manipulator system as a constrained multi-body system. As an immediate consequence, a closed-form model, incorporating the manipulators' kinematics and forces, is derived based on the Gauss principle. Moreover, the vital role of the kinematic constraints imposed to the manipulator ensemble is discussed, enforcing an all-to-all coupling in terms of the emerging interaction forces between the manipulators. From a multi-agent point of view, this might be interpreted as an implicit all-to-all communication through the force/torque sensors. On the other hand, this rigid coupling emphasizes the intrinsically centralized character of the interaction dynamics when aiming for cooperative force/motion tracking.

In Chapter 3 fundamental properties of the manipulator model presented in Chapter 2 are derived. This includes a result on the robust stability of the cooperative manipulator system under inaccurate feedback linearization of the individual manipulators as encountered in many practical situations. This finding is the thorough theoretical proof that common cooperative manipulator implementations maintain important system properties such as passivity (in case the end effector dynamics themselves are passive) and that the individually feedback controlled end effector remains stable when interacting with the object, the rest of the manipulators and a properly defined environment. It is the first stability result which is based on an explicit expression of the emerging end effector wrenches and valid for arbitrary dynamic manipulation tasks.

This chapter introduces also a shift of paradigm for the analysis of internal force/torques. Previously, the decomposition of internal and external wrench components is performed exclusively based on the measured end effector force/torques. As a result of the interpretation of the cooperative manipulator system as a constrained multi-body system, a new characterization of internal wrenches is presented which is compliant to the principle of virtual work. As a direct consequence, novel degrees of freedom for the load distribution between the manipulators are available and it is demonstrated that a proper internal force analysis needs to incorporate the kinematics of the end effectors.

In Chapter 4 the challenge of kinematic manipulator coordination without a global coordinate frame is introduced and formulated as an adaptive control problem. The relevant case of cooperative manipulation tasks without access to an accurate, common reference frame is discussed and the disturbing impact on the force/motion tracking objective is illustrated by means of several examples. As a first step within the adaptive control design, the identifiability of the kinematic grasp parameters is derived for manipulation tasks in $SE(3)$ but also in the particular case of planar manipulation tasks in $SE(2)$. In the latter case, a proper identification of the kinematic grasp parameters requires the object's motion to meet a condition involving its angular *and* translational velocity (opposed to tasks conducted in $SE(3)$ where only the angular velocity is relevant for the parameter identification).

In view of achieving robust force/motion tracking under uncertain kinematic grasp parameters, an adaptive control law for planar manipulation tasks is proposed. The presented scheme guarantees asymptotic tracking of the force/motion setpoints and performs an identification of the unknown grasp parameters under the assumption that the inertial forces required to manipulate the object remain small.

Conclusions

This thesis contributes to the field of cooperative manipulation by insisting continuously on a clear distinction between the modeling of the cooperative system dynamics and the control and coordination design for the manipulator ensemble in task space. Thanks to this precise differentiation, the dynamics of cooperative manipulator systems may be conveniently split into components commonly used in control design as depicted in Fig. 5.1.
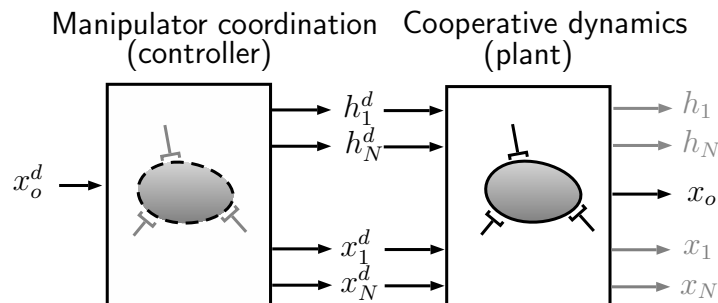
Fig. 5.1: Block scheme representation of the cooperative manipulator dynamics and the employed coordination strategy

Chapter 2 discusses thoroughly the cooperative manipulator dynamics as depicted by

the block on the right-hand side of Fig. 5.1. The individual manipulator force/motion set-points serve as input to the kinematically constrained multi-robot ensemble manipulating the object. The output of this block is the actual object pose (from which in turn the manipulator poses can be derived through the kinematic constraints) but also the actual end effector wrenches rendering the system of manipulators and object compatible to the imposed constraints.

Chapter 3 deals in depth with the analysis of the coordination strategies depicted by the block on the left-hand side of Fig. 5.1 interconnected with the cooperative system dynamics. This includes the force/motion tracking control scheme in Section 3.3 but also a completely new perspective on the design of internal/external wrench control as discussed in Sections 3.1 and 3.6, respectively.

From a high-level control engineering perspective, the cooperative dynamics block in in Fig. 5.1 represents a specific plant model while the manipulator coordination block represents the controller. Note however that the cooperative dynamics block itself contains the individual, local manipulator feedback loops rendering the apparent, individual end effector dynamics in task space. This distinction between plant dynamics (i.e. the constrained cooperative manipulator system) and controller (i.e. the applied coordination strategy for cooperative force/motion tracking) is essential for the design of more sophisticated coordination strategies with the force/motion setpoints in task space serving as convenient interface between coordination strategy and manipulator dynamics.

From an object-centered perspective, the manipulator coordination block in Fig. 5.1 realizes an inverse dynamics control law while simultaneously distributing the desired applied object wrench to the manipulator ensemble by means of suitable force/motion setpoints. Consequently, the computations in the manipulator coordination block have a straightforward interpretation as a redundancy resolution for input redundant systems.

From a multi-robot system perspective, Chapter 2 and Chapter 3 point out the vital role of the kinematic constraints imposed through the object for the system dynamics *and* the control design. Chapter 4 picks up this observation in view of the situation encountered in most practical implementations, where these crucial kinematic parameters are either not measurable at all or only with limited accuracy. The presented adaptive control scheme in Section 4.4 achieves robust force/motion tracking for planar manipulation tasks, in which the object's inertial effects remain small.

Future work

Cooperative multi-robot manipulator systems have drawn the attention of many researchers since more than three decades. Yet the number of cooperative manipulator systems successfully deployed in real world scenarios is very limited. This surely will not last long due to several reasons. On one hand, there is the recent technological trend of robotic manipulators becoming more reliable, more robust and more accessible to a broader professional and non-professional audience in regard to the available interfaces and generally decreasing deployment costs. In the field of aerial manipulation, a fully operational quadcopter equipped with on-board camera, wireless communication and inertial measurement units for stabilization of the flight dynamics is nowadays available at the price of a tablet computer. On the other hand, the conceptual design of coordination strategies for

multi-robot systems is progressively advancing towards algorithms which are able to deal efficiently with the arising uncertainties in distributed systems. However, various open research questions in the field of cooperating manipulators must be addressed in the future to comply with the expectation of its potential.

Generalization to dynamic manipulation tasks An open issue is the conceptual generalization of the adaptive control design approach presented in Chapter 4 to more general, dynamic manipulation tasks without global coordinate frame in $SE(3)$. Common parameterizations of the task space, i.e. the special Euclidean group, impede a straightforward application of standard stability results from adaptive control due to the nonlinear occurrence of the rotational parameters in the manipulator model. A potentially more general approach for this purpose might be found by employing tools from differential geometry for the parameter estimation and exploiting passivity properties of the cooperative dynamics and a suitably designed controller.

Distributed control strategies Current cooperative multi-robot manipulator setups are characterized by the increasingly autonomous character of the individual robot and the resulting distributed hardware architecture in terms of the available sensing and actuation equipment. Chapter 4 deals with the particular challenge of distributed coordinate knowledge leading to uncertain kinematic grasp parameters. The presented adaptive control algorithm is clearly a centralized scheme since it evaluates and combines continuously the sensor data of all robots in a single computational entity. No restriction on the available communication bandwidth and no delay in the sensor data transmission, which occur in real world applications, are taken into account. In case of non-ideal information exchange over the communication network, a performance loss is expected, which degrades the force/motion tracking performance of the multi-robot team. A thorough analysis of the manipulation performance and the design of distributed control algorithms appears indispensable whenever the manipulation task is conducted by means of non-ideal communication networks.

Multi-robot team reconfiguration The manipulators' autonomy in view of the numerous challenges encountered in more complex cooperative manipulation tasks can only be maintained when a coordination layer on top of the system dynamics and control design level is introduced. This means that the manipulator ensemble is eventually capable to reconfigure itself facing a task in which the objective or the requirements change over time. A typical example for this is cooperative regrasping of the object in order to increase the achievable dexterity or to render a desired apparent object dynamics. On the other hand, it appears also beneficial that manipulators flexibly join or quit the multi-robot team when needed without destabilizing or degrading the cooperative manipulation task. It is obvious that such performance-related reconfiguration builds on a concise model of the interaction dynamics as presented in this thesis.

Multi-agent reasoning With the increasing autonomy of single robotic manipulator systems and potentially heterogeneous on-board sensing, actuation and computation capaci-

ties in the multi-robot team, decision relevant to the current task objective may be negotiated during the task and subtasks may be reallocated to specific robots. The desired trajectory for the object and the manipulator ensemble should be updated and redistributed as a function of the available visual sensor information if obstacles in the environment or new directives from a human operator are detected. This negotiation about task objectives should include the human who is able to communicate at least implicitly by means of the applied force/torque to the object with the entire multi-robot team. Based on the captured sensor data, task-relevant signals such as haptic cues induced by a human operator might be extracted and learned by the manipulators in order to improve the interaction comfort for the human.

A Basic adaptive control concepts

This section introduces some fundamental concepts from adaptive control theory. The content follows the compact presentation in [91]. For a more detailed treatment of related concepts, the reader is referred to more comprehensive textbooks such as [89, 92]. Adaptive control is employed in this thesis in order to achieve accurate force/motion tracking under unknown plant parameters.

Adaptive control model

Throughout this section the joint space dynamics of a single robotic manipulator as presented in (2.4) is used in order to illustrate the adaptive control concepts. Recall that the joint space dynamics are given by

$$\Lambda_i(\xi_i)\ddot{\xi}_i + \Gamma_i(\xi_i, \dot{\xi}_i) = \tau_i. \tag{A.1}$$

It can be verified that the individual manipulator dynamics are linear in terms of suitably selected set of p_i physical robot parameters $\Theta_i \in \mathbb{R}^{p_i}$ as e.g. the link inertias or the end-effector payload. In adaptive control this *linear parameterization* property is commonly exploited to rewrite the plant dynamics as

$$\tau_i = Y_i(\xi_i, \dot{\xi}_i, \ddot{\xi}_i)\,\Theta_i, \tag{A.2}$$

wherein $Y_i \in \mathbb{R}^{n_i \times p_i}$ is a non-linear matrix function called the *regressor matrix*.

Remark In case the joint acceleration $\ddot{\xi}_i$ is not measurable, the following modification can be implemented. In order to eliminate $\ddot{\xi}_i$ from (A.2), both sides of (A.2) are filtered by an exponentially stable and strictly proper filter with impulse response $w_i(t)$. By defining the filtered torque as

$$y_i(t) = \int_0^t w_i(t-r)\tau_i(r)dr \tag{A.3}$$

and using partial integration one has

$$\int_0^t w_i(t-r)[\Lambda_i(\xi_i)\ddot{\xi}_i] = w_i(t-r)\Lambda_i(\xi_i)\dot{\xi}_i \mid_0^t - \int_0^t \frac{d}{dr}[w_i\Lambda_i(\xi_i)]\dot{\xi}_i dr \tag{A.4}$$

which clearly is a function of ξ_i and $\dot{\xi}_i$ only. Thus one can write

$$y_i = W_i(\xi_i, \dot{\xi}_i)\,\Theta_i \tag{A.5}$$

wherein W_i is the filtered version of Y_i, which can be computed by means of the measurements ξ_i and $\dot{\xi}_i$.

Based on the parameter estimate $\hat{\Theta}_i \in \mathbb{R}^{p_i}$, a prediction of the (filtered) torque is generated according to

$$\hat{y}_i = W_i(\xi_i, \dot{\xi}_i)\, \hat{\Theta}_i. \tag{A.6}$$

The prediction error is thus

$$e_i = \hat{y}_i - y_i = W_i(\xi_i, \dot{\xi}_i)\, \tilde{\Theta}_i \tag{A.7}$$

and hence e_i linear in the parameter error

$$\tilde{\Theta}_i = \hat{\Theta}_i - \Theta_i. \tag{A.8}$$

Parameter estimation methods

In the sequel parameter estimators of the form

$$\dot{\hat{\Theta}}_i = -P_i W_i^T e_i \tag{A.9}$$

are considered wherein $P_i \in \mathbb{R}^{p_i \times p_i}$ is a constant or time-varying, positive definite gain matrix.

Gradient estimator

The gradient estimator results from choosing

$$P_i = \bar{P}_i = \text{const.}, \tag{A.10}$$

which is equivalent to minimizing the instantaneous prediction error, i.e.

$$\min_{\hat{\Theta}_i} \|e_i\|^2. \tag{A.11}$$

The gradient estimator is suitable to track time-varying parameters and performs well in the presence of disturbances. If the regressor matrix W_i is *persistently exciting*, the parameter estimate converges exponentially. However, if W_i is not persistently exciting, the parameters will not converge - even in the absence of uncertainties. Therefore, persistency of excitation plays a crucial role for the parameter identification in adaptive control schemes.

Persistent excitation   A matrix $M \in \mathbb{R}^{d \times d}$ is said to be persistently exciting if there exist positive constants α_1, α_2 and ΔT such that

$$\forall t \geq 0 \quad \alpha_1 I_d \leq \int_t^{t+\Delta T} M^T(r)M(r)dr \leq \alpha_2 I_d. \tag{A.12}$$

Note that although the matrix product $M^T M$ might in general be singular for all r, the integral of $M^T M$ is uniformly positive definite for any interval of length L. The concept of persistent excitation is closely linked to the uniform observability condition of non-linear systems and the observability Gramian in linear systems. In the context of adaptive control, persistent excitation means unambiguous observability of the parameters from the observed system trajectory. In view of the manipulator example with $W(\xi_i, \dot{\xi}_i)$, persistent excitation means that the joint space trajectory $\xi_i(t)$ is sufficiently rich in order to allow a unique conclusion on the parameter vector Θ_i.

Least-squares estimator

An alternative estimator guaranteeing convergence to a constant parameter vector is obtained by

$$\dot{P}_i = -P_i W_i^T W_i P_i \tag{A.13}$$

minimizing the squared integral of the prediction error, i.e.

$$\min_{\hat{\Theta}_i} \int_0^t \|e_i(r)\|^2 dr. \tag{A.14}$$

However, even if W_i is persistently exciting, the estimator does not converge exponentially. See [89, Section 4.3] for alternative estimators and a thorough analysis of the individual convergence properties.

Bibliography

[1] Y. Shoham and K. Leyton-Brown, *Multiagent Systems: Algorithmic, Game-Theoretic, and Logical Foundations.* New York, NY, USA: Cambridge University Press, 2008.

[2] M. Woolridge and M. J. Wooldridge, *Introduction to Multiagent Systems.* New York, NY, USA: John Wiley & Sons, Inc., 2001.

[3] R. Olfati-Saber, J. Fax, and R. Murray, "Consensus and cooperation in networked multi-agent systems," *Proceedings of the IEEE*, vol. 95, pp. 215–233, Jan 2007.

[4] J. Lin, A. S. Morse, and B. D. O. Anderson, "The multi-agent rendezvous problem. part 1: The synchronous case," *SIAM Journal on Control and Optimization*, vol. 46, no. 6, pp. 2096–2119, 2007.

[5] K.-K. Oh, M.-C. Park, and H.-S. Ahn, "A survey of multi-agent formation control," *Automatica*, vol. 53, pp. 424 – 440, 2015.

[6] J. Cortes, S. Martinez, T. Karatas, and F. Bullo, "Coverage control for mobile sensing networks," *Robotics and Automation, IEEE Transactions on*, vol. 20, pp. 243–255, April 2004.

[7] D. V. Dimarogonas and K. H. Johansson, "Bounded control of network connectivity in multi-agent systems," *IET control theory & applications*, vol. 4, no. 8, pp. 1330–1338, 2010.

[8] R. Olfati-Saber and R. M. Murray, "Graph rigidity and distributed formation stabilization of multi-vehicle systems," in *Decision and Control, 2002, Proceedings of the 41st IEEE Conference on*, vol. 3, pp. 2965–2971, IEEE, 2002.

[9] A. Sarlette, S. Bonnabel, and R. Sepulchre, "Coordinated motion design on Lie groups," *Automatic Control, IEEE Transactions on*, vol. 55, pp. 1047–1058, May 2010.

[10] D. Katz and O. Brock, "A factorization approach to manipulation in unstructured environments," in *14th International Symposium of Robotics Research*, (Lucerne, Switzerland), pp. 1–16, Springer Verlag, August 31-September 3 2009.

[11] S. Erhart and S. Hirche, "Model and analysis of the interaction dynamics in cooperative manipulation tasks," *IEEE Transactions on Robotics*, vol. 32, pp. 672–683, June 2016.

[12] S. Erhart and S. Hirche, "Internal force analysis and load distribution for cooperative multi-robot manipulation," *IEEE Transactions on Robotics (T-RO)*, vol. 31, no. 5, pp. 1238 – 1243, 2015.

[13] L. D. Pascali, "Interaction force decomposition in cooperative multi-robot manipulation tasks," Masters's thesis, Institute of Information-oriented Control (ITR), Techniche Universität München, Germany, Mar. 2015.

[14] A. Z. Bais, "Dynamic load distribution in cooperative multi-robot manipulation tasks," Masters's thesis, Institute of Information-oriented Control (ITR), Techniche Universität München, Germany, Mar. 2015.

[15] S. Erhart and S. Hirche, "Adaptive force/velocity control for multi-robot cooperative manipulation under uncertain kinematic parameters," in *Intelligent Robots and Systems (IROS), 2013 IEEE/RSJ International Conference on*, pp. 307–314, Nov 2013.

[16] D. Cehajic, S. Erhart, and S. Hirche, "Grasp pose estimation in human-robot manipulation tasks using wearable motion sensors," in *Proceedings of the 2015 IEEE/RSJ International Conference on Intelligent Robots and Systems (IROS 2015)*, pp. 1031–1036, 2015.

[17] S. Hayati, "Hybrid position/force control of multi-arm cooperating robots," in *Robotics and Automation. Proceedings. 1986 IEEE International Conference on*, vol. 3, pp. 82–89, Apr 1986.

[18] O. Khatib, "Object manipulation in a multi-effector robot system," in *Proceedings of the 4th International Symposium on Robotics Research*, (Cambridge, MA, USA), pp. 137–144, MIT Press, 1988.

[19] M. Unseren and A. Koivo, "Reduced order model and decoupled control architecture for two manipulators holding an object," in *Robotics and Automation, 1989. Proceedings., 1989 IEEE International Conference on*, pp. 1240–1245 vol.2, May 1989.

[20] M. D. Djurovic and M. K. Vukobratovic, "A contribution to dynamic modeling of cooperative manipulation," *Mechanism and Machine Theory*, vol. 25, no. 4, pp. 407 – 415, 1990.

[21] X. Yun and V. R. Kumar, "An approach to simultaneous control of trajectory and interaction forces in dual-arm congurations," *IEEE Transactions on Robotics and Automation*, pp. 618–624, 1991.

[22] J. Gudino-Lau and M. A. Arteaga, "Dynamic model and simulation of cooperative robots: a case study," *Robotica*, vol. 23, pp. 615–624, 9 2005.

[23] H. Bruyninckx and O. Khatib, "Gauss' Principle and the Dynamics of Redundant and Constrained Manipulators," in *International Conference on Robotics and Automation*, vol. 3, pp. 2563–2568, 2000.

[24] V. De Sapio and O. Khatib, "Operational space control of multibody systems with explicit holonomic constraints," in *Robotics and Automation, 2005. ICRA 2005. Proceedings of the 2005 IEEE International Conference on*, pp. 2950–2956, April 2005.

[25] S. Stramigioli, *Modeling and IPC Control of Interactive Mechanical Systems: A Coordinate-Free Approach.* Secaucus, NJ, USA: Springer-Verlag New York, Inc., 2001.

[26] A. van der Schaft, "Port-hamiltonian systems: an introductory survey," in *Proceedings of the International Congress of Mathematicians Vol. III: Invited Lectures* (M. Sanz-Sole, J. Soria, J. Varona, and J. Verdera, eds.), (Madrid, Spain), pp. 1339–1365, European Mathematical Society Publishing House (EMS Ph), 2006.

[27] H. Yoshimura and J. E. Marsden, "Representations of Dirac structures and implicit port-controlled Lagrangian systems," in *18th International Symposium on Mathematical Theory of Networks and Systems*, 2008.

[28] F. Aghili, "A unified approach for inverse and direct dynamics of constrained multi-body systems based on linear projection operator: applications to control and simulation," *Robotics, IEEE Transactions on*, vol. 21, pp. 834–849, Oct 2005.

[29] A. Bicchi, D. Prattichizzo, and C. Melchiorri, "Force and dynamic manipulability for cooperating robot systems," in *in Proc. Int. Symp. on Robotic Systems (IROS) 97*, pp. 1479–1484, 1997.

[30] S. Arimoto, K. Tahara, J.-H. Bae, and M. Yoshida, "A stability theory of a manifold: concurrent realization of grasp and orientation control of an object by a pair of robot fingers," *Robotica*, vol. 21, no. 02, pp. 163–178, 2003.

[31] D. Prattichizzo and A. Bicchi, "Dynamic analysis of mobility and graspability of general manipulation systems," *Robotics and Automation, IEEE Transactions on*, vol. 14, pp. 241–258, Apr 1998.

[32] J. Fink, N. Michael, S. Kim, and V. Kumar, "Planning and control for cooperative manipulation and transportation with aerial robots," *The International Journal of Robotics Research*, vol. 30, no. 3, pp. 324–334, 2011.

[33] K. Sreenath and V. Kumar, "Dynamics, control and planning for cooperative manipulation of payloads suspended by cables from multiple quadrotor robots," in *Robotics: Science and Systems (RSS)*, 2013.

[34] B. Siciliano, L. Sciavicco, L. Villani, and G. Oriolo, *Robotics: Modelling, Planning and Control.* Springer Publishing Company, Incorporated, 1st ed., 2008.

[35] O. Khatib, "A unified approach for motion and force control of robot manipulators: The operational space formulation," *Robotics and Automation, IEEE Journal of*, vol. 3, pp. 43–53, February 1987.

[36] C. Ott, A. Albu-Schaffer, A. Kugi, S. Stamigioli, and G. Hirzinger, "A passivity based cartesian impedance controller for flexible joint robots," in *Robotics and Automation, 2004. Proceedings. ICRA '04. 2004 IEEE International Conference on*, vol. 3, pp. 2659–2665 Vol.3, April 2004.

[37] J. Diebel, "Representing attitude: Euler angles, unit quaternions, and rotation vectors." `http://citeseerx.ist.psu.edu/viewdoc/summary?doi=10.1.1.110.5134`, 2006.

[38] F. Caccavale, P. Chiacchio, A. Marino, and L. Villani, "Six-dof impedance control of dual-arm cooperative manipulators," *Mechatronics, IEEE/ASME Transactions on*, vol. 13, no. 5, pp. 576–586, 2008.

[39] D. Lawrence, "Impedance control stability properties in common implementations," in *Robotics and Automation, 1988. Proceedings., 1988 IEEE International Conference on*, pp. 1185–1190 vol.2, Apr 1988.

[40] B. Siciliano, "Kinematic control of redundant robot manipulators: A tutorial," *Journal of Intelligent and Robotic Systems*, vol. 3, no. 3, pp. 201–212, 1990.

[41] R. Volpe and P. Khosla, "A theoretical and experimental investigation of explicit force control strategies for manipulators," *IEEE Transactions on Automatic Control*, vol. 38, pp. 1634–1650, 1993.

[42] A. Albu-Schäffer and G. Hirzinger, "Cartesian impedance control techniques for torque controlled light-weight robots," in *Robotics and Automation, 2002. Proceedings. ICRA '02. IEEE International Conference on*, vol. 1, pp. 657–663 vol.1, 2002.

[43] A. Bicchi, "Hands for dexterous manipulation and robust grasping: A difficult road toward simplicity," *Robotics and Automation, IEEE Transactions on*, vol. 16, no. 6, pp. 652–662, 2000.

[44] M. Uchiyama and P. Dauchez, "A symmetric hybrid position/force control scheme for the coordination of two robots," in *Robotics and Automation, 1988. Proceedings., 1988 IEEE International Conference on*, pp. 350–356 vol.1, Apr 1988.

[45] F. E. Udwadia and R. E. Kalaba, "A new perspective on constrained motion," *Proceedings: Mathematical and Physical Sciences*, vol. 439, no. 1906, pp. 407–410, 1992.

[46] T. A. Johansen and T. I. Fossen, "Control allocation a survey," *Automatica*, vol. 49, no. 5, pp. 1087 – 1103, 2013.

[47] R. Bonitz and T. Hsia, "Internal force-based impedance control for cooperating manipulators," *Robotics and Automation, IEEE Transactions on*, vol. 12, pp. 78–89, Feb 1996.

[48] D. Heck, D. Kostic, A. Denasi, and H. Nijmeijer, "Internal and external force-based impedance control for cooperative manipulation," in *Control Conference (ECC), 2013 European*, pp. 2299–2304, July 2013.

[49] T. Alberts and D. Soloway, "Force control of a multi-arm robot system," in *Robotics and Automation, 1988. Proceedings., 1988 IEEE International Conference on*, pp. 1490–1496 vol. 3, Apr 1988.

[50] Y. Nakamura, K. Nagai, and T. Yoshikawa, "Dynamics and stability in coordination of multiple robotic mechanisms," *The International Journal of Robotics Research*, vol. 8, no. 2, pp. 44–61, 1989.

[51] I. D. Walker, R. A. Freeman, and S. I. Marcus, "Analysis of motion and internal loading of objects grasped by multiple cooperating manipulators," *The International Journal of Robotics Research*, vol. 10, no. 4, pp. 396–409, 1991.

[52] R. Bonitz and T. Hsia, "Force decomposition in cooperating manipulators using the theory of metric spaces and generalized inverses," in *Robotics and Automation, 1994. Proceedings., 1994 IEEE International Conference on*, pp. 1521–1527 vol.2, May 1994.

[53] J. Chung, B.-J. Yi, and W. Kim, "Analysis of internal loading at multiple robotic systems," *Journal of Mechanical Science and Technology*, vol. 19, no. 8, pp. 1554–1567, 2005.

[54] V. Kumar and K. Waldron, "Force distribution in closed kinematic chains," in *Robotics and Automation, 1988. Proceedings., 1988 IEEE International Conference on*, pp. 114–119 vol. 1, Apr 1988.

[55] V. Lippiello, B. Siciliano, and L. Villani, "A grasping force optimization algorithm for multiarm robots with multifingered hands," *Robotics, IEEE Transactions on*, vol. 29, pp. 55–67, Feb 2013.

[56] T. Yoshikawa and K. Nagai, "Manipulating and grasping forces in manipulation by multifingered robot hands," *Robotics and Automation, IEEE Transactions on*, vol. 7, pp. 67–77, Feb 1991.

[57] D. Williams and O. Khatib, "The virtual linkage: a model for internal forces in multi-grasp manipulation," in *Robotics and Automation, 1993. Proceedings., 1993 IEEE International Conference on*, pp. 1025–1030 vol. 1, 1993.

[58] A. Zambelli, S. Erhart, L. Zaccarian, and S. Hirche, "Dynamic load distribution in cooperative manipulation tasks," in *Proceedings of the 2015 IEEE/RSJ International Conference on Intelligent Robots and Systems (IROS 2015)*, (Hamburg, Germany), pp. 2380 – 2385, 2015.

[59] N. Hogan, "Impedance control: An approach to manipulation," in *American Control Conference, 1984*, pp. 304–313, June 1984.

[60] S. Schneider and J. Cannon, R.H., "Object impedance control for cooperative manipulation: theory and experimental results," *Robotics and Automation, IEEE Transactions on*, vol. 8, pp. 383–394, Jun 1992.

[61] K. Kosuge, H. Yoshida, T. Fukuda, M. Sakai, K. Kanitani, and K. Hariki, "Unified control for dynamic cooperative manipulation," in *Intelligent Robots and Systems. Proceedings of the IEEE/RSJ/GI International Conference on*, vol. 2, pp. 1042–1047 vol.2, Sep 1994.

[62] J. Szewczyk, G. Morel, and P. Bidaud, "Distributed impedance control of multiple robot systems," in *Robotics and Automation, 1997. Proceedings., 1997 IEEE International Conference on*, vol. 2, pp. 1801–1806 vol.2, Apr 1997.

[63] F. Caccavale, V. Lippiello, G. Muscio, F. Pierri, F. Ruggiero, and L. Villani, "Grasp planning and parallel control of a redundant dual-arm/hand manipulation system," *Robotica*, vol. 31, pp. 1169–1194, 10 2013.

[64] T. Wimböck, C. Ott, A. Albu-Schäffer, and G. Hirzinger, "Comparison of object-level grasp controllers for dynamic dexterous manipulation," *The International Journal of Robotics Research*, vol. 31, no. 1, pp. 3–23, 2012.

[65] A. Macchelli, "Passivity-based control of implicit port-hamiltonian systems," in *Control Conference (ECC), 2013 European*, pp. 2098–2103, July 2013.

[66] D. Lee and P. Li, "Passive decomposition of mechanical systems with coordination requirement," *Automatic Control, IEEE Transactions on*, vol. 58, pp. 230–235, Jan 2013.

[67] M. Tognon and A. Franchi, "Control of motion and internal stresses for a chain of two underactuated aerial robots," in *Control Conference (ECC), 2015 European*, pp. 1620–1625, July 2015.

[68] A. Bicchi, "On the problem of decomposing grasp and manipulation forces in multiple whole-limb manipulation," *Robotics and Autonomous Systems*, vol. 13, no. 2, pp. 127 – 147, 1994.

[69] J. Gentle, *Matrix Algebra: Theory, Computations, and Applications in Statistics.* Springer Texts in Statistics, Springer, 2007.

[70] H.-C. Lin, T.-C. Lin, and K. Yae, "On the skew-symmetric property of the newton-euler formulation for open-chain robot manipulators," in *American Control Conference, Proceedings of the 1995*, vol. 3, pp. 2322–2326 vol.3, Jun 1995.

[71] J. Loncaric, "Normal forms of stiffness and compliance matrices," *Robotics and Automation, IEEE Journal of*, vol. 3, pp. 567–572, December 1987.

[72] H. Khalil, *Nonlinear Systems.* Prentice Hall, 2002.

[73] R. Ortega and M. Spong, "Adaptive motion control of rigid robots: a tutorial," in *Decision and Control, 1988., Proceedings of the 27th IEEE Conference on*, pp. 1575–1584 vol.2, Dec 1988.

[74] T. Caughey and M. Okelly, "Classical normal modes in damped linear dynamic systems," *Journal of Applied Mechanics*, vol. 32, no. 3, pp. 583–588, 1965.

[75] C. Cheah, C. Liu, and J. Slotine, "Adaptive Jacobian tracking control of robots with uncertainties in kinematic, dynamic and actuator models," *Automatic Control, IEEE Transactions on*, vol. 51, pp. 1024 – 1029, June 2006.

[76] F. Aghili, "Self-tuning cooperative control of manipulators with position/orientation uncertainties in the closed-kinematic loop," in *Intelligent Robots and Systems (IROS), 2011 IEEE/RSJ International Conference on*, pp. 4187–4193, Sept 2011.

[77] Y. Karayiannidis, C. Smith, F. Vina, P. Ögren, and D. Kragic, ""open sesame!" - adaptive force/velocity control for opening unknown doors," in *IEEE/RSJ International Conference on Intelligent Robots and Systems*, pp. 4040–4047, 2012.

[78] J. Markdahl, Y. Karayiannidis, X. Hu, and D. Kragic, "Distributed cooperative object attitude manipulation," in *Robotics and Automation (ICRA), 2012 IEEE International Conference on*, pp. 2960–2965, IEEE, 2012.

[79] A. Belabbas, S. Mou, A. Morse, and B. Anderson, "Robustness issues with undirected formations," in *Decision and Control (CDC), 2012 IEEE 51st Annual Conference on*, pp. 1445–1450, Dec 2012.

[80] S. Erhart, D. Sieber, and S. Hirche, "An impedance-based control architecture for multi-robot cooperative dual-arm mobile manipulation," in *Intelligent Robots and Systems (IROS), 2013 IEEE/RSJ International Conference on*, pp. 315–322, Nov 2013.

[81] B. Mooring, M. Driels, and Z. Roth, *Fundamentals of Manipulator Calibration*. New York, NY, USA: John Wiley & Sons, Inc., 1991.

[82] J. Spletzer, A. Das, R. Fierro, C. Taylor, V. Kumar, and J. Ostrowski, "Cooperative localization and control for multi-robot manipulation," in *Intelligent Robots and Systems, 2001. Proceedings. 2001 IEEE/RSJ International Conference on*, vol. 2, pp. 631–636 vol.2, 2001.

[83] D. Fox, W. Burgard, H. Kruppa, and S. Thrun, "A probabilistic approach to collaborative multi-robot localization," *Autonomous Robots*, vol. 8, no. 3, pp. 325–344, 2000.

[84] H. Krishnan and N. H. McClamroch, "Tracking in nonlinear differential-algebraic control systems with applications to constrained robot systems," *Automatica*, vol. 30, no. 12, pp. 1885–1897, 1994.

[85] C.-S. Chiu, K.-Y. Lian, and T.-C. Wu, "Robust adaptive motion/force tracking control design for uncertain constrained robot manipulators," *Automatica*, vol. 40, no. 12, pp. 2111–2119, 2004.

[86] G. Wahba, "A least squares estimate of satellite attitude," *SIAM Review*, vol. 7, no. 3, pp. 409–409, 1965.

[87] J. L. Crassidis, F. L. Markley, and Y. Cheng, "Survey of nonlinear attitude estimation methods," *Journal of Guidance, Control, and Dynamics*, vol. 30, no. 1, pp. 12–28, 2007.

[88] F. Aghili, "Adaptive control of manipulators forming closed kinematic chain with inaccurate kinematic model," *Mechatronics, IEEE/ASME Transactions on*, vol. 18, pp. 1544–1554, Oct 2013.

[89] P. A. Ioannou and J. Sun, *Robust Adaptive Control.* Upper Saddle River, NJ, USA: Prentice-Hall, Inc., 1995.

[90] D. Q. Huynh, "Metrics for 3D rotations: Comparison and analysis," *Journal of Mathematical Imaging and Vision*, vol. 35, no. 2, pp. 155–164, 2009.

[91] F. J. Vijverstra, *Direct, Indirect and Composite Adaptive Control of Robot.* Technische Universiteit Eindhoven, 1992.

[92] J. Slotine and W. Li, *Applied Nonlinear Control.* Prentice Hall, 1991.